



National Library
of Canada

Bibliothèque nationale
du Canada

Canadian Theses Service

Service des thèses canadiennes

Ottawa, Canada
K1A 0N4

NOTICE

The quality of this microform is heavily dependent upon the quality of the original thesis submitted for microfilming. Every effort has been made to ensure the highest quality of reproduction possible.

If pages are missing, contact the university which granted the degree.

Some pages may have indistinct print especially if the original pages were typed with a poor typewriter ribbon or if the university sent us an inferior photocopy.

Reproduction in full or in part of this microform is governed by the Canadian Copyright Act, R.S.C. 1970, c. C-30, and subsequent amendments.

AVIS

La qualité de cette microforme dépend grandement de la qualité de la thèse soumise au microfilmage. Nous avons tout fait pour assurer une qualité supérieure de reproduction.

S'il manque des pages, veuillez communiquer avec l'université qui a conféré le grade.

La qualité d'impression de certaines pages peut laisser à désirer, surtout si les pages originales ont été dactylographiées à l'aide d'un ruban usé ou si l'université nous a fait parvenir une photocopie de qualité inférieure.

La reproduction, même partielle, de cette microforme est soumise à la Loi canadienne sur le droit d'auteur, SRC 1970, c. C-30, et ses amendements subséquents.

**SHIELDING EFFECTIVENESS OF
ENCLOSURES PREDICTED VIA THE FINITE
ELEMENT METHOD**

by
Luc B. Gravelle

A thesis submitted to the
School of Graduate Studies and Research
in partial fulfillment of the requirements for the degree of
Master of Applied Science

Ottawa-Carleton Institute for Electrical Engineering

Department of Electrical Engineering

Faculty of Engineering

University of Ottawa



Luc B. Gravelle, Ottawa, Canada, 1990



National Library
of Canada

Bibliothèque nationale
du Canada

Canadian Theses Service Service des thèses canadiennes

Ottawa, Canada
K1A 0N4

The author has granted an irrevocable non-exclusive licence allowing the National Library of Canada to reproduce, loan, distribute or sell copies of his/her thesis by any means and in any form or format, making this thesis available to interested persons.

The author retains ownership of the copyright in his/her thesis. Neither the thesis nor substantial extracts from it may be printed or otherwise reproduced without his/her permission.

L'auteur a accordé une licence irrévocable et non exclusive permettant à la Bibliothèque nationale du Canada de reproduire, prêter, distribuer ou vendre des copies de sa thèse de quelque manière et sous quelque forme que ce soit pour mettre des exemplaires de cette thèse à la disposition des personnes intéressées.

L'auteur conserve la propriété du droit d'auteur qui protège sa thèse. Ni la thèse ni des extraits substantiels de celle-ci ne doivent être imprimés ou autrement reproduits sans son autorisation.

ISBN 0-315-59997-9

Canada



UNIVERSITÉ D'OTTAWA
UNIVERSITY OF OTTAWA

I hereby declare that I am the sole author of this document. I authorize the University of Ottawa to lend this document to other institutions or individuals for the purpose of scholarly research.

Luc B. Gravelle

I further authorize the University of Ottawa to reproduce this document by photocopying or by other means, in total or in part, at the request of other institutions or individuals for the purpose of scholarly research.

Luc B. Gravelle

Acknowledgement

I would like to express my sincere gratitude to my supervisor Dr. G.I. Costache for his guidance and encouragement during the preparation of this thesis, thank you very much for always being available for your students when we needed you, it is exceptional.

I would also like to extend sincere thanks to Dr. R. Vaillancourt, from the Mathematics department of the University of Ottawa, for his great help in locating a finite-difference algorithm appropriate to the analysis.

The financial support of the National Science and Engineering Research Council of Canada is gratefully acknowledged.

Abstract

This thesis presents the application of the numerical finite element method (FEM) in solving the electromagnetic shielding effectiveness of enclosures. The emphasis is placed on the solution of time-dependant varying fields, as for example an NEMP or a digital signal, directly in the time domain. Previous numerical prediction of shielding effectiveness on complicated structures have been analyzed with the FEM in the frequency domain whereas no study, to the author's knowledge, has been conducted in the time domain. EMP type varying fields impinging on enclosures are studied with this new CAD tool and compared to the analytical solution of a simple parallel plate shield. Following the validation of the technique for the one-dimensional case, the shielding effectiveness of a more general two dimensional structure is investigated and validated with the introduction of a second numerical technique, TLM. Included in this study are two user-friendly, general, interactive Fortran codes. One analyze the field penetration through rectangular enclosures (with apertures) of various EMP type plane waves (TE or TM) having a certain angle of incidence on enclosures. The other analyze the field radiation from enclosures (with apertures) due to currents in signal lines.

Contents

List of Figures	iv
List of Tables	vii
1 Introduction	1
1.1 Goal	3
1.2 The Numerical Techniques	4
1.2.1 FEM	4
1.2.2 TLM	5
2 One-Dimensional Test Enclosure	6
2.1 Analytical Formulation	7
2.1.1 Frequency Domain	8
2.1.2 Time Domain	9
3 Finite Element Method	12
3.1 Introduction	12
3.2 Mathematical Formulation	13
3.3 Frequency Domain	18
3.3.1 Solving the System of Equations	19
3.3.2 Realistic Frequency Diffusion Problems and Validation	19

3.4	Time Domain	21
3.4.1	Solving the System of Equations	21
3.4.2	Realistic Time Diffusion Problems	25
3.4.3	Validation	26
4	Transmission-Line-Matrix	29
4.1	Introduction	29
4.2	Mathematical Formulation	33
4.2.1	Lossless Medium	33
4.2.2	Lossy and Dielectric Medium	35
4.2.3	Variable Mesh Size	37
4.3	Realistic Diffusion Problems to be Solved	39
4.4	Validation	44
4.4.1	Number of Iterations Needed for Steady-State	44
4.4.2	Effect of Varying the Length of the Step Size	46
4.5	Discussion	47
5	Application of FEM to General Problems	49
5.1	Introduction	49
5.2	Immunity Case	50
5.2.1	Mathematical Formulation	52
5.2.2	Frequency Domain Comparison Between FEM and TLM	53
5.2.3	Time Domain Comparison Between FEM and TLM	55
5.3	Emission Case	58
5.3.1	Mathematical Formulation	59
5.3.2	Frequency Domain Comparison Between FEM and TLM	65
5.3.3	Time Domain Comparison Between FEM and TLM	67
5.4	Discussion	69

6	Time-Domain Analysis of Complex Shielding Situations with FEM	70
6.1	Introduction	70
6.2	Immunity Analysis	71
6.2.1	Considerations	72
6.2.2	Results	73
6.3	Emission Analysis	78
6.3.1	Considerations	79
6.3.2	Results	80
7	Conclusion	83
A	Time Domain Analytical Formulation	85
B	Infinite Element Contribution to the System of Equations	88
C	FEM Computer Program for Immunity Problems in Time Domain	90
D	FEM Computer Program for Emission Problems in Time Domain	91

List of Figures

1.1	Problems to be analysed.	2
2.1	One-dimensional approximation.	7
3.1	Finite element subregions.	13
3.2	Basic triangular element.	16
3.3	Division into FEs for frequency domain.	20
3.4	Time signatures of the EMP type fields.	22
3.5	Division into FEs for time-domain.	27
3.6	One-dimensional time-domain comparison of analytical solution with FEM.	28
4.1	Formation of wave fronts as explained by Huygens principle.	30
4.2	Interconnecting transmission lines (TLs).	30
4.3	Scattered field from one Dirac impulse in a homogeneous region.	32
4.4	Basic shunt network.	33
4.5	Top view of node loaded with $\frac{\Delta l}{2}$ open stub and infinite loss stub.	36
4.6	Shunt network with variable branch length.	37
4.7	One-dimensional TLM.	39
4.8	Dispersion vs frequency of TLM network.	41
4.9	TLM division of the one-dimensional problem.	44
4.10	TLM vs analytical solution as a function of iteration.	45
4.11	Frequency plot of TLM vs analytical solution as a function of iteration.	46

4.12	Analytical solution vs TLM as a function of Δl	48
5.1	Mirror image concept for (a)TE and (b) TM modes of propagating plane waves.	51
5.2	Immunity problem under investigation.	52
5.3	Finite element division (immunity).	53
5.4	TLM division (immunity).	54
5.5	Frequency domain comparison between FEM and TLM, immunity case.	55
5.6	Time domain comparison between FEM and TLM for $x = y = 25mm$, immunity case.	57
5.7	Time domain comparison between FEM and TLM for $x = 38mm$; $y = 25mm$, immunity case.	57
5.8	Constant magnetic field on a back plane.	58
5.9	Emission problem under investigation.	59
5.10	TLM mesh division for the emission study.	60
5.11	Inhomogeneous Neumann boundary.	63
5.12	The infinite element.	64
5.13	FEM boundary condition for the emission study.	66
5.14	Frequency domain comparison between FEM and TLM, emission case.	67
5.15	Time domain comparison between FEM and TLM, emission case. . .	68
6.1	General immunity problem to investigate.	71
6.2	Distance from the real and image source to a boundary point.	73
6.3	The analysed enclosure (immunity).	74
6.4	Division into FEs of region (immunity).	74
6.5	Position of the field calculation.	75
6.6	Electric field penetration at positions 1 & 2.	76
6.7	Time domain electric SE at position 2.	77
6.8	Magnetic field penetration at positions 1 & 2.	77

6.9 Time domain magnetic SE at position 2. 78
6.10 General emission problem under investigation. 78
6.11 Current time signature. 79
6.12 The analysed enclosure (emission). 80
6.13 FEM boundary conditions (emission). 81
6.14 Magnetic field radiation for different positions of source. 82

List of Tables

3.1	Comparison between FEM and analytical solution for various δ / d	20
3.2	EMP type fields characteristics.	22
3.3	Realistic diffusion problems.	26
4.1	Calculating the maximum step size as a function of σ	43

Chapter 1

Introduction

Electromagnetic shielding of sensitive equipment is receiving a growing interest in the electromagnetic interference and compatibility (EMI/EMC) community as the density of electronic equipment in the working environment is continuously increasing. The effect of the overloaded environment is to reduce the reliability of devices improperly protected from potentially damaging ambient fields. To remedy this problem, federal agencies throughout the world have regulated the radiation levels of any electronic device to specified limits. In the United States, for example, the Federal Communication Commission (FCC) has listed these requirements in the “FCC Rules and Regulations” under the section “Part 15J” [40]. It is now required, by law, that the radiation levels of an equipment be lower than a specified level. Furthermore natural phenomena such as lightning and electrostatic discharges (ESD) are also very threatening to the performance of sensitive equipment as their associated rise and fall times generate wide frequency band electromagnetic waves. Along with these inherent passive EMI sources (passive in the sense of unprovoked) one more major catastrophic source to be included in the EMI shielding analysis is a possible high-altitude electromagnetic burst. The characteristic of these cataclysmic bursts lie in the fact that with a single nuclear war head explosion at a certain altitude in the atmosphere (typically around 400 km) the entire North-American continent could be

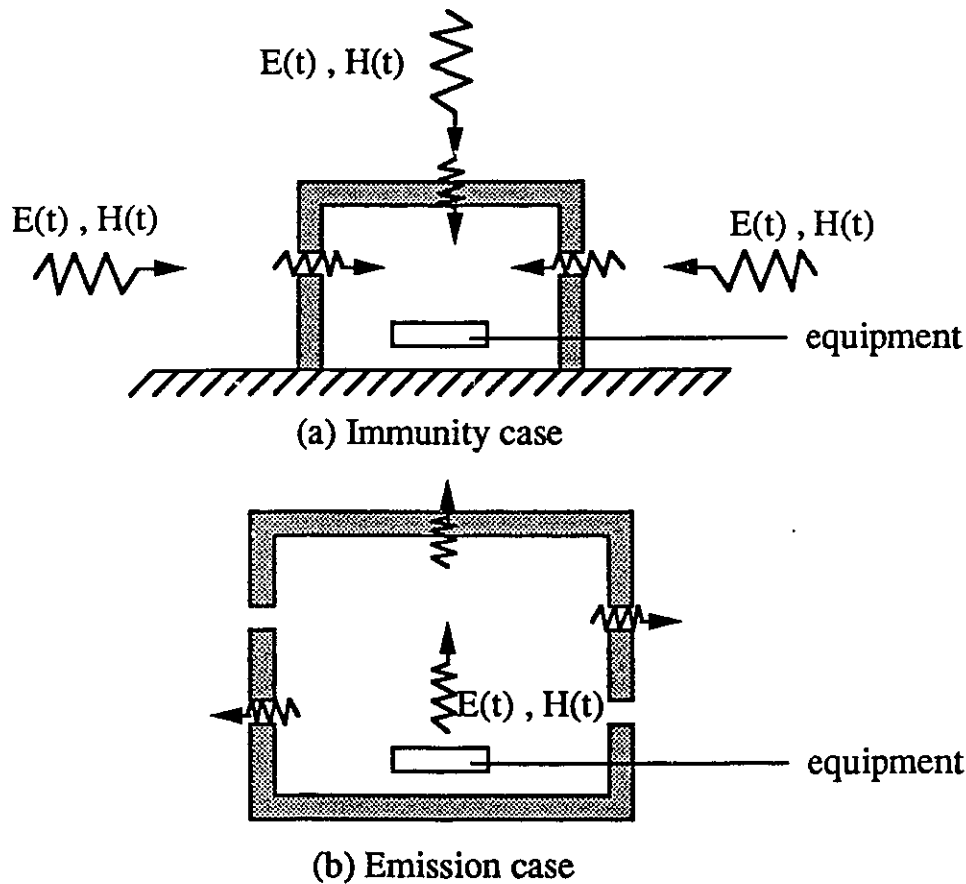


Figure 1.1: Problems to be analysed.

illuminated by this devastating high-altitude nuclear electromagnetic pulse (HNEMP) causing malfunction and even breakdown of improperly shielded sensitive electronic equipment.

The wide interest in assuring the reliability of equipment under normal to severe conditions has focused our attention on the need for an effective, inexpensive and easy to use tool intended to predict the shielding effectiveness of arbitrarily shaped enclosures. As it was implied above, there are two cases to study when referring to the shielding effectiveness of an enclosure. One type of study to include in the tool is the immunity analysis, in which the shield is intended to prevent ambient fields from perturbing the electronic device it contains (see figure 1.1 (a)). The other is the emission analysis, where the shield restrains energy, generated by the device, from affecting nearby equipment (see figure 1.1 (b)).

1.1 Goal

The object of this thesis is to bring forward a novel approach to predict the shielding effectiveness of enclosures. It consists of developing a computer aided design (CAD) tool via the numerical technique of finite element method (FEM). This particular numerical technique was chosen as it is one of the most flexible methods for solving problems as general as the ones presented here.

The CAD tool will have to be applicable to both the emission and the immunity problems as these are two very different situations. In the latter case, the impinging field will be assumed known at a certain distance from the enclosure; where as in the former, a current, flowing in a wire or on a microstrip's ground plane, will generate a magnetic field which will be assumed to be known very close to the conductor.

Furthermore, the tool shall perform the analysis in both the frequency and time domains. The added feature of a time domain analysis will reveal to be extremely important, especially in the study of EMP type fields such as lightning, ESD and NEMP and also in the study of the effect of digital signals on the radiated fields.

To achieve these objectives with assurance, we divide the task into four stages.

- Analytical solution of one-dimensional problem to validate the technique.
- Introduction of a second numerical technique.
- Comparison between two numerical techniques for more involved situations.
- Application of the CAD tool to complex problems.

In the first task, an analytical solution to a diffusion problem is derived for both the frequency and time domains. With the availability of this analytical formulation, the range of operation of the CAD tool is determined. To validate the prediction of the tool for a higher degree of complexity, a completely different numerical technique is introduced. The transmission-line matrix (TLM) method, the new technique, need also to be validated through the analytical problem to determine its operating range.

Once the confidence in solving one-dimensional diffusion problems is established, both techniques are applied to two-dimensional problems and the results are compared. The CAD tool, now validated, may be applied to complex situations that are more practical.

1.2 The Numerical Techniques

1.2.1 FEM

The method of finite elements originates from the variational method which may be traced back to the past century. This method was mainly applied, initially, by civil engineers to calculate structural stress and fluid dynamics. Although it was first attributed the name of "finite element method" by Clough in 1960 [1], it was extensively used in the late fifties.

The finite element method consists of characterizing the equations of a boundary-value problem through an appropriate functional which generally relates to the energy stored in the field (for electrical situations). Once this functional is determined, the region of interest is then discretized into finite elements in which the unknown field is approximated by suitable interpolation functions. Introducing these functions into the appropriate functional and taking the first variation with respect to the unknown, leads to a final system of equation that, in some cases, may be solved directly.

The finite element method (FEM) was first applied in electrical engineering in the middle of the 60's by Winslow [2] for the study of saturation effects in accelerator magnets. Since then, the application of the finite element method in electrical engineering has become a current topic, it is considered one of the fastest growing techniques in this field [43]. Its applications vary from eddy currents and skin effect problems [3], [4], [5] to the study of transformers [6] [7] , electrostatic [7], turbo-alternators [8], anisotropic magnetic problems [9] and much more. The flexibility of

this numerical technique is its driving force, the elements may be adapted to practically any boundary and interface geometry as they may be defined in various shapes and sizes.

1.2.2 TLM

The transmission-line matrix (TLM) method was first introduced by Johns and Beurle [33] in 1971. This method is a direct application of Huygen's principle of light [32] which explains a wavefront propagation as a combination of secondary wave sources on the wave front giving rise to a new front formed by the envelope of the secondary wavefronts. The TLM method consists of discretizing the region of interest into interconnecting transmission lines in which a travelling field would be scattered upon reaching a junction as there is impedance discontinuity. Thus each junction could then be seen as the secondary wave sources mentioned above.

The initial application of the TLM method was directed to the modeling of field propagation into a waveguide and the study of the scattered fields due to a waveguide discontinuity [33]. The method was then rapidly extended to analyse inhomogeneous [34] and lossy waveguides [10]. Then the interest was shifted to three-dimensional implementation of the technique [39], [11], [12]. Following this, some refinements on the two-dimensional formulation were brought forward such as non-uniform mesh [36], [13], and coarseness error elimination [14]. The applications of TLM have been reported in the analysis of fin lines [15], transients in transmission-lines [16], anisotropic media [17], dielectric loaded cavities [39], and many more. An excellent review paper on TLM, by Hoefler, can be found in [18]. The merits of TLM are also its flexibility and most definitely its versatility. The fact that the analysis is conducted in the time domain directly is also very interesting.

Chapter 2

One-Dimensional Test Enclosure

The evaluation of any type of measurement or prediction schemes is problematic; one has to be extremely careful when “conceiving” a test problem aimed at determining their proper range of operation. When evaluating a computer aided design (CAD) tool, an individual may choose among three options: either he/she compares the results from the tool with measurements, another tool, or an analytical solution. The latter option, in our opinion, is advantageous when available, as it yields more information in less time at a very low cost and particularly because the analytical (closed-form) results are absolutely accurate.

When predicting the field penetration into an enclosure, a limiting factor arises from the diffusion process. In particular, one would ask the following question, will the tool be able to follow the exponential decay of the field? If so, up to what point? A novel approach is presented here which predicts the shielding effectiveness of enclosures; it consists of the application of two numerical techniques, namely the finite element method (FEM) and the transmission line matrix (TLM) method. To validate these CAD tools, an analytical solution is derived for both the frequency and time domains.

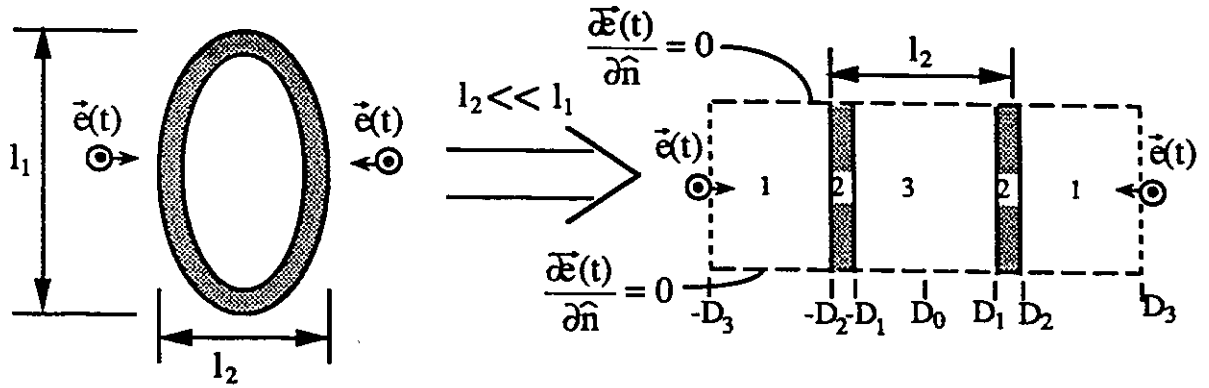


Figure 2.1: One-dimensional approximation.

2.1 Analytical Formulation

The analytical diffusion test problem may be regarded as a two-dimensional enclosure that extends much more in one direction than in the other thus making a one-dimensional analysis possible, see figure 2.1. The field is assumed to impinge on both sides of the enclosure and to be of equal magnitude and phase.

The full equation describing the field propagation through air and conducting materials is obtained directly from Maxwell's equations and given as

$$\frac{\partial^2}{\partial x^2} \vec{e}(x, t) - \mu\sigma \frac{\partial}{\partial t} \vec{e}(x, t) - \mu\epsilon \frac{\partial^2}{\partial t^2} \vec{e}(x, t) = 0 \quad (2.1)$$

for the one-dimensional problems. Now taking the Laplace transform of equation (2.1) leads to

$$\begin{aligned} \frac{\partial^2}{\partial x^2} \vec{E}(x, s) - s\mu\sigma \vec{E}(x, s) + \mu\sigma \vec{e}(x, t = 0^-) - \\ s^2 \mu\epsilon \vec{E}(x, s) + s\mu\epsilon \vec{e}(x, t = 0^-) + \mu\epsilon \frac{\partial}{\partial t} \vec{e}(x, t = 0^-) = 0 \end{aligned} \quad (2.2)$$

but as the impinging field is initially zero, thus equation (2.2) becomes of the following form

$$\frac{\partial^2}{\partial x^2} \vec{E}(x, s) - s\mu\sigma \vec{E}(x, s) - s^2 \mu\epsilon \vec{E}(x, s) = 0 \quad (2.3)$$

where μ , ϵ and σ are respectively the permeability, permittivity and conductivity of the region.

2.1.1 Frequency Domain

The wave equation in the frequency domain is written as (from equation (2.3))

$$\frac{\partial^2}{\partial x^2} \vec{E}(x) + (\omega^2 \mu \epsilon - j\omega \mu \sigma) \vec{E}(x) = 0 \quad (2.4)$$

in which ω is a frequency variable. Referring to figure 2.1, the equation to be solved in region 1 and 3 (in air) is

$$\frac{\partial^2}{\partial x^2} \vec{E}_{1/3}(x) + \omega^2 \mu_0 \epsilon_0 \vec{E}_{1/3}(x) = 0 \quad (2.5)$$

and in region 2 (in the conducting walls)

$$\frac{\partial^2}{\partial x^2} \vec{E}_2(x) - j\omega \mu \sigma \vec{E}_2(x) = 0 \quad (2.6)$$

where in the conducting walls the displacement current term ($\omega^2 \mu \epsilon \vec{E}(x)$) may be neglected. From equations (2.5) and (2.6), the general solution for the three different regions is given in the following

$$\vec{E}_1(x) = \hat{z}(Ae^{jK_1x} + Be^{-jK_1x}) \quad (2.7)$$

$$\vec{E}_2(x) = \hat{z}(Ce^{jK_2x} + De^{-jK_2x}) \quad (2.8)$$

$$\vec{E}_3(x) = \hat{z}F \cosh(K_1x) \quad (2.9)$$

where $K_1 = \sqrt{\omega^2 \mu_0 \epsilon_0}$ and $K_2 = \sqrt{-j\omega \mu \sigma}$. The constants A through F are derived by imposing the boundary conditions on equations (2.7)-(2.9).

Boundary conditions:

1. $\vec{E}_1(\pm D_3) = \hat{z}E_0$
2. $\frac{\partial}{\partial x} \vec{E}_3(D_0) = 0$
3. Matching the electric and magnetic field at the interfaces,
i.e. at $x = \pm D_1$ and $x = \pm D_2$.

Applying these boundary conditions, for positive x , to equations (2.7), (2.8) and (2.9) leads to the following global system of equations

$$\begin{pmatrix}
e^{jK_1 D_3} & e^{-jK_1 D_3} & 0 & 0 & 0 \\
e^{jK_1 D_2} & e^{-jK_1 D_2} & -e^{jK_2 D_2} & -e^{-jK_2 D_2} & 0 \\
k_1 e^{jK_1 D_2} & -K_1 e^{-jK_1 D_2} & -\frac{K_2}{\mu_r} e^{jK_2 D_2} & \frac{K_2}{\mu_r} e^{-jK_2 D_2} & 0 \\
0 & 0 & e^{jK_2 D_1} & e^{-jK_2 D_1} & \cosh(K_1 D_1) \\
0 & 0 & -\frac{jK_2}{\mu_r} e^{jK_2 D_1} & \frac{jK_2}{\mu_r} e^{-jK_2 D_1} & K_1 \sinh(K_1 D_1)
\end{pmatrix} \times
\begin{pmatrix}
A \\
B \\
C \\
D \\
F
\end{pmatrix} = \begin{pmatrix}
E_0 \\
0 \\
0 \\
0 \\
0
\end{pmatrix}. \quad (2.10)$$

This system of equation may be solved analytically or via a matrix reduction technique once the parameters are known.

2.1.2 Time Domain

To obtain the time domain analytical solution, the formulation is first conducted in Laplacian domain and transformed, in the last stage of analysis, back to the time domain via Heaviside's formulation [19]. To decrease the complexity of the problem, the impinging field will be assumed known on the outside wall of the enclosure, at $\pm D_2$ (see figure 2.1). The time signature of the incident field is modeled as

$$\vec{e}(t) = \hat{z} E_0 \{e^{-\alpha t} - e^{-\beta t}\} \quad (2.11)$$

which may represent a nuclear electromagnetic pulse (NEMP), an electrostatic discharge (ESD) or lightning [20]. The mathematical model describing the wave propagation through air and conducting materials in the Laplace domain is given in (2.3). Thus, neglecting the displacement current in the conducting material, the equation to be solved in region 2 becomes

$$\frac{\partial^2}{\partial x^2} \vec{E}_2(x, s) - s\mu\sigma \vec{E}_2(x, s) = 0 \quad (2.12)$$

and in region 3 (in the air)

$$\frac{\partial^2}{\partial x^2} \vec{E}_3(x, s) - s^2 \mu_0 \epsilon_0 \vec{E}_3(x, s) = 0 \quad (2.13)$$

where s is the Laplace variable. The general solution in each region is given as

$$\vec{E}_2(x, s) = \hat{z}[A \cos(\sqrt{-s\mu\sigma} x) + B \sin(\sqrt{-s\mu\sigma} x)] \quad (2.14)$$

$$\vec{E}_3(x, s) = \hat{z}C \cosh(\sqrt{s^2 \mu_0 \epsilon_0} x) \quad (2.15)$$

where A , B and C are constants to be determined. To obtain these constants we need to impose the boundary conditions on equations (2.14) and (2.15).

Boundary conditions:

1. $\vec{E}_2(\pm D_2, s) = \mathcal{L}\{\hat{z}E_0(e^{-\alpha t} - e^{-\beta t})\} = \hat{z} \frac{E_0(\beta - \alpha)}{(s + \alpha)(s + \beta)} = \hat{z}L(s)$
2. $\frac{\partial}{\partial x} \vec{E}_3(D_0, s) = 0$
3. $\vec{E}_2(\pm D_1, s) = \vec{E}_3(\pm D_1, s)$
4. $\vec{H}_2(\pm D_1, s) = \vec{H}_3(\pm D_1, s)$.

Applying the boundary conditions 1-4, for positive x , to equations (2.14) and (2.15), the constants A , B and C may be derived by solving the following global system of equations:

$$\begin{pmatrix} \cos \theta & \sin \theta & 0 \\ \cos \gamma & \sin \gamma & -\cosh \phi \\ \sin \gamma & -\cos \gamma & \delta \sinh \phi \end{pmatrix} \begin{pmatrix} A \\ B \\ C \end{pmatrix} = \begin{pmatrix} L(s) \\ 0 \\ 0 \end{pmatrix} \quad (2.16)$$

where

$$\delta = \left(\eta_0 \sqrt{\frac{\sigma}{-s\mu}} \right)^{-1}; \quad \theta = \sqrt{-s\mu\sigma} D_2; \quad \gamma = \sqrt{-s\mu\sigma} D_1; \quad \phi = \sqrt{s^2 \mu_0 \epsilon_0} D_1$$

and

$$\eta_0 = \sqrt{\frac{\epsilon_0}{\mu_0}}$$

Solving (2.16) for A , B , and C leads to:

$$A = L(s)(\cosh \phi \cos \gamma - \delta \sinh \phi \sin \gamma)/R(s) \quad (2.17)$$

$$B = L(s)(\cosh \phi \sin \gamma + \delta \sinh \phi \cos \gamma)/R(s) \quad (2.18)$$

$$C = L(s)/R(s) \quad (2.19)$$

where $R(s)$ is the determinant of the 3x3 matrix in (2.16), given as :

$$R(s) = [\cosh \phi \cos(\gamma - \theta) - \delta \sinh \phi \sin(\gamma - \theta)]$$

and

$$L(s) = \mathcal{L}\{E_0(e^{-\alpha t} - e^{-\beta t})\} = \frac{E_0(\beta - \alpha)}{(s + \alpha)(s + \beta)}.$$

To obtain the time domain counterpart of equations (2.14) and (2.15) one may use Heaviside's formulation as stated below, if

$$G(s) = \frac{P(s)}{Q(s)} \quad (2.20)$$

then

$$g(t) = \sum_{k=1}^{\infty} \frac{P(s_k)}{\dot{Q}(s_k)} e^{s_k t} \quad (2.21)$$

where s_k are the poles of $Q(s)$ and \dot{Q} is the derivative of Q with respect to the variable s . As the derivation of $\vec{e}(t)$, the time domain electric field, is quite involved, it will not be written here (the reader is referred to Appendix A for more details).

Chapter 3

Finite Element Method

3.1 Introduction

The finite element method is a numerical technique based on the variational method [21]. It consists of describing the mathematical model (i.e. the equation defining the particular situation), along with the boundary conditions, with an appropriate functional

$$\mathcal{F}(\phi) = \int_{\Omega} L\phi d\Omega \quad (3.1)$$

where ϕ is the unknown quantity, L , the operator and Ω is the region of interest. The functional, which frequently coincides with the energy stored in the field for electrical problems, as given in (3.1), is an integral equation which will be made stationary by taking its first variation with respect to the unknown

$$\frac{\partial \mathcal{F}(\phi)}{\partial \phi} = 0 \quad (3.2)$$

thus yielding the solution to the unknown ϕ (approximated by an interpolation function in the region Ω). Now to better approximate the field variations, the region is divided into subregions, such as triangles, of various shapes and sizes as shown in figure 3.1. In each of these subregions Ω_i , the unknown quantity is represented by suitable interpolation functions. Thus the functional becomes a summation over the

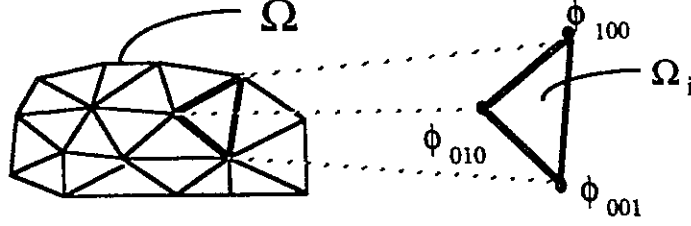


Figure 3.1: Finite element subregions.

total number of subregions of the integrals

$$\mathcal{F}(\phi) = \sum_{i=1}^{NSUB} \int_{\Omega_i} L \hat{\phi} d\Omega_i \quad (3.3)$$

where NSUB is the total number of subregions and

$$\hat{\phi} = \underline{\phi}_j \zeta(x, y)$$

in which $\underline{\phi}_j$ is the unknown nodal vector [$\underline{\phi}_j = (\phi_{100} \phi_{010} \phi_{001})$] of the corresponding subregion and $\zeta(x, y)$, the interpolation function. Equation (3.2) is then satisfied by taking the first variation of (3.3) with respect to all unknown nodal field quantities ($\phi_1, \phi_2, \dots, \phi_m$) which in turn produces a system of equations

$$S \underline{\phi} = \underline{b} \quad (3.4)$$

which when linear may be solved via a matrix reduction technique.

3.2 Mathematical Formulation

The idea behind the finite element method is to find an energy related functional describing the particular situation and make it stationary by taking its first variation with respect to the unknown. The functional associated with the problem of interest is determined by both the mathematical model (i.e. the equation describing the field propagation through conducting material and air), as given in the following

$$\nabla^2 \vec{g}(t) - \mu\sigma \frac{\partial}{\partial t} \vec{g}(t) - \mu\epsilon \frac{\partial^2}{\partial t^2} \vec{g}(t) = 0 \quad (3.5)$$

and the boundary conditions such as inhomogeneous Neumann boundaries. In equation (3.5), $\vec{g}(t)$ represents either the electric or the magnetic field, or even the magnetic vector potential which will be derived later in section 5.3. Equation (3.5) may be rewritten in a more general form as

$$\nabla^2 \vec{g}(t) - k\vec{g}(t) = 0 \quad (3.6)$$

in which k is a time differentiation operator ($k \equiv \mu\sigma \frac{\partial}{\partial t} + \mu\epsilon \frac{\partial^2}{\partial t^2}$).

The functional associated with the mathematical model given in (3.6), is [22]

$$\mathcal{F}(\vec{g}(t)) = \int_{\Omega} \vec{g}(t) \cdot \nabla^2 \vec{g}(t) d\Omega - k \int_{\Omega} \vec{g}(t) \cdot \vec{g}(t) d\Omega \quad (3.7)$$

where the integrals cover the total region of interest, Ω . To include Neumann boundary conditions, the first integral in the functional may be modified by Green's first formula [23]

$$\int_{\Omega} [\vec{f} \cdot \nabla^2 \vec{h} + \nabla \vec{f} \cdot \nabla \vec{h}] d\Omega = \int_S \vec{f} \cdot \frac{\partial \vec{h}}{\partial \hat{n}} dS \quad (3.8)$$

where the right hand side integral is performed on the surface of the region with the normal pointing outward. The use of Green's identity will also reduce the Laplacian operator, ∇^2 (a second order derivative), to a vector product of two gradients, first order derivatives, making the analysis more stable. Equation (3.7) then becomes

$$\mathcal{F}(\vec{g}(t)) = - \int_{\Omega} \nabla \vec{g}(t) \cdot \nabla \vec{g}(t) d\Omega - k \int_{\Omega} \vec{g}(t) \cdot \vec{g}(t) d\Omega + 2 \int_S \vec{g}(t) \cdot \frac{\partial \vec{g}(t)}{\partial \hat{n}} dS. \quad (3.9)$$

Now to verify that (3.9) is an appropriate functional associated to equation (3.6), let's take the first variation of the functional with respect to the unknown, $\vec{g}(t)$, and set it equal to zero as it is a sufficient condition for the solution to be stationary [24].

$$\Delta \mathcal{F}(\vec{g}(t)) = 0. \quad (3.10)$$

The first variation of (3.9) is

$$\begin{aligned} \Delta \mathcal{F}(\vec{g}(t)) = & - \int_{\Omega} 2 \nabla \vec{g}(t) \cdot \Delta(\nabla \vec{g}(t)) d\Omega - k \int_{\Omega} 2 \vec{g}(t) \cdot \Delta \vec{g}(t) d\Omega + \\ & 2 \int_S \left[\Delta \vec{g}(t) \cdot \frac{\partial \vec{g}(t)}{\partial \hat{n}} + \vec{g}(t) \cdot \Delta \left(\frac{\partial \vec{g}(t)}{\partial \hat{n}} \right) \right] dS. \end{aligned} \quad (3.11)$$

Making use of Green's identity once more along with the knowledge that both operators, Δ and ∇ , are interchangeable, the first integral in the previous equation is modified to

$$-2 \int_{\Omega} \nabla \vec{g}(t) \cdot \nabla(\Delta \vec{g}(t)) d\Omega = 2 \int_{\Omega} \nabla^2 \vec{g}(t) \cdot \Delta \vec{g}(t) d\Omega - 2 \int_S \Delta \vec{g}(t) \cdot \frac{\partial \vec{g}(t)}{\partial \hat{n}} dS \quad (3.12)$$

thus (3.11) may be written as

$$\begin{aligned} \Delta \mathcal{F}(\vec{g}(t)) &= 2 \int_{\Omega} \nabla^2 \vec{g}(t) \cdot \Delta \vec{g}(t) d\Omega - 2 \int_S \Delta \vec{g}(t) \cdot \frac{\partial \vec{g}(t)}{\partial \hat{n}} dS - k \int_{\Omega} 2\vec{g}(t) \cdot \Delta \vec{g}(t) d\Omega + \\ & 2 \int_S \Delta \vec{g}(t) \cdot \frac{\partial \vec{g}(t)}{\partial \hat{n}} dS + 2 \int_S \vec{g}(t) \cdot \Delta \left(\frac{\partial \vec{g}(t)}{\partial \hat{n}} \right) dS. \end{aligned} \quad (3.13)$$

The last surface integral in (3.13) reduces to zero as, in the problems solved here, the Neumann boundary conditions are dependent on an external source and not on the unknown, $\vec{g}(t)$

$$\Delta \left(\frac{\partial \vec{g}(t)}{\partial \hat{n}} \right) = 0. \quad (3.14)$$

Then the first variation of the functional with respect to the unknown, $\vec{g}(t)$, is

$$\Delta \mathcal{F}(\vec{g}(t)) = 2 \int_{\Omega} [\nabla^2 \vec{g}(t) \cdot \Delta \vec{g}(t) - k\vec{g}(t) \cdot \Delta \vec{g}(t)] d\Omega. \quad (3.15)$$

But since the vector product is distributive the following is obtained

$$\Delta \mathcal{F}(\vec{g}(t)) = 2 \int_{\Omega} [\nabla^2 \vec{g}(t) - k\vec{g}(t)] \cdot \Delta \vec{g}(t) d\Omega. \quad (3.16)$$

Returning to the necessary condition given in (3.10), we must then have

$$\nabla^2 \vec{g}(t) - k\vec{g}(t) = 0 \quad (3.17)$$

which is the original mathematical model describing the field propagation through a medium. We therefore see that the functional in (3.9) is appropriate for this type of problem.

Having determined the functional to be made stationary throughout the region of interest, the region is then subdivided into finite elements, such as triangles, making

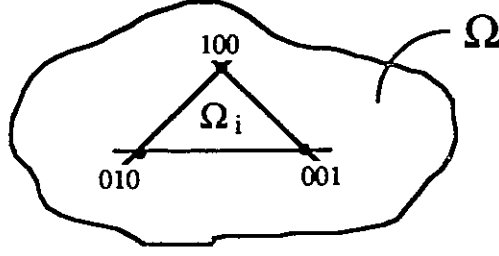


Figure 3.2: Basic triangular element.

it easier to follow the field variations. The field in each subregion is then approximated by n^{th} order polynomials. The derivation of the two-dimensional first order polynomial is given in (3.18) to (3.21). As the extension to higher orders is fairly straightforward when using simplex coordinates [25], it will not be shown here.

A first order polynomial approximating a field oriented in the \hat{z} direction may be given as

$$\vec{g}(t) = (a(t)x + b(t)y + c(t))\hat{z} \quad (3.18)$$

where a , b and c are unknowns and (x,y) are the physical positions of the field. Now when approximating the field by equation (3.18), the solution to the problem would be determined in terms of the unknowns a , b and c of each subregions. But since the solution of these unknowns is insufficient by itself (a substitution is needed to calculate the field), it is in our interest to represent a , b and c as a function of the node potentials (at each vertex of a triangle), and then solve directly for the field at each node.

The field potential at each vertex of a triangle, g_{100} , g_{010} and g_{001} , may be related to the unknowns a , b and c of the same triangle (figure 3.2) by the following system of equations

$$\begin{pmatrix} g_{100}(t) & g_{010}(t) & g_{001}(t) \end{pmatrix} = \begin{pmatrix} a(t) & b(t) & c(t) \end{pmatrix} \begin{pmatrix} x_{100} & x_{010} & x_{001} \\ y_{100} & y_{010} & y_{001} \\ 1 & 1 & 1 \end{pmatrix}. \quad (3.19)$$

The unknowns a , b and c may then be represented by the node potentials g_{100} , g_{010}

and g_{001} as

$$\begin{pmatrix} a(t) & b(t) & c(t) \end{pmatrix} = \begin{pmatrix} g_{100}(t) & g_{010}(t) & g_{001}(t) \end{pmatrix} \begin{pmatrix} x_{100} & x_{010} & x_{001} \\ y_{100} & y_{010} & y_{001} \\ 1 & 1 & 1 \end{pmatrix}^{-1} \quad (3.20)$$

Then equation (3.18) becomes

$$\vec{g}(t) = \begin{pmatrix} a(t) & b(t) & c(t) \end{pmatrix} \begin{pmatrix} x \\ y \\ 1 \end{pmatrix} \hat{z} = \underline{g}(t) \underline{\zeta}(x, y) \hat{z} \quad (3.21)$$

where $\underline{g}(t)$ is a 1x3 row vector with the node potentials as its elements and $\underline{\zeta}(x, y)$ is a 3x1 column vector given as follow

$$\underline{\zeta}(x, y) = \begin{pmatrix} x_{100} & x_{010} & x_{001} \\ y_{100} & y_{010} & y_{001} \\ 1 & 1 & 1 \end{pmatrix}^{-1} \begin{pmatrix} x \\ y \\ 1 \end{pmatrix} \quad (3.22)$$

in which -1 is the symbol for the inverse and T for the transpose and (x_{---}, y_{---}) are the physical position of the triangle vertices.

Introducing the shape functions of equation (3.21) into the functional and taking its first variation with respect to the node potential yields a system of equations since the functional must be satisfied *simultaneously* in each subregion. The overall functional then becomes the summation of each subregion integrals

$$\begin{aligned} \mathcal{F}(\vec{g}(t)) = & \sum_{i=1}^{NSUB} \left[- \int_{\Omega_i} \{ \nabla(\underline{g}(t) \underline{\zeta}(x, y) \hat{z}) \cdot \nabla(\underline{g}(t) \underline{\zeta}(x, y) \hat{z}) \} d\Omega_i - \right. \\ & \left. k_i \int_{\Omega_i} \{ (\underline{g}(t) \underline{\zeta}(x, y) \hat{z}) \cdot (\underline{g}(t) \underline{\zeta}(x, y) \hat{z}) \} d\Omega_i \right] + \\ & \sum_{l=1}^{NS} \left[2 \int_{S_l} \left\{ \underline{g}(t) \underline{\zeta}(x, y) \hat{z} \cdot \frac{\partial(\underline{g}(t) \underline{\zeta}(x, y) \hat{z})}{\partial \hat{n}} \right\} dS_l \right] \end{aligned} \quad (3.23)$$

where $NSUB$ is the total number of subregions, NS is the number of Neumann boundaries and k_i is given as $k_i \equiv \mu_i \sigma_i \frac{\partial}{\partial t} + \mu_i \epsilon_i \frac{\partial^2}{\partial t^2}$. Now to solve (3.21), the first

variation with respect to the node potentials is set to zero which produces the following system of equations

$$(S + T + U)\underline{g} = 0 \quad (3.24)$$

where the elements of matrices S , T and U are given as

$$\begin{aligned} S_{mn} &= -\frac{\partial}{\partial g_m} \left\{ \sum_{i=1}^{NSUB} \int_{\Omega_i} [\nabla(\underline{g}(t)\underline{\zeta}(x, y))]^2 d\Omega_i \right\} \\ T_{mn} &= -\frac{\partial}{\partial g_m} \left\{ \sum_{i=1}^{NSUB} k_i \int_{\Omega_i} (\underline{g}(t)\underline{\zeta}(x, y))^2 d\Omega_i \right\} \\ U_{mn} &= \frac{\partial}{\partial g_m} \left\{ \sum_{l=1}^{NS} 2 \int_{S_l} \left[\underline{g}(t)\underline{\zeta}(x, y)\hat{z} \cdot \frac{\partial(\underline{g}(t)\underline{\zeta}(x, y)\hat{z})}{\partial \hat{n}} \right] dS_l \right\} \end{aligned}$$

where m varies from one to the total number of unknowns, n is related to the unknown node potentials inside the integrals and \underline{g} is a column vector including all the node potentials at time t .

3.3 Frequency Domain

The frequency domain is a good starting position to evaluate a numerical technique for a diffusion problem. The major limiting factor is due to the field's attenuation as it propagates into a conducting material. The rate at which the field decays is dictated by the conductivity and permeability of the material as well as the wavelength components of the field in relation to the thickness of the shield's wall. To have a better understanding of their influence, they (with the exception of the wall thickness) have been incorporated into a single parameter, the skin depth δ

$$\delta = \sqrt{\frac{2}{\omega\mu\sigma}} \quad (3.25)$$

where $\omega = 2\pi f$. The skin depth defined as in (3.25) is the required thickness of a material with parameters μ & σ , to attenuate an incident field, at frequency f , by a factor of $e^{-1} \simeq 0.368$ [26].

3.3.1 Solving the System of Equations

For the frequency domain analysis, the Fourier transform needs to be performed on all time dependent variables defined in section 3.2. Therefore, the final system of equations to be solved becomes the following

$$(Q + R)\underline{G} = 0 \quad (3.26)$$

where the matrix Q is the Fourier transform of the summation of S and T matrices (see equation (3.24)), given as

$$Q_{mn} = -\frac{\partial}{\partial G_m} \left\{ \sum_{i=1}^{NSUB} \left[\int_{\Omega_i} [\nabla(\underline{G}\zeta(x, y))]^2 d\Omega_i + K_i \int_{\Omega_i} [\underline{G}\zeta(x, y)]^2 d\Omega_i \right] \right\}$$

and R is the transform of matrix U in (3.24),

$$R_{mn} = \frac{\partial}{\partial G_m} \left\{ \sum_{i=1}^{NS} 2 \int_{S_i} \underline{G}\zeta(x, y) \hat{z} \cdot \frac{\partial(\underline{G}\zeta(x, y) \hat{z})}{\partial \hat{n}} dS_i \right\}$$

in which G defines the Fourier transform of g and the variable K_i is the transform of k_i , given as

$$K_i = \mathcal{F} \left\{ \mu_i \epsilon_i \frac{\partial^2}{\partial t^2} + \mu_i \sigma_i \frac{\partial}{\partial t} \right\} = -\omega^2 \mu_i \epsilon_i + j\omega \mu_i \sigma_i \quad (3.27)$$

in which j denotes the imaginary part of a complex variable. As the final system of equations is linear, it may be directly solved by a matrix reduction technique such as the Gaussian elimination [27].

3.3.2 Realistic Frequency Diffusion Problems and Validation

In the FEM, the field variations are approximated by shape functions in each discrete subregion. As the skin depth increases, it becomes harder for the shape functions associated with the subregions to follow the field variation. Therefore, to make the task possible and easier, one may increase the order of the polynomials used in the shape functions and/or decrease the area of the subregions. Considering the computer

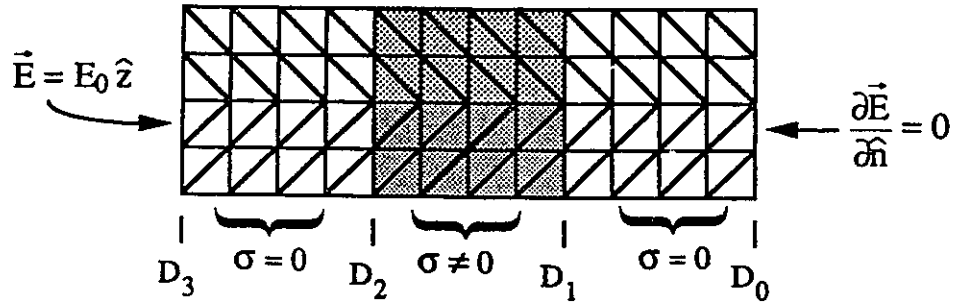


Figure 3.3: Division into FEs for frequency domain.

Table 3.1: Comparison between FEM and analytical solution for various δ / d .

δ / d (%)	Attenuation $\frac{E(D_2)}{E(D_0)}$ (dB)	Analytical		FEM		
		$E(D_2)$	$E(D_0)$	$E(D_2)$	$E(D_0)$	order of polynomials
39	1.63E01	3.470	0.527E+00	3.470	0.535E+00	1 st
21	3.48E01	1.890	0.343E-01	1.890	0.361E-01	1 st
15	5.18E01	1.340	0.346E-02	1.340	0.411E-02	1 st
11	7.57E01	0.945	0.156E-03	0.945	0.155E-03	3 rd
8	1.03E02	0.707	0.493E-05	0.707	0.371E-05	3 rd
6.5	1.28E02	0.577	0.239E-06	0.577	0.805E-06	3 rd
5.6	1.48E02	0.500	0.191E-07	0.500	0.693E-06	3 rd
5.3	1.66E02	0.447	0.210E-08	0.447	0.412E-06	3 rd

limitations, diffusion problems can be solved practically for a certain range of skin depth, δ , and wall thickness, d . It isn't independently the skin depth nor the wall thickness that determines this range but the relation between the two. To have an idea of the limits that the FEM poses to the solution of diffusion problems, the numerical technique is applied to calculate the field penetration through a wall, for various thickness and constitutive parameters, and the results are compared with the analytical solution derived in section 2.1.1.

The results of this analysis are shown in Table 3.1, where the leftmost column refers to the percentage of the skin depth in relation to the wall thickness. The

solution by FEM was set up with first order polynomials and four divisions in the wall for δ/d down to 15% and, for lower percentage, with third order polynomials with the same number of divisions (see figure 3.3 for the finite element division). As seen from Table 3.1, the FEM can be used practically (with the available computer memory limits), in relatively large regions, for skin depth as low as seven percent of the wall thickness. Obviously, for one-dimensional problems the FEM could be used for much lower δ/d percentage as the computer memory limits present no longer a problem.

3.4 Time Domain

The time domain analysis concentrates on the diffusion process of electromagnetic pulse (EMP) types impinging plane waves. EMP type fields are defined here as time varying fields that can be modeled as a double exponential of the following general form

$$e(t) = E_0\{e^{-\alpha t} - e^{-\beta t}\} \quad (3.28)$$

Three different sources of EMP type fields are analysed throughout this chapter, namely lightning, ESD and NEMP. Although the emphasis is on NEMP generated fields, the added analysis of lightning and ESD sources will facilitate the understanding of the implications that NEMP type fields have on the shielding performances of enclosures. Table 3.2 gives the characteristics of the three EMP type fields to be analysed [28] and shown in figure 3.4 are their time signatures.

3.4.1 Solving the System of Equations

The method of solution in the time domain is a combination of two numerical techniques, namely the FEM and a time integration or differentiation method.

The final system of equations, (3.24), may be rewritten in a more practical manner

$$V\underline{g} + W\frac{\partial}{\partial t}\underline{g} + Z\frac{\partial^2}{\partial t^2}\underline{g} = 0 \quad (3.29)$$

Table 3.2: EMP type fields characteristics.

Type of EMP field	E_0 (V/m)	α (s^{-1})	β (s^{-1})
Lightning	E_0	10^4	0.5×10^6
ESD	E_0	1.6×10^6	10^9
NEMP	5.25×10^4	4×10^6	4.76×10^8

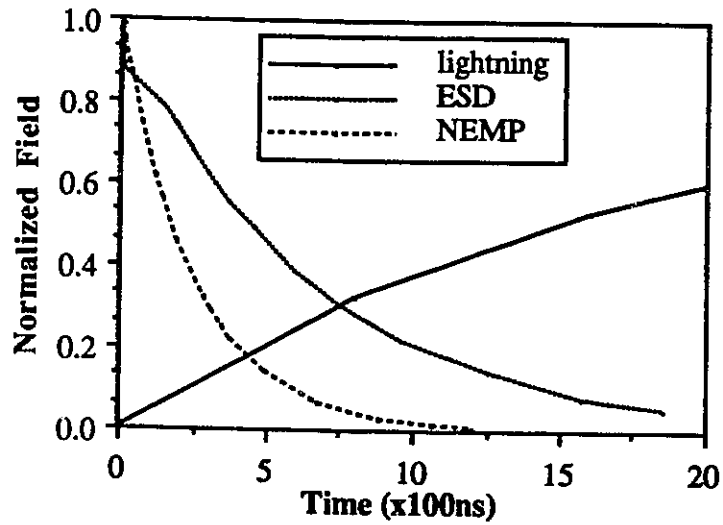


Figure 3.4: Time signatures of the EMP type fields.

with matrix V , being the summation of S and U matrices in (3.24),

$$V_{mn} = -\frac{\partial}{\partial g_m} \left\{ \sum_{i=1}^{NSUB} \int_{\Omega_i} [\nabla(\underline{g}(t)\underline{\zeta}(x, y))]^2 d\Omega_i - \sum_{l=1}^{NS} 2 \int_{S_l} \left[\underline{g}(t)\underline{\zeta}(x, y)\hat{z} \cdot \frac{\partial(\underline{g}(t)\underline{\zeta}(x, y)\hat{z})}{\partial \hat{n}} \right] dS_l \right\}$$

and matrices W and Z are obtained directly from the T matrix by parting k_i ,

$$W_{mn} = -\frac{\partial}{\partial g_m} \left\{ \sum_{i=1}^{NSUB} \mu_i \sigma_i \int_{\Omega_i} [\underline{g}(t)\underline{\zeta}(x, y)]^2 d\Omega_i \right\}$$

$$Z_{mn} = -\frac{\partial}{\partial g_m} \left\{ \sum_{i=1}^{NSUB} \mu_i \epsilon_i \int_{\Omega_i} [\underline{g}(t)\underline{\zeta}(x, y)]^2 d\Omega_i \right\}.$$

Now the effect of the displacement current (the term related to $\mu\epsilon\frac{\partial^2}{\partial t^2}$ in equation (3.29)) could be neglected for fields varying relatively slowly with time (fields with frequency components lower than about 10 GHz). But as most, possibly all, numerical integration techniques available in software packages require that the ordinary differential equations (ODE) have the following format

$$\dot{y} = f(t, y)$$

$$y(t_0) = y_0 \tag{3.30}$$

one would need to find the inverse of the matrix W which is singular, as in some regions $\sigma = 0$. Thus this formulation of an ODE, for the situation of interest, is unattainable when neglecting the displacement current term. To overcome this, one might instinctively reduce equation (3.29) to a differential equation of the first order by setting the first derivative with respect to time of \underline{g} to a vector \underline{f}

$$\underline{f} = \dot{\underline{g}} \tag{3.31}$$

and transform equation (3.29) into

$$Z\underline{\dot{f}} = -W\underline{f} - V\underline{g}. \tag{3.32}$$

Now as the matrix Z is a non-singular matrix, this leads to the following system of equations

$$\begin{bmatrix} \dot{\underline{g}} \\ \dot{\underline{f}} \end{bmatrix} = \begin{bmatrix} 0 & I \\ -Z^{-1}V & -Z^{-1}W \end{bmatrix} \begin{bmatrix} \underline{g} \\ \underline{f} \end{bmatrix} \quad (3.33)$$

where I is a unit matrix and Z^{-1} is the inverse of Z .

At the first glance, it might seem that the system of equations presented in (3.33) is now ready to be solved by an available ODE solver such as DVERK (found in IMSL Fortran package [29]). However, it turns out that (3.29) is a highly unstable system of equations, it is ill-posed as the elements of the matrix Z are orders of magnitude lower than those of matrices V and W . In order to solve the ODE in (3.33), one would need ridiculously small time steps, and even so, the system would still be very unstable. Thus the solution of (3.29) in a practical time frame requires that the displacement current term be neglected. Since the matrix W is singular, an ODE is out of the question, and the system to be solved becomes a differential/algebraic equation(DAE) system described as [30]

$$\begin{aligned} f(t, y, \dot{y}) &= 0 \\ y(t_0) &= y_0 \\ \dot{y}(t_0) &= \dot{y}_0. \end{aligned} \quad (3.34)$$

After an extensive search, the author came across a program called DDASSL developed by Linda R. Petzold, from Sandia National Laboratories [31]. This program is a DAE solver based on backward differentiation formulas which solves equation (3.34) directly by replacing the derivative with a difference approximation, and then solve the resulting equation using Newton's method at the current time t_n . DDASSL approximates the derivative via k^{th} order backward differentiation formula, where k ranges from one to five. For example, replacing the derivative by the backward difference in (3.34), the first order formula can be written as

$$F\left(t_n, y_n, \frac{y_n - y_{n-1}}{\Delta t_n}\right) = 0. \quad (3.35)$$

Then using Newton's method, the equation is solved at t_n for y_n as

$$y_n^{m+1} = y_n^m - \left(\frac{\partial F}{\partial y} + \frac{1}{\Delta t_n} \frac{\partial F}{\partial y} \right)^{-1} F \left(t_n, y_n^m, \frac{y_n^m - y_{n-1}^m}{\Delta t_n} \right) \quad (3.36)$$

where m is the iteration index. As will be seen in section 3.4.3, the method used in DDASSL is very well suited to the type of problems considered herein.

3.4.2 Realistic Time Diffusion Problems

In the time domain investigation, we are confronted with two possible limitations. One is related to the rise and fall times of the incident field; the faster the rise or fall time, the smaller the time steps in the differentiation technique needs to be. As in EMP type fields there is a combination of a fast rise time compared to a much lower fall time, the technique must then have variable time steps to be effective, which is the case for the program DDASSL. The second limitation is again related to the steepness of the rise and fall time but is due to the approximation of the field by the polynomials in the FEM. The steeper they get, the higher the field frequency components will reach. We are then limited by the skin depth related to the higher frequencies and the wall thickness.

The effect of the skin depth and wall thickness was demonstrated in section 3.3.2. Now to apply this information to the time-domain problem of interest, the EMP type fields first need to be transformed in the frequency domain

$$\underline{E}(\omega) = \mathcal{F}\{E_0[e^{-\alpha t} - e^{-\beta t}]\} \quad (3.37)$$

given in (3.38) as the magnitude normalized to E_0 .

$$\frac{|\underline{E}(\omega)|}{E_0} = \frac{\beta - \alpha}{\sqrt{\omega^4 + \omega^2(\alpha^2 + \beta^2) + \alpha^2\beta^2}}. \quad (3.38)$$

To properly characterize the field penetration, the subregions within the walls should be defined in a way to follow the field variations up to the frequency for which

$$|E(2\pi f_{max})| \leq 0.02 \times |E(0Hz)|. \quad (3.39)$$

Table 3.3: Realistic diffusion problems.

Type of EMP field	f_{max} (MHz)	Copper ($\mu_r = 1; \sigma = 0.56E8S/m$)		Steel ($\mu_r = 200; \sigma = 0.1E8S/m$)	
		Skin depth for f_{max} (μm)	max. wall thickness (1 st ord)(mm)	Skin depth for f_{max} (μm)	max. wall thickness (1 st ord)(mm)
Lightning	0.05	301.0	2.010	50.30	0.333
ESD	10.00	21.3	0.142	3.56	0.024
NEMP	20.00	15.0	0.100	2.52	0.017

Here two one hundredths is chosen as the limiting factor since most of the damaging energy is situated in the lower spectrum. Once the maximum frequency, f_{max} , is determined, the lowest skin depth can be calculated for various materials as in Table 3.3.

The code made use of first order polynomials to follow the field variations and four divisions in the walls, therefore realistic diffusion problems in this case relate to situations for which the percentage of skin depth over the wall thickness is greater or equal to fifteen percent (see Table 3.1). Applying this virtual limit to the skin depth calculated in Table 3.3 gives the maximum wall thickness for which the shielding effectiveness can be solved.

3.4.3 Validation

The numerical technique presented in section 3.4 is validated against the analytical solution of a one-dimensional diffusion problem as presented in section 2.1.2. The test problem was analysed for various geometries and impinging fields to show the effect that the constitutive parameters and the thickness of the shield has on the accuracy of the numerical method. The field of interest consists of lightning, ESD and NEMP

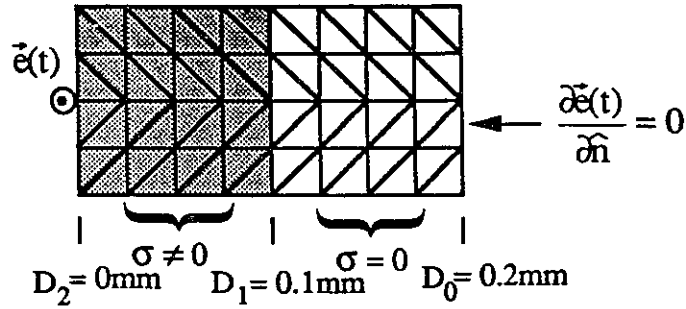


Figure 3.5: Division into FEs for time-domain.

with the characteristics as given in Table 3.2.

The division into triangular finite elements of the one-dimensional test problem (see figure 2.1) is shown in figure 3.5. Figures 3.6(a-c) show the comparison between the analytical and the finite element solution for copper walls of one-tenth of a millimeter thick with three types of impinging fields (the electric field is normalized to the outside peak field). As may be observed, there is a perfect agreement between the FEM and the analytical solution. In figure 3.6(d), both methods were applied to the diffusion of an NEMP field through steel walls of the same thickness. Notice that the diffused field inside the steel walls is more attenuated, has a slower rise time and a flatter response than that of the copper shield (see figure 3.6(c)). It can be seen that the FEM can still follow fairly well the field penetration even when the width of the wall is five times greater than the computed maximum wall thickness (refer to Table 3.3).

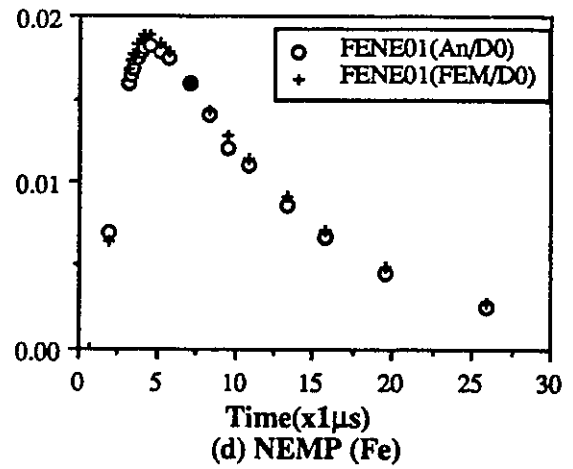
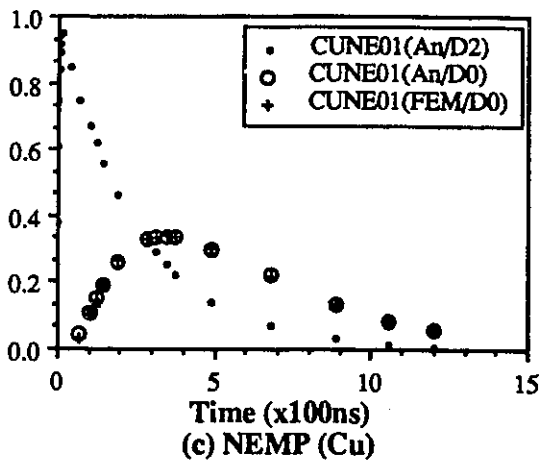
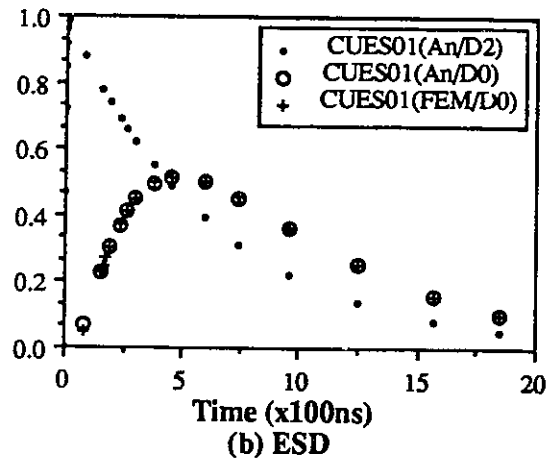
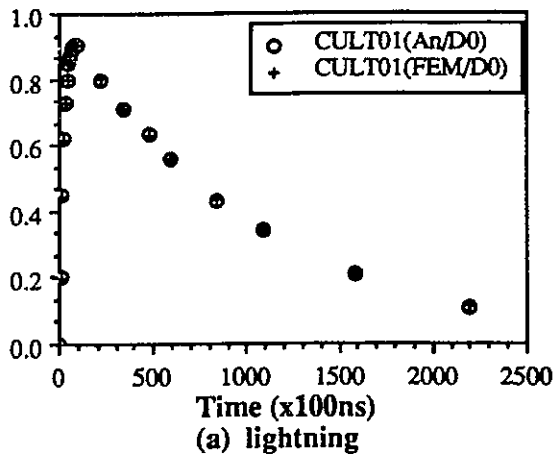


Figure 3.6: One-dimensional time-domain comparison of analytical solution with FEM.

Chapter 4

Transmission-Line-Matrix

4.1 Introduction

The transmission line matrix method finds its origin in Huygen's principle of light [32] which states that a wave front consists of secondary wave sources which in turn radiate thus creating a new wave front with the envelope of these secondary wavelets (see figure 4.1).

John's and Beurle's idea [33] was to implement this principle to solve electromagnetic problems. To accomplish this, they discretized a two-dimensional region into interconnecting transmission lines in which each junction (node) would then become a secondary radiator due to the reflection and transmission of an incoming wave on a node (see figure 4.2).

Thus a field, in this model, travelling along a transmission line would be scattered in four directions upon reaching a junction as there are impedance discontinuities at each junction. In a lossless and homogeneous region with characteristic impedance of Z_c , a field travelling towards a node with an amplitude of $1V$ is reflected back with an amplitude of $-\frac{1}{2}V$ since the node impedance seen from the incident branch is $\frac{Z_c}{3}$,

$$\Gamma = \frac{\frac{Z_c}{3} - Z_c}{\frac{Z_c}{3} + Z_c} = -\frac{1}{2}. \quad (4.1)$$

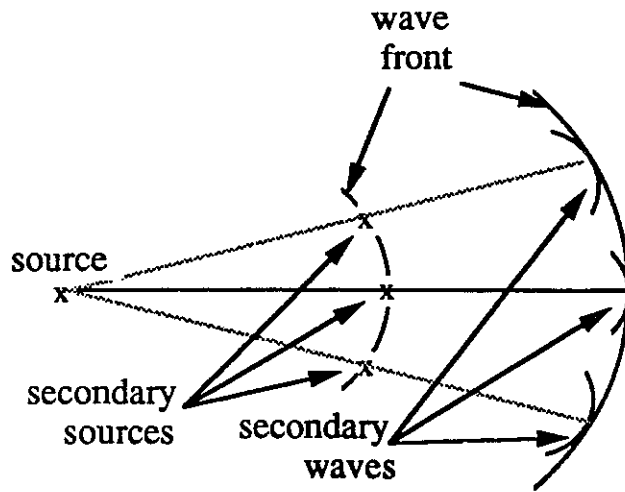


Figure 4.1: Formation of wave fronts as explained by Huygens principle.

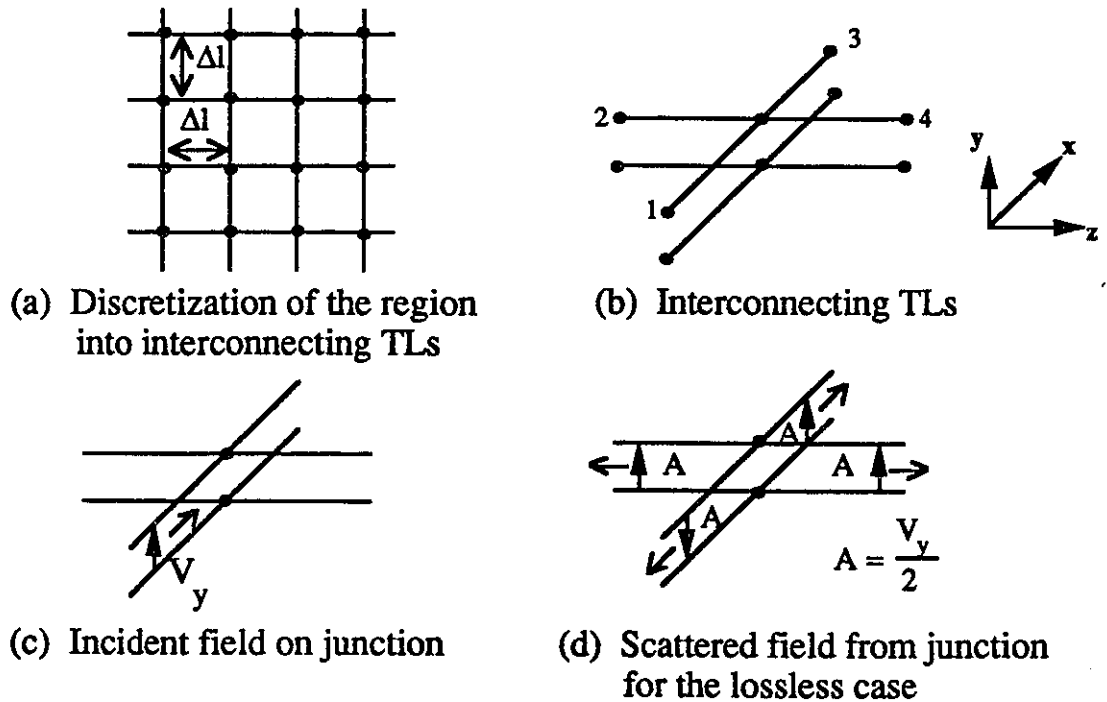


Figure 4.2: Interconnecting transmission lines (TLs).

A field is also generated in the three other branches having an amplitude of $(1 + \Gamma) \cdot 1V = +\frac{1}{2}V$ in each one of them.

The analysis in the TLM method is conducted directly in the time domain for which the impinging field's or point source's time signature is discretized in time as a succession of Dirac impulses. These impulses are spaced by

$$\Delta t = \Delta l / c_0 \quad (4.2)$$

in a uniformly gridded region.

The reflected voltages in the four branches of a unit cell at the time $(k + 1) * \Delta t$ is then related to the incident voltages on the node at time $k * \Delta t$ by the scattering matrix S [33] given below

$$\begin{bmatrix} V_1 \\ V_2 \\ V_3 \\ V_4 \end{bmatrix}_{k+1}^r = S \begin{bmatrix} V_1 \\ V_2 \\ V_3 \\ V_4 \end{bmatrix}_k^i \quad (4.3)$$

where

$$S = \frac{1}{2} \begin{bmatrix} -1 & 1 & 1 & 1 \\ 1 & -1 & 1 & 1 \\ 1 & 1 & -1 & 1 \\ 1 & 1 & 1 & -1 \end{bmatrix}.$$

To give a visual representation of the propagation of the field in such a structure, one Dirac impulse is sent from one node in the four directions and the scattered fields are calculated for two iterations (see figure 4.3).

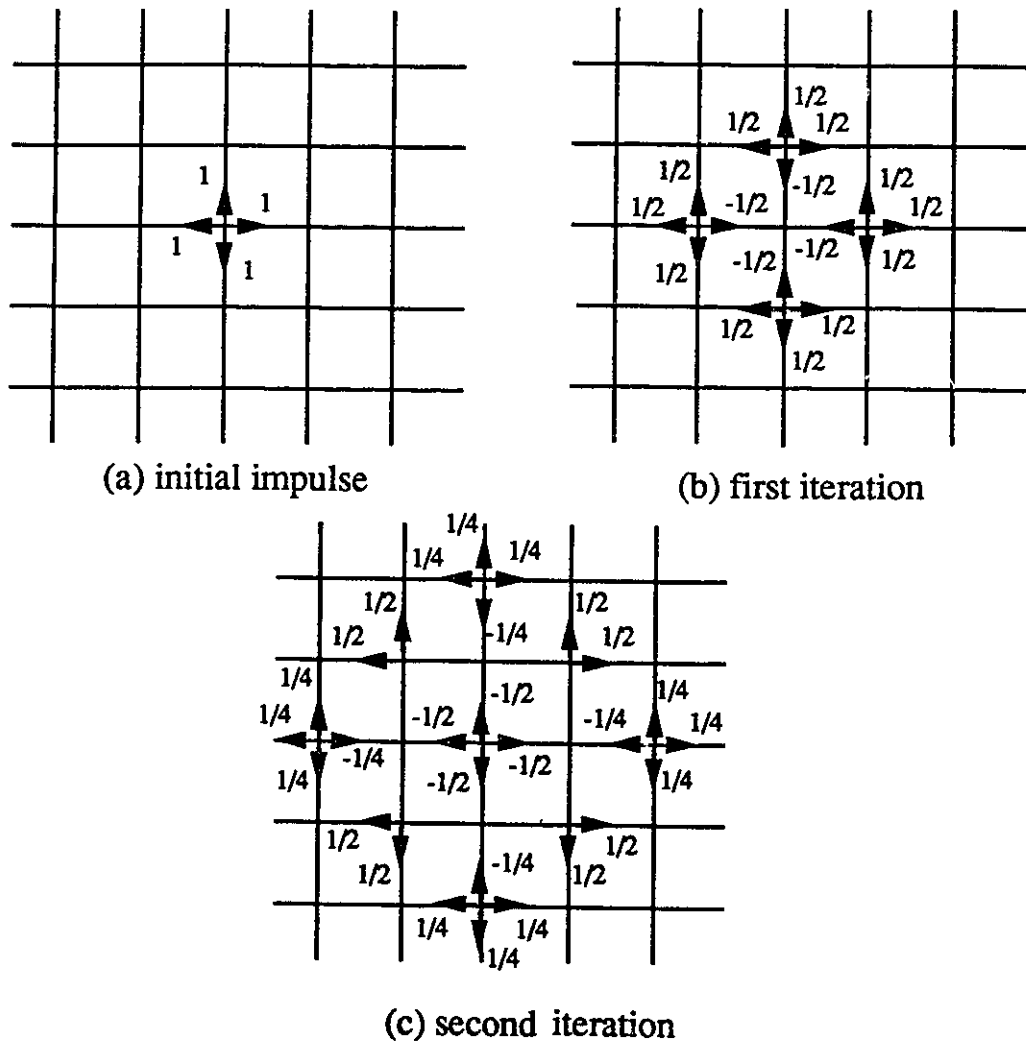


Figure 4.3: Scattered field from one Dirac impulse in a homogeneous region.

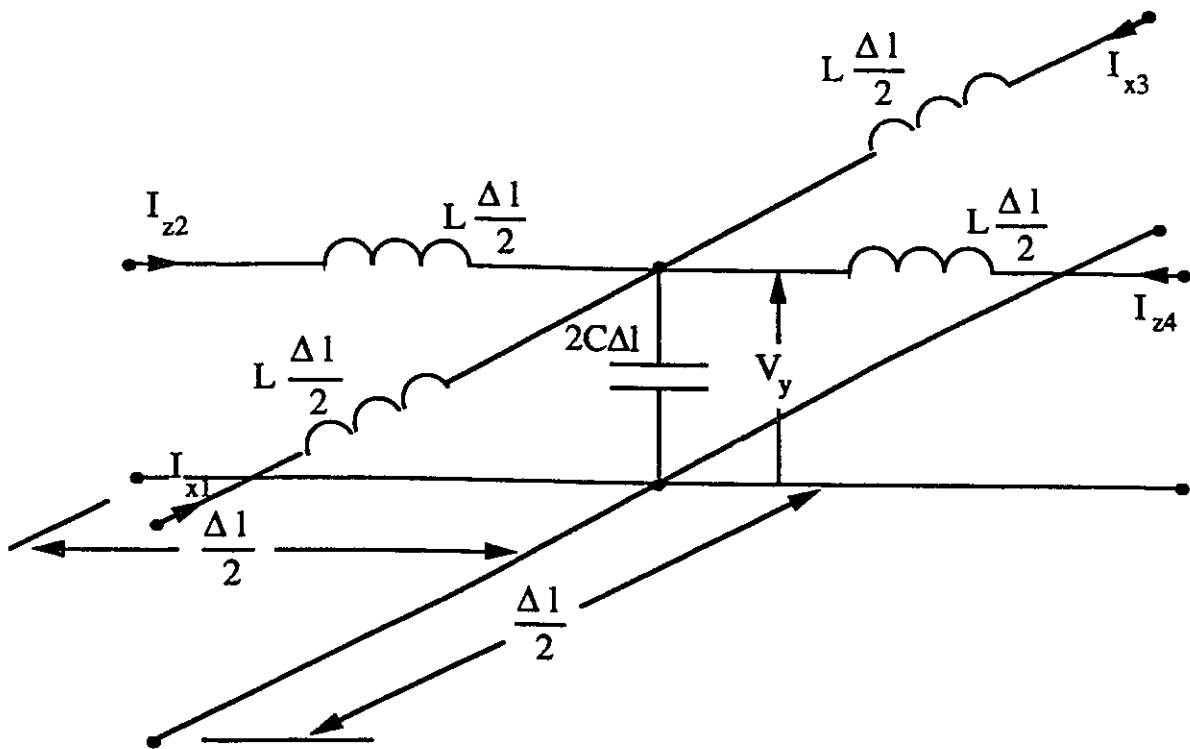


Figure 4.4: Basic shunt network.

4.2 Mathematical Formulation

4.2.1 Lossless Medium

The mapping, for a lossless medium, of the voltages and currents in the transmission lines to the field quantities being modeled is obtained by replacing the transmission lines with their equivalent lumped parameters such as inductances and capacitances. Then, for a certain inductance and capacitance per unit length represented respectively by L and C , the basic network in the two-dimensional analysis may be represented as shown in figure 4.4, known as the shunt configuration.

The simulation of a transverse electric (TE) field propagating in a certain medium is conducted by discretizing the region with the use of the basic shunt network. In such a model, the voltages and currents may be approximated by the following equations

when the spacing between the junctions, Δl , is relatively small with respect to the wavelength [33]

$$-\frac{\partial}{\partial x}(I_{x_1} - I_{x_3}) - \frac{\partial}{\partial z}(I_{x_2} - I_{x_4}) = 2C \frac{\partial V_y}{\partial t} \quad (4.4)$$

$$-\frac{\partial V_y}{\partial x} = L \frac{\partial}{\partial t}(I_{x_1} - I_{x_3}) \quad (4.5)$$

$$-\frac{\partial V_y}{\partial z} = L \frac{\partial}{\partial t}(I_{x_2} - I_{x_4}) \quad (4.6)$$

which may be combined to give a wave equation

$$\frac{\partial^2 V_y}{\partial x^2} + \frac{\partial^2 V_y}{\partial z^2} = 2LC \frac{\partial^2 V_y}{\partial t^2}. \quad (4.7)$$

The corresponding field equations for a propagating TE wave are given by Maxwell's equations as

$$\frac{\partial H_x}{\partial z} - \frac{\partial H_z}{\partial x} = \epsilon \frac{\partial E_y}{\partial t} \quad (4.8)$$

$$\frac{\partial E_y}{\partial z} = \mu \frac{\partial H_x}{\partial t} \quad (4.9)$$

$$\frac{\partial E_y}{\partial x} = -\mu \frac{\partial H_z}{\partial t} \quad (4.10)$$

which combined give the wave equation

$$\frac{\partial^2 E_y}{\partial x^2} + \frac{\partial^2 E_y}{\partial z^2} = \mu\epsilon \frac{\partial^2 E_y}{\partial t^2}. \quad (4.11)$$

By relating equations (4.4)–(4.7) to equations (4.8)–(4.11) the following mapping may be established, for lossless transmission lines,

$$E_y \equiv V_y ; H_x \equiv (I_{x_1} - I_{x_3}) ; H_z \equiv -(I_{x_2} - I_{x_4})$$

$$\mu \equiv L ; \epsilon \equiv 2C.$$

The implication of this mapping is well understood when considering wave propagation in free space ($\mu_r = 1$ and $\epsilon_r = 1$). As the inductance and capacitance per unit length are related by

$$\frac{1}{\sqrt{LC}} = \frac{1}{\sqrt{\mu_0 \epsilon_0}} = c_0,$$

a field propagating in free space at the speed of light would then be simulated, in TLM, as propagating in a medium with a relative permittivity twice that of free space. To account for this inherent error, one has to be careful of how they relate the propagation constant of the network to that of the actual situation.

In the lossless case, the reflected fields are related to the incident fields by the scattering matrix as given in equation (4.3).

4.2.2 Lossy and Dielectric Medium

To represent a TE field propagating in a lossy and/or dielectric medium, the shunt transmission lines are loaded with infinite loss shunt stubs and/or $\Delta l/2$ open stubs respectively (see figure 4.5). In such a medium, equations (4.4) and (4.8) become [34]-[35]

$$-\frac{\partial}{\partial x}(I_{x_1} - I_{x_3}) - \frac{\partial}{\partial z}(I_{x_2} - I_{x_4}) = 2C(1 + Y_0/4)\frac{\partial V_y}{\partial t} + \frac{G_0 C c_0}{\Delta l} V_y \quad (4.12)$$

$$\frac{\partial H_x}{\partial z} - \frac{\partial H_z}{\partial x} = \epsilon_0 \epsilon_r \frac{\partial E_y}{\partial t} + \sigma E_y \quad (4.13)$$

where G_0 is the characteristic admittance of the infinite loss stub normalized to the characteristic admittance of the mainlines. The mapping of the field quantities to those of the model is then

$$E_y \equiv V_y \quad ; \quad H_z \equiv (I_{x_1} - I_{x_3}) \quad ; \quad H_x \equiv -(I_{x_2} - I_{x_4})$$

$$\mu_0 \equiv L \quad ; \quad \epsilon_0 \equiv 2C \quad ; \quad \epsilon_r \equiv 1 + Y_0/4 \quad ; \quad \sigma \equiv \frac{G_0 C c_0}{\Delta l} \equiv \frac{G_0}{\Delta l} \sqrt{\frac{\epsilon_0}{\mu_0}}$$

when a lossy and dielectric medium is present. With the added representation of losses, the basic shunt network is now a six port network.

In this model, the incident fields are discretized in time and injected in the mesh, at certain nodes, as impulses of different amplitude. The reflected voltages from a node at time $(k + 1) * \Delta t$ are related to the incident voltages on the same node at

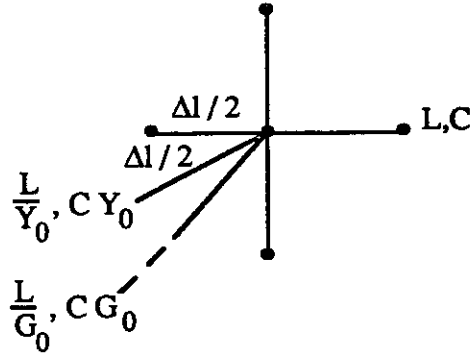


Figure 4.5: Top view of node loaded with $\frac{\Delta l}{2}$ open stub and infinite loss stub.

time $k * \Delta t$ by the scattering matrix S [35]

$$\begin{bmatrix} V_1 \\ V_2 \\ V_3 \\ V_4 \\ V_5 \end{bmatrix}_{k+1}^r = S \begin{bmatrix} V_1 \\ V_2 \\ V_3 \\ V_4 \\ V_5 \end{bmatrix}_k^i \quad (4.14)$$

where

$$S = \frac{2}{Y} \begin{bmatrix} 1 & 1 & 1 & 1 & Y_0 \\ 1 & 1 & 1 & 1 & Y_0 \\ 1 & 1 & 1 & 1 & Y_0 \\ 1 & 1 & 1 & 1 & Y_0 \\ 1 & 1 & 1 & 1 & Y_0 \end{bmatrix} - I$$

and $Y = 4 + Y_0 + G_0$; $Y_0 = 4(\epsilon_r - 1)$; $G_0 = \sigma \Delta l \sqrt{\mu_0 / \epsilon_0}$, and I is a unit matrix.

Equation (4.14) gives the generalized scattering matrix, S , when modeling a dielectric and lossy medium. Notice that the voltage scattered into the infinite loss shunt (V_0) is not needed in the calculation as none of the lost energy is reflected back to the node.

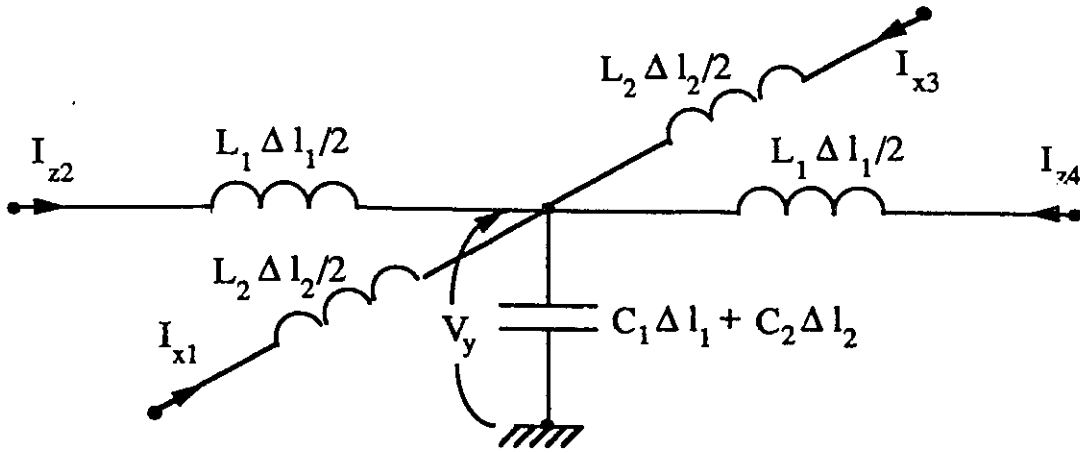


Figure 4.6: Shunt network with variable branch length.

4.2.3 Variable Mesh Size

In order to analyse a large region in which small discontinuities are present, one would need to discretize the whole region in small square meshes, when using the conventional TLM method. This would then lead to a great number of nodes in regions where it is not needed, thus immensely increasing the memory requirements and more importantly, the processing time. To overcome this problem, rectangular mesh (or variable mesh size) have been introduced by Saguet and Pic [36].

In a variable mesh configuration, the basic cell, as shown in figure 4.4, is modified to include different branch length and impedances. An intersection of two transmission lines of length Δl_1 and Δl_2 and of inductance and capacitance per unit length of L_1 , C_1 , and L_2 , C_2 is then described as (see figure 4.6)

$$-\Delta l_1 \frac{\partial}{\partial x} (I_{x1} - I_{x3}) - \Delta l_2 \frac{\partial}{\partial z} (I_{z2} - I_{z4}) = (C_1 \Delta l_1 + C_2 \Delta l_2) \frac{\partial V_y}{\partial t} \quad (4.15)$$

$$-\frac{\partial V_y}{\partial x} = L_1 \frac{\partial}{\partial t} (I_{x1} - I_{x3}) \quad (4.16)$$

$$-\frac{\partial V_y}{\partial z} = L_2 \frac{\partial}{\partial t} (I_{z2} - I_{z4}). \quad (4.17)$$

Now to alleviate the complexity of the network Δl_2 is chosen to be an integer multiplier (N) of Δl_1 . Thus by setting $\Delta l_2 = N \Delta l_1$, equations (4.15) to (4.17) reduce

to

$$-\frac{\partial}{\partial x}(I_{x_1} - I_{x_3}) - N\frac{\partial}{\partial z}(I_{z_2} - I_{z_4}) = 2C_1\frac{\partial V_y}{\partial t} \quad (4.18)$$

$$-\frac{\partial V_y}{\partial x} = L_1\frac{\partial}{\partial t}(I_{x_1} - I_{x_3}) \quad (4.19)$$

$$-\frac{\partial V_y}{\partial z} = NL_1\frac{\partial}{\partial t}(I_{z_2} - I_{z_4}) \quad (4.20)$$

since $L_2 = NL_1$ and $C_2 = C_1/N$. When combined, equations (4.18) to (4.20) represent a wave equation

$$\frac{\partial^2 V_y}{\partial x^2} + \frac{\partial^2 V_y}{\partial z^2} = 2L_1C_1\frac{\partial^2 V_y}{\partial t^2}. \quad (4.21)$$

The speed of propagation in a variable mesh configuration is conserved,

$\sqrt{L_1C_1} = \sqrt{L_2C_2}$, but the characteristic impedances are different

$$\sqrt{\frac{L_1}{C_1}} = \frac{1}{N}\sqrt{\frac{L_2}{C_2}}. \quad (4.22)$$

This difference in the characteristic impedances means that the scattering matrix will differ from the uniform mesh division. For the rectangular mesh, the reflected voltages are related to the incident ones by the following equation

$$V_{n+1}^r = \frac{2\sum_m Y_m V_m^i}{\sum_m Y_m} - V_n^i \quad (4.23)$$

or

$$\begin{bmatrix} V_1 \\ V_2 \\ V_3 \\ V_4 \end{bmatrix}_{k+1}^r = S \begin{bmatrix} V_1 \\ V_2 \\ V_3 \\ V_4 \end{bmatrix}_k^i \quad (4.24)$$

with

$$S = \frac{2}{\sum_{m=1}^4 Y_m} \begin{bmatrix} Y_1 & Y_2 & Y_3 & Y_4 \\ Y_1 & Y_2 & Y_3 & Y_4 \\ Y_1 & Y_2 & Y_3 & Y_4 \\ Y_1 & Y_2 & Y_3 & Y_4 \end{bmatrix} - I$$

where $Y_3 = Y_1$ and $Y_4 = Y_2$.

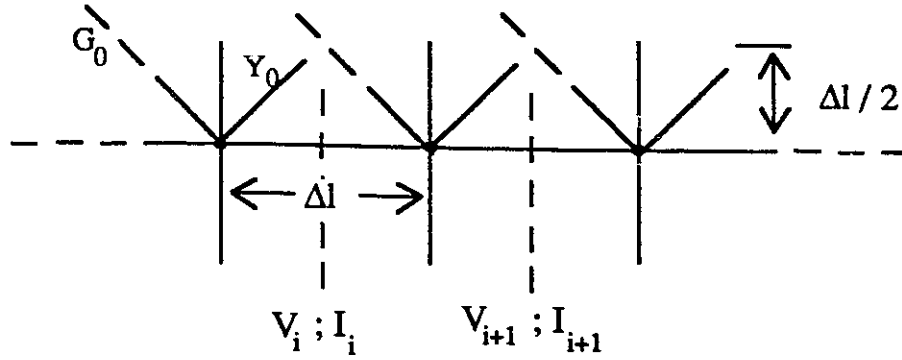


Figure 4.7: One-dimensional TLM.

4.3 Realistic Diffusion Problems to be Solved

As the regions analysed by the TLM method are discretized into interconnecting transmission lines, problems might occur if one isn't careful. Depending on the frequencies of operation and the angle of propagation, the mesh may present a cutoff network to the fields. To calculate the range of frequencies for which the network is valid, the transmission line matrix is analysed for a plane wave travelling in the axial direction (this gives the worst case situation for the network) within a homogeneous region. Since the transmission lines are in a homogeneous region and the impinging fields are plane waves, the analysis of the propagating wave may be conducted via a one-dimensional TLM. In this case the wave travels along a transmission line which is periodically loaded with open circuited stubs of length $\Delta l/2$ as shown in figure 4.7. Now relating V_i & I_i to V_{i+1} & I_{i+1} in figure 4.4, one finds the following [37]

$$\begin{aligned}
 \begin{vmatrix} V_i \\ I_i \end{vmatrix} &= \begin{vmatrix} \cosh \gamma \frac{\Delta l}{2} & \sinh \gamma \frac{\Delta l}{2} \\ \sinh \gamma \frac{\Delta l}{2} & \cosh \gamma \frac{\Delta l}{2} \end{vmatrix} \times \begin{vmatrix} 1 & 0 \\ (2 + Y_0) \tanh \gamma \frac{\Delta l}{2} & 1 \end{vmatrix} \times \\
 &\begin{vmatrix} \cosh \gamma \frac{\Delta l}{2} & \sinh \gamma \frac{\Delta l}{2} \\ \sinh \gamma \frac{\Delta l}{2} & \cosh \gamma \frac{\Delta l}{2} \end{vmatrix} \times \begin{vmatrix} V_{i+1} \\ I_{i+1} \end{vmatrix} \quad (4.25)
 \end{aligned}$$

A wave propagating in a periodic structure such as this one, with a propagating constant $\gamma_n = \alpha_n + j\beta_n$, would then have the following relationship

$$\begin{vmatrix} V_i \\ I_i \end{vmatrix} = \begin{vmatrix} e^{\gamma_n \Delta l} & 0 \\ 0 & e^{\gamma_n \Delta l} \end{vmatrix} \times \begin{vmatrix} V_{i+1} \\ I_{i+1} \end{vmatrix}. \quad (4.26)$$

The solution to equations (4.25) and (4.26) gives

$$\left(2 + \frac{Y_0}{2}\right) \cosh \gamma \Delta l - \left(1 + \frac{Y_0}{2}\right) = \cosh \gamma_n \Delta l. \quad (4.27)$$

Replacing γ by $\alpha + j\beta$ and γ_n by $\alpha_n + j\beta_n$ in (4.27) and equating the real and imaginary parts respectively, the following relations are obtained

$$\left(2 + \frac{Y_0}{2}\right) \cos \beta \Delta l \cosh \alpha \Delta l - \left(1 + \frac{Y_0}{2}\right) = \cos \beta_n \Delta l \cosh \alpha_n \Delta l \quad (4.28)$$

$$\left(2 + \frac{Y_0}{2}\right) \sin \beta \Delta l \sinh \alpha \Delta l = \sin \beta_n \Delta l \sinh \alpha_n \Delta l \quad (4.29)$$

in which (4.28) corresponds to the real part and (4.29) to the imaginary. Assuming that both $\alpha \Delta l$ and $\alpha_n \Delta l$ are much smaller than one ($\alpha \Delta l$ & $\alpha_n \Delta l \ll 1$), equations (4.28) and (4.29) may be rewritten as

$$\frac{\beta}{\beta_n} = \frac{\pi \left(\frac{\Delta l}{\lambda}\right)}{\sin^{-1} \left\{ \sqrt{2 \left(1 + \frac{Y_0}{4}\right)} \sin \left(\pi \frac{\Delta l}{\lambda}\right) \right\}} \quad (4.30)$$

$$\frac{\alpha}{\alpha_n} = \frac{\sqrt{1 - 2 \left(1 + \frac{Y_0}{4}\right) \sin^2 \left(\pi \frac{\Delta l}{\lambda}\right)}}{\sqrt{2 \left(1 + \frac{Y_0}{4}\right) \cos \left(\pi \frac{\Delta l}{\lambda}\right)}} \quad (4.31)$$

where $\alpha = \frac{G_0}{4\Delta l \left(1 + \frac{Y_0}{4}\right)}$. From equations (4.30) and (4.31), the first network cutoff frequency is then found to be

$$\left(\frac{\Delta l}{\lambda}\right)_{cutoff} = \frac{1}{\pi} \sin^{-1} \left(\frac{1}{\sqrt{2 \left(1 + \frac{Y_0}{4}\right)}} \right). \quad (4.32)$$

At relatively low frequencies, well below cutoff, the propagation constants α_n and β_n of the network are relatively constant, thus equation (4.30) and (4.31) reduce to

$$\gamma_n = \sqrt{2 \left(1 + \frac{Y_0}{4}\right)} \gamma. \quad (4.33)$$

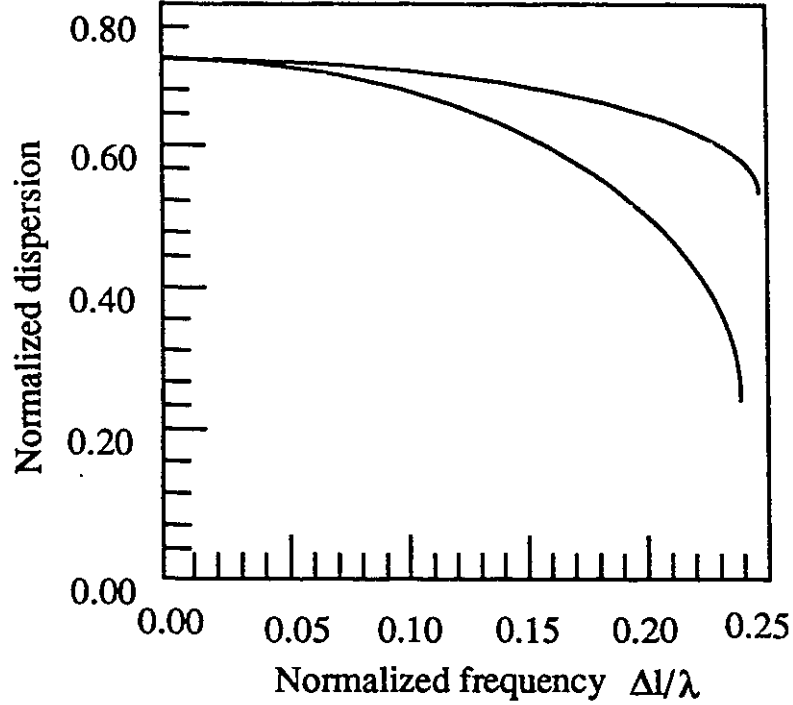


Figure 4.8: Dispersion vs frequency of TLM network.

As demonstrated, when the wavelength of propagation approaches the transmission line mesh size, the equivalence between the network constants and the constant of a continuous medium collapses (see figure 4.8). Equation (4.33) implies that, for non-dielectric medium, the network wavelength λ_n actually represents an effective wavelength of $\sqrt{2}\lambda$ and, similarly, the network conductivity σ_n represents effectively a conductivity of $\sqrt{2}\sigma$.

The introduction of conducting materials brings another limiting factor as the relationship between the attenuation constant of the network and that of the medium, given in equation (4.31), is only valid when

$$\alpha\Delta l \ll 1. \quad (4.34)$$

Replacing α by $G_0 / (4\Delta l(1 + \frac{Y_0}{4}))$ and G_0 by $\sigma\Delta l\sqrt{\mu_0/\epsilon_0}$ in equation (4.34),

$$\alpha\Delta l \cong \frac{\sigma\Delta l \cdot 120\pi}{4 \cdot (1 + \frac{Y_0}{4})} \leq 0.1 \quad (4.35)$$

we obtain, in a non-dielectric medium ($Y_0 = 0$),

$$\Delta l \leq (300\pi\sigma)^{-1}. \quad (4.36)$$

Combining the limiting factor (4.36) with the fact that the relationship between the propagation constant of the network and of the medium, equation (4.30), is valid for non-dielectric medium when (see figure 4.8)

$$\frac{\Delta l}{\lambda} \leq 0.07, \quad (4.37)$$

one may determine the ranges in which TLM will effectively analyse a diffusion problem.

Now with the upper limit defined in (4.37), we may determine f_{max} , the maximum frequency, for a given conductivity, σ , for which TLM may be effectively used. Thus with the following two limits

$$\Delta l_{max} = (300\pi\sigma)^{-1} \quad (4.38)$$

$$\lambda_{min} = \frac{\Delta l_{max}}{0.07} \quad (4.39)$$

f_{max} is obtained

$$f_{max} = \frac{c_0}{\lambda_{min}} = 21\pi\sigma c_0. \quad (4.40)$$

In Table 4.1, the maximum step size is given as a function of the conductivity, σ . As may be observed, the limiting factor for the step size is the conductivity as opposed to the wavelength when considering a non-dielectric material.

At first glance it might seem contradictory that as the conductivity increases, the maximum frequency also increases. But this is an illusion since as the conductivity increases, the maximum step size decreases at the same rate as the maximum frequency increases (see equation (4.39)). When relating the conductivity, the maximum step size and frequency to the skin depth, δ (given in equation (3.25)), we see that

$$\Delta l_{max} \simeq \frac{\delta_{min}}{3.4} = \frac{1}{3.4\sqrt{\pi f_{max}\mu\sigma}} \quad (4.41)$$

Therefore in the limiting case there are approximately four steps per skin depth.

Table 4.1: Calculating the maximum step size as a function of σ .

Conductivity (S/m)	Maximum step ¹ size $\Delta l(\mu m)$	Maximum frequency ² $f_{max}(GHz)$	Skin depth in (μm) for σ & f_{max}	Typical frequencies- # iterations/cycle ³	
				1GHz	10GHz
10	106.1	197.9	357.8	2830	283
20	53.0	395.8	178.9	5660	566
50	21.1	989.9	71.5	14151	1415
100	10.6	1979.0	35.8	28300	2830
200	5.3	3958.0	17.9	56600	5660
500	2.1	⋮	⋮	⋮	⋮
1E03	1.1	⋮	⋮	⋮	⋮
1E05	10.6E-03	⋮	⋮	⋮	⋮
1E08	10.6E-06	⋮	⋮	⋮	⋮

1 for $Y_0 = 0$
2 the maximum frequency (f_{max}) is determined from equation (4.40) once Δl is found from (4.38)
3 # of iterations = $\frac{c_0}{\Delta l \times f}$

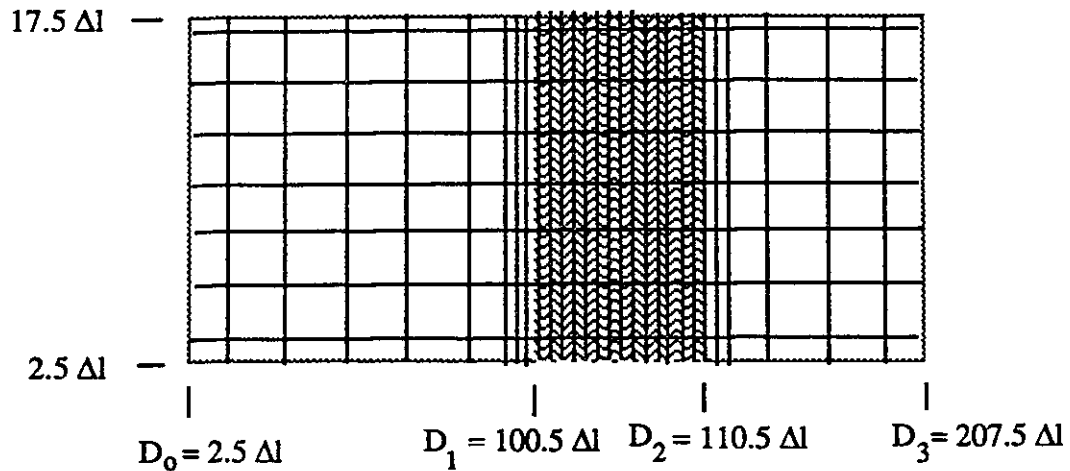


Figure 4.9: TLM division of the one-dimensional problem.

4.4 Validation

The validation of the TLM method, used to analyse diffusion problems, is conducted in the frequency domain for it yields more information. Since TLM is a time domain numerical technique, the result of the analysis will be converted to the frequency domain via the Fourier transform. The effect that both the total number of iterations and the mesh size, Δl , have on the numerical results of TLM are compared to the analytical solution derived in section 2.1.2.

The one-dimensional test problem (see figure 2.1) is discretized into interconnecting transmission lines as shown in figure 4.9. The total region analysed is approximately $210 \Delta l$ long by $20 \Delta l$ high. Using variable mesh size the region is divided into steps of Δl between $93 \Delta l$ and $117 \Delta l$, the rest is divided into steps of $5 \Delta l$. As a consequence, for an impulse to travel from $x = D_3$ to $x = D_0$ and back, 400 iterations are needed.

4.4.1 Number of Iterations Needed for Steady-State

The number of iterations required to reach a steady-state for a problem depends on the size of both the step and the region under investigation as a function of the

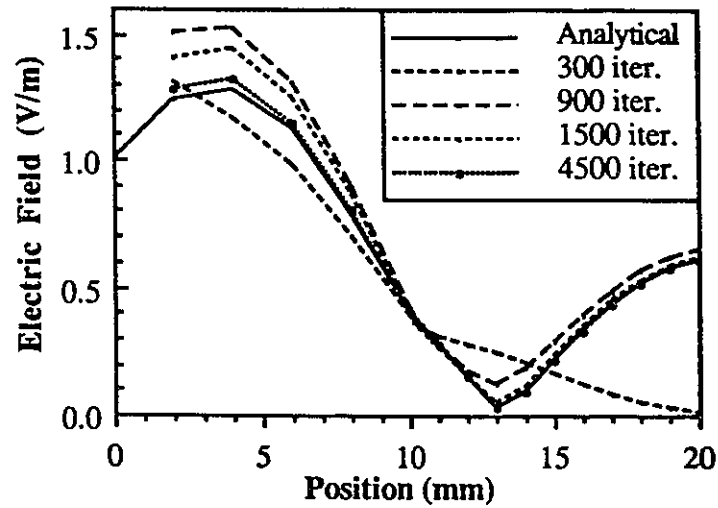


Figure 4.10: TLM vs analytical solution as a function of iteration.

frequencies of interest. To show what effect the number of iterations considered has on the steady-state results, a one-dimensional diffusion problem was solved for various number of iterations and compared to the analytical solution as shown in figure 4.10. The problem geometry and parameters are

$$D_0 = 0.25mm ; D_1 = 10.05mm ; D_2 = 11.05mm ; D_3 = 20.75mm$$

$$f = 10GHz ; \sigma = 10 ; \Delta l = 100\mu m$$

$$\# \text{ of iterations for 1 cycle} = \frac{c_0}{f\Delta l} = 300$$

It is seen that the results obtained with 300 iterations is far from being accurate, for two reasons:

- only one full cycle was considered which isn't enough for a steady-state solution.
- also it takes 400 iterations for one impulse to travel to D_3 and back

Although one cycle isn't enough, TLM converges very rapidly; with only three cycles considered, already TLM results are close to the signature, and with 15 cycles, the results are in good agreement.

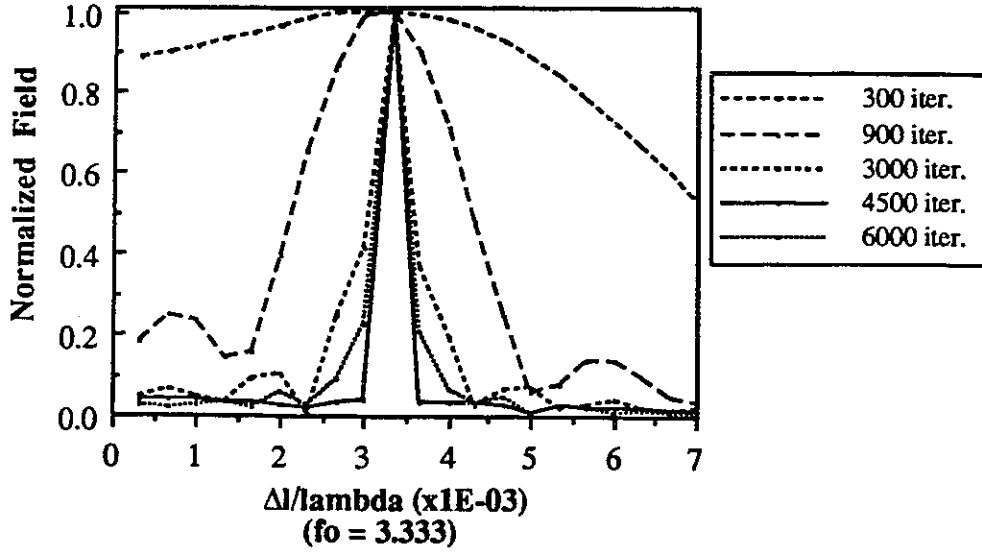


Figure 4.11: Frequency plot of TLM vs analytical solution as a function of iteration.

The implications of the number of iterations considered can also be analysed by plotting the Fourier transform of the signal, at a certain position, for various iterations. In figure 4.11 the convergence to the frequency of interest as a function of the number of iterations is very well demonstrated. It should be noted that there is an optimum number of iterations since, as one increases this number beyond a certain point, the errors from the imperfect terminations become more and more apparent. For this particular situation, fifteen cycles seem to be an optimum.

4.4.2 Effect of Varying the Length of the Step Size

In section 4.3 it was shown that the determining factor for the step size is mainly the conductivity and not the wavelength in a non-dielectric region. The step size Δl will now be increased up to a breaking point such as to verify the presented rule of thumb relating the conductivity to the step size

$$\alpha \Delta l \leq 0.1 \quad \text{or} \quad \Delta l_{max} = (300\pi\sigma)^{-1}. \quad (4.42)$$

In figures 4.12(a) & (b), the analytical solution is compared to TLM's for various step sizes. In each case the geometry and parameters are as follow:

$$D_0 = 2.5\Delta l \ ; \ D_1 = 100.5\Delta l \ ; \ D_2 = 110.5\Delta l \ ; \ D_3 = 207.5\Delta l$$

$$f = 10GHz \ ; \ \sigma = 10 \ ; \ \# \ of \ iterations = 15 \times [\# \ of \ iter./cycle]$$

As the parameter $\alpha\Delta l$ increases from 0.05 to 0.1, there is a very good correlation between TLM and the analytical solution. The TLM results are still in good order for $\alpha\Delta l$ near 0.2, but as $\alpha\Delta l$ increases beyond 0.3, the TLM method cannot follow the field variations anymore. This breakdown phenomenon is well observed with $\alpha\Delta l$ equal to 0.5.

4.5 Discussion

In section 4.3, some rules of thumb regarding modeling of diffusion problems via the TLM method were derived through a one-dimensional analysis. These rules revealed to be very useful in understanding the limits imposed by TLM and in knowing, prior to any analysis, the projected accuracy of the model.

The validation of the TLM method was carried out in the frequency domain because it yields more useful information. The convergence of the technique was demonstrated by increasing the number of iterations considered. It was seen with the comparison to the analytical solution and also with the fourier transform that the convergence is fairly rapid (about 15 cycles were needed to reach steady state) and that there is an optimum number of iterations. The effect of the cutoff of the network is well demonstrated in section 4.4.2 by varying the length of the step size.

The TLM method may now be applied to more complex diffusion problems as its range of operation has been determined.

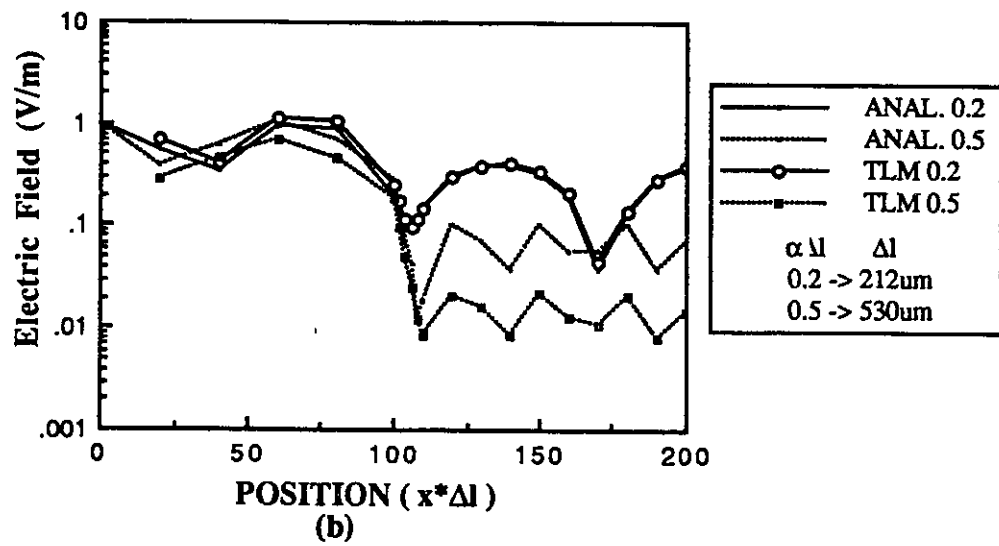
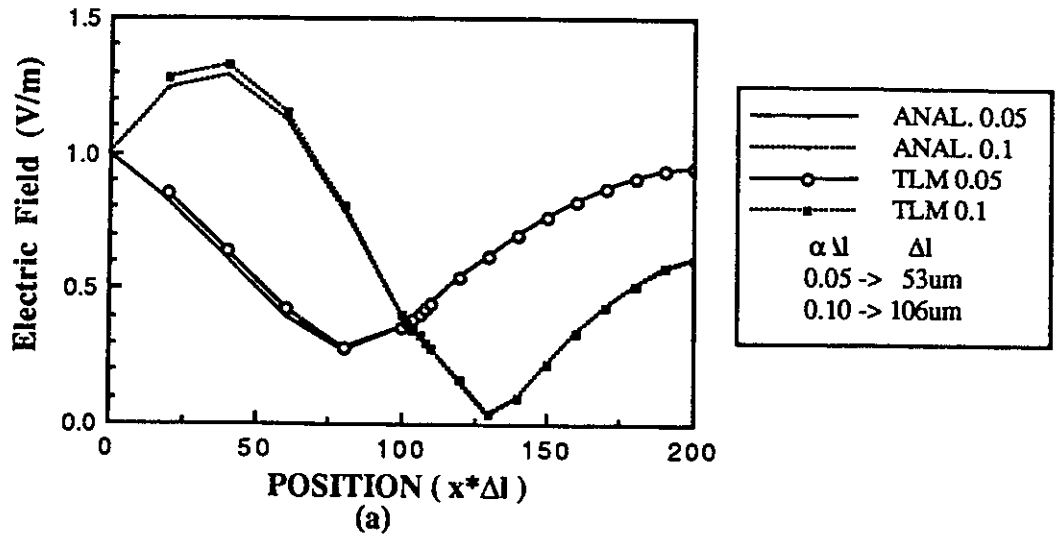


Figure 4.12: Analytical solution vs TLM as a function of Δl .

Chapter 5

Application of FEM to General Problems

5.1 Introduction

In chapter 2, an analytical solution was derived for the diffusion problem in both time and frequency domain. The availability of this theoretical formulation has given us the opportunity to validate both numerical techniques, the FEM and TLM, in solving diffusion problems. It also provided us with means to determine the range of operation of the techniques for following the field penetration into a conducting material.

Having full confidence in the FEM and the TLM method for solving the one-dimensional diffusion problems, we can apply both numerical techniques to more general and realistic problems. The actual enclosures used as shields, for damaging fields, are comprised of conducting materials as well as apertures. Since the shielded equipment has to communicate with the outside world, apertures (or holes) are needed for the link and also they are needed to dissipate the heat generated by the electrical equipment. Now to obtain an analytical solution of field penetration through apertures would require a very complicated formulation, if one exists. Thus to validate

the presented techniques, the same problem will be solved by these two completely different numerical methods.

There are two distinct situations to analyse when talking about the shielding effectiveness of enclosures. In one case, the shield is needed to prevent the damaging field from penetrating while in the other, the shield is intended to confine the field within the enclosure. The first situation is referred to as the immunity case, in which impinging fields are to be reflected and attenuated by the enclosures such as to minimize the effect of the ambient fields on the electronic equipment (see figure 1.1(a)). In the second situation, the emission case, fields generated by the electronic equipment are constrained within the enclosure as much as possible to prevent the emitted fields from corrupting nearby susceptible apparatus (see figure 1.1(b)).

In the following, assumptions are introduced to simplify the problem which in turn reduces the CPU time required for the calculation of the solution; they are by no means an indication of the restrictions imposed by the methods. The most important assumption made in this analysis is as follows: *“the length of the enclosure is assumed to be much longer than its width or height”*. This enables a reduction of a three-dimensional problem into a two-dimensional one thereby alleviating the complexity of the situation without sacrificing too much the generality of the analysis. Although only two-dimensional problems are considered here, three-dimensional studies are feasible with FEM [38] and TLM [39] as these numerical methods have been extended to include that type of investigation. Another assumption made in this thesis is with respect to the ground plane: *“the conductivity of the ground plane, over which lies the shield, is assumed to be infinite”*. Thus no loss is accounted for within the ground.

5.2 Immunity Case

The analysis of the immunity of a system, assured by an enclosure, is crucial as the system's performance may deteriorate due to the ambient fields. To properly

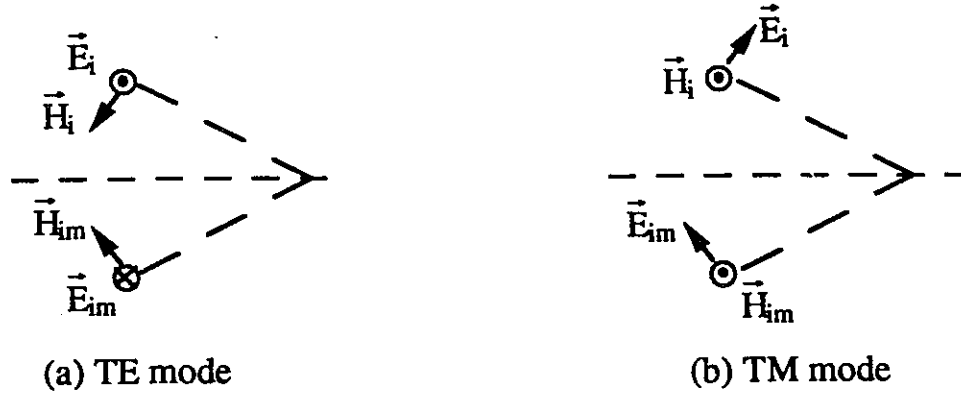


Figure 5.1: Mirror image concept for (a)TE and (b) TM modes of propagating plane waves.

characterize the immunity via a CAD tool, it has to solve problems as realistic as possible. Therefore both the material's conductivity and the aperture geometries have to be included as parameters along with the geometry of the enclosure.

The enclosure, in the immunity analysis, is lying over a perfectly conducting ground plane ($\sigma \equiv \infty$), which may be taken into consideration by making use of the mirror image concept. Figure 5.1 shows the effect of the ground plane on the region's fields when it is replaced by the image concept. The field at a certain point is given as the superposition of the impinging field and its image. Thus for the TE case, the electric field is set equal to zero everywhere on the ground plane at any time t ; whereas for the TM case, the magnetic field is set to be twice that of the field directly above the ground plane ($y = 0^+$) which is dependent on the time t and its position. For the TM case, the ground plane may also be replaced by a homogeneous Neumann boundary since the magnetic field has no variations with respect to the normal of the ground plane near the plane [24]. This will facilitate somewhat the code. In this type of analysis, the ambient field is assumed to impinge uniformly on two sides of the enclosure. With this assumption, a Dirichlet boundary may be set at a certain distance from the enclosure (see figure 5.2) and also at a distance far enough over the enclosure, the field may be assumed invariant with respect to the normal ($\frac{\partial H}{\partial n} = 0$).

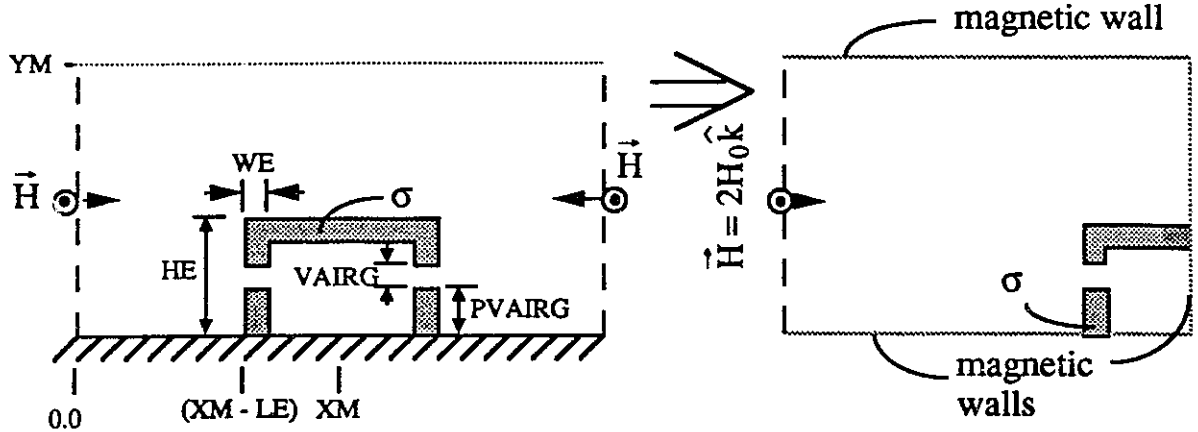


Figure 5.2: Immunity problem under investigation.

5.2.1 Mathematical Formulation

In the previous two chapters, we have solved the field penetration of an incident TE field. Here we shall predict the shielding effectiveness of enclosures to TM impinging fields thus showing the flexibility of both techniques. The mathematical formulation for solving TM fields with FEM and TLM is very similar to the one derived in chapters 3 and 4 respectively, since the wave equations are the same:

$$\nabla^2 \vec{e}(t) - \mu\sigma \frac{\partial}{\partial t} \vec{e}(t) - \mu\epsilon \frac{\partial^2}{\partial t^2} \vec{e}(t) = 0 \quad (5.1)$$

$$\nabla^2 \vec{h}(t) - \mu\sigma \frac{\partial}{\partial t} \vec{h}(t) - \mu\epsilon \frac{\partial^2}{\partial t^2} \vec{h}(t) = 0. \quad (5.2)$$

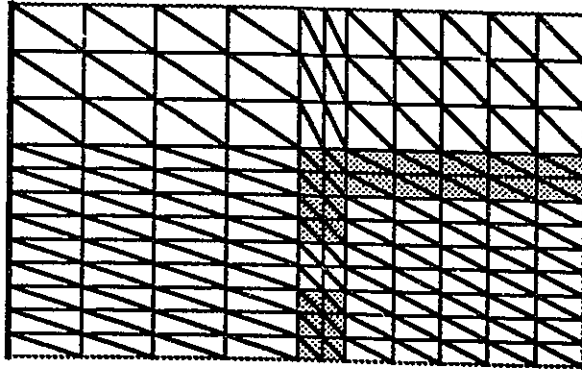
The formulation in the FEM is exactly the same as the one derived in section 3.2 as it was given in a very general form, one only needs to replace the general unknown $\vec{g}(t)$ by $\vec{h}(t)$. The variation is introduced by the boundary conditions.

Now in the TLM method, the mapping of the field quantities to the voltages and currents in the transmission lines is obtained from the following sets of equations for the TM case [37],

$$-\frac{\partial}{\partial x}(I_{x1} - I_{x3}) - \frac{\partial}{\partial z}(I_{z2} - I_{z4}) = 2C(1 + Y_0/4) \frac{\partial V_y}{\partial t} \quad (5.3)$$

$$-\frac{\partial V_y}{\partial x} = L \frac{\partial}{\partial t}(I_{x1} - I_{x3}) + \frac{G_0 C c_0}{\Delta l}(I_{x1} - I_{x3}) \quad (5.4)$$

$$-\frac{\partial V_y}{\partial z} = L \frac{\partial}{\partial t}(I_{z2} - I_{z4}) + \frac{G_0 C c_0}{\Delta l}(I_{z2} - I_{z4}) \quad (5.5)$$



where :

— Homogeneous Neumann boundary

— Dirichlet boundary

Figure 5.3: Finite element division (immunity).

for the transmission lines and

$$\frac{\partial E_x}{\partial z} - \frac{\partial E_z}{\partial x} = -\mu \frac{\partial H_y}{\partial t} \quad (5.6)$$

$$\frac{\partial H_y}{\partial z} = -\epsilon \frac{\partial E_x}{\partial t} - \sigma E_x \quad (5.7)$$

$$\frac{\partial H_y}{\partial x} = \epsilon \frac{\partial E_z}{\partial t} + \sigma E_z \quad (5.8)$$

for the field quantities. The mapping then becomes

$$H_y \equiv V_y ; E_z \equiv -(I_{x1} - I_{x3}) ; E_x \equiv (I_{z2} - I_{z4})$$

$$\mu_0 \equiv 2C ; \mu_r \equiv 1 + Y_0/4 ; \epsilon_0 \equiv L ; \sigma \equiv \frac{G_0 C \epsilon_0}{\Delta l} \equiv \frac{G_0}{\Delta l} \sqrt{\frac{\epsilon_0}{\mu_0}}$$

which is reciprocal to the TE case (see chapter 4). In this particular mapping, a voltage travelling in the transmission lines will represent a propagating magnetic field. Also, materials with a relative permeability different from 1 may be considered by introducing $\Delta l/2$ open shunt stubs at the proper nodes.

The discretization of the region into finite elements and transmission lines is given in figures 5.3 and 5.4 respectively along with the appropriate boundary conditions.

5.2.2 Frequency Domain Comparison Between FEM and TLM

In the TLM formulation some rules of thumb regarding the possible diffusion problems to analyse were presented. In Table 4.1, the maximum step size is depicted for

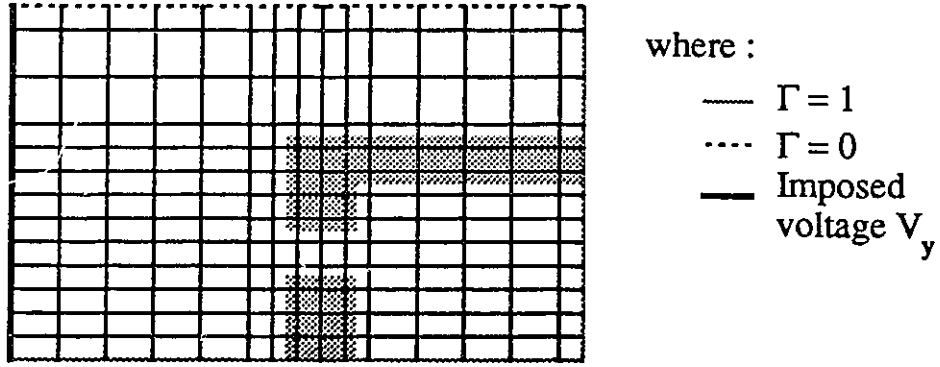


Figure 5.4: TLM division (immunity).

various conductivity and calculated also are the maximum frequency of analysis and its associated skin depth as well as some typical frequencies of analysis with the corresponding number of iterations they require to complete one cycle. It is then seen that in order to investigate diffusion problems in a realistic manner, the best combination of conductivity, wall thickness, and frequency is a shield with a wall thickness in the order of millimeters with conductivity of around $10S/m$ on which a field is impinging at the frequency greater than $1GHz$.

With these considerations in mind, the immunity problem was solved via the two techniques, in the frequency domain, for the following parameters (see figure 5.2)

$$\begin{aligned}
 LE &= 11.2mm & ; & & WE &= 2.0mm & ; & & HE &= 19.75mm \\
 XM &= 21.75mm & ; & & YM &= 49.75mm \\
 PVAIRG &= 9.75mm & ; & & VAIRG &= 5mm \\
 f &= 10.0GHz & ; & & \sigma &= 10.0
 \end{aligned}$$

$$TLM \left\{ \begin{array}{l} \#ofiterations = 14 \times [\#ofiter./cycle] \\ \Delta l = 100\mu m \end{array} \right\}.$$

The comparison between the FEM and TLM is presented in figure 5.5 where the magnitude of the magnetic field is given at $y = 12.25mm$ (through the middle of the aperture) for x varying from $1mm$ to $21.75mm$. As may be observed, there is a very good agreement between both methods.

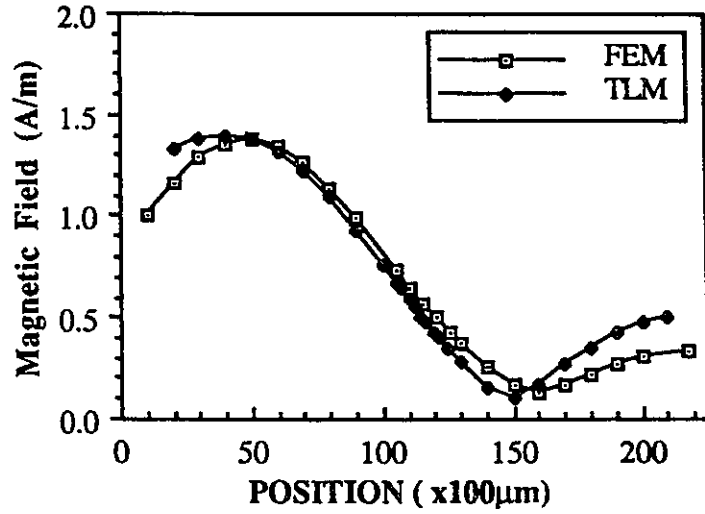


Figure 5.5: Frequency domain comparison between FEM and TLM, immunity case.

5.2.3 Time Domain Comparison Between FEM and TLM

To ensure that the TLM method be able to follow the field variations through the lossy material, we will limit the “maximum frequency component” of the EMP type impinging field to $50GHz$. The period of a $50GHz$ signal is $T|_{50GHz} = 20psec$, therefore by setting the time, t' , at which the peak of the EMP occurs to $t' = T|_{50GHz}$, we make certain that most of the energy will be below $15GHz$ (about one quarter of $50GHz$).

The value of α and β are determined by taking the first derivative of equation (2.11) with respect to time and setting it equal to zero; from this the time at which the peak occurs may be determined

$$t' = \frac{1}{(\beta - \alpha)} \ln \left(\frac{\beta}{\alpha} \right) = T|_{50GHz}. \quad (5.9)$$

Thus α and β are obtained by setting one to a certain value and then determining the corresponding value of the other. In this analysis the value of α and β were chosen as

$$\alpha = 10^9 \text{ \& } \beta = 3 \times 10^{11}.$$

When using these values, the exact peak time t_l is calculated to be

$$t_l = 19.08psec.$$

The minimum number of iterations needed to properly characterize the situation is then determined. Ideally one would like to investigate the effect of the pulse until it dies out, but this isn't feasible. Therefore we shall analyse the problem from the initial time to the time at which the amplitude of the field is equal to or lower than one tenth of the peak pulse value, this will give a final time of

$$t_{fin} = 120t_l. \quad (5.10)$$

Also since the time step of TLM, Δt , is equal to the smallest step size, Δl , divided by the speed of light, c_0 , it is then directly related to the conductivity (see equations (4.38) - (4.40)). Therefore to obtain a practical number of iterations to complete the analysis, the conductivity of the material will be chosen to be equal to or lower than $5S/m$ (see Table 4.1). By choosing a conductivity of $5S/m$, the maximum step size (for TLM), Δl_{max} , then becomes approximately $200\mu m$, and this in turn gives us a maximum time step of $0.67psec$. Therefore to follow the pulse up to $t = 120t_l$ we need:

$$\frac{120 \times 19.08psec}{0.67psec} \simeq 3400 \text{ iterations.}$$

With this in mind, the time domain immunity analysis is solved for the following parameters (refer to figure 5.2)

$$\begin{aligned} LE &= 22.4mm & ; & & WE &= 4.0mm & ; & & HE &= 39.75mm \\ XM &= 43.5mm & ; & & YM &= 99.5mm & ; & & \alpha &= 10^9 \\ PVAIRG &= 19.5mm & ; & & VAIRG &= 10mm & ; & & \beta &= 3 \times 10^{11} \end{aligned}$$

$$TLM\{\#ofiterations = 3400; \Delta l = 200\mu m\}.$$

In figures 5.6&5.7, the comparison between FEM and TLM is presented for the magnitude of the magnetic field as a function of time taken at two positions inside the enclosure, ($x = 25mm, y = 25mm$) and ($x = 38mm, y = 25mm$) respectively.

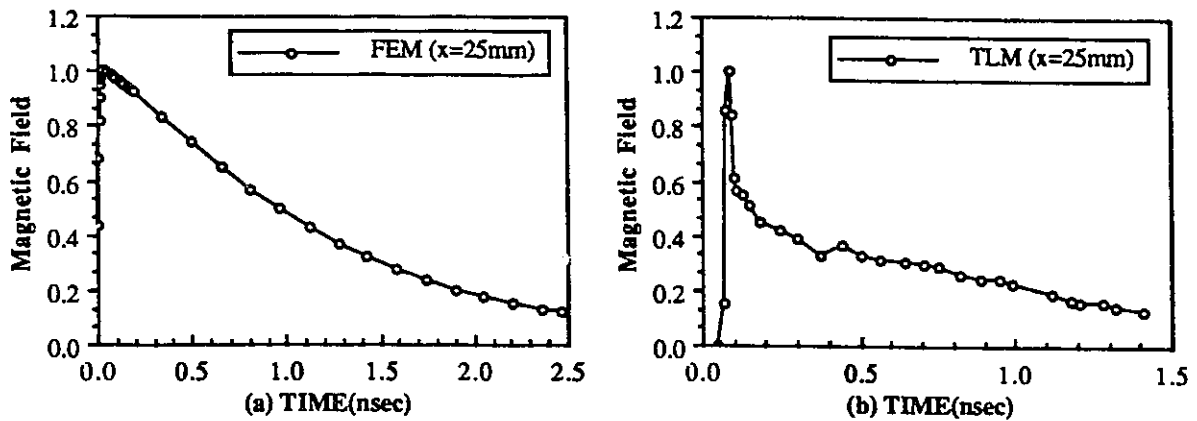


Figure 5.6: Time domain comparison between FEM and TLM for $x = y = 25mm$, immunity case.

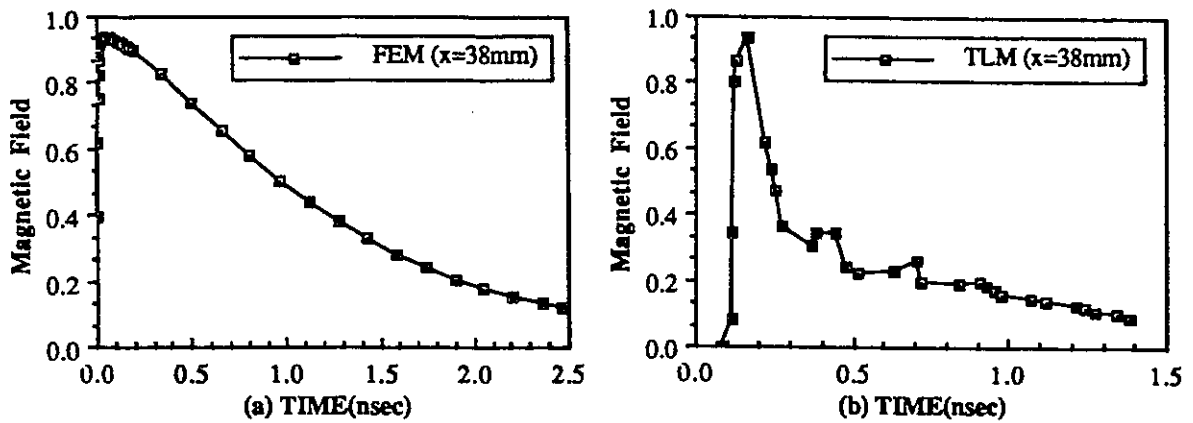


Figure 5.7: Time domain comparison between FEM and TLM for $x = 38mm$; $y = 25mm$, immunity case.

When comparing the results of both techniques one should keep in mind that in TLM, the frequency components lower than $1GHz$ ($f = \frac{c_0}{\Delta l \cdot \#iterations}$) do not contribute to the results since not enough iterations are considered for these frequencies. The effect that TLM has on the time response is observed in figures 5.6&5.7, since the lower frequency components do not figure in the results (too much iterations would be needed to include them), it lowers the overall field penetration.

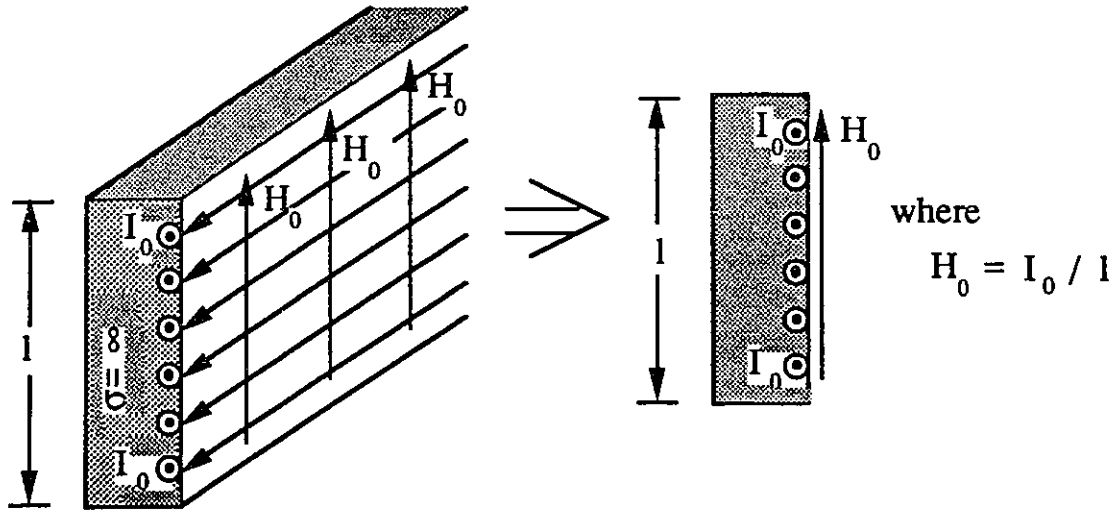


Figure 5.8: Constant magnetic field on a back plane.

5.3 Emission Case

Electromagnetic interference (EMI) caused by radiating electronic instruments is potentially harmful to nearby equipment. It is then of great importance to predict the shielding effectiveness of an enclosure used for confining fields.

In this section, the effect of the radiation from an electronic equipment surrounded by an enclosure with apertures is analysed via FEM and TLM. The comparison of both numerical techniques will validate the results of the analysis.

As the radiations from electronic devices is due to the fields associated with the currents flowing in a conductor or a back plane, for example, the analysis will be carried out through the magnetic field, \vec{H} . Now to be able to relate the conditions in both numerical techniques, the source current will be assumed to flow on the ground plane of a microstrip. The current will also be assumed to be uniformly distributed on the plane thus creating a constant magnetic field very close to the ground plane (see figure 5.8) [41]. To reduce memory requirements as well as the processing time, we have solved for two back planes in one enclosure so as to obtain a symmetry with respect to one axis as shown in figure 5.9. This will reduce the region to be analysed by one half and the processing time by at least one fourth. Furthermore, the thickness

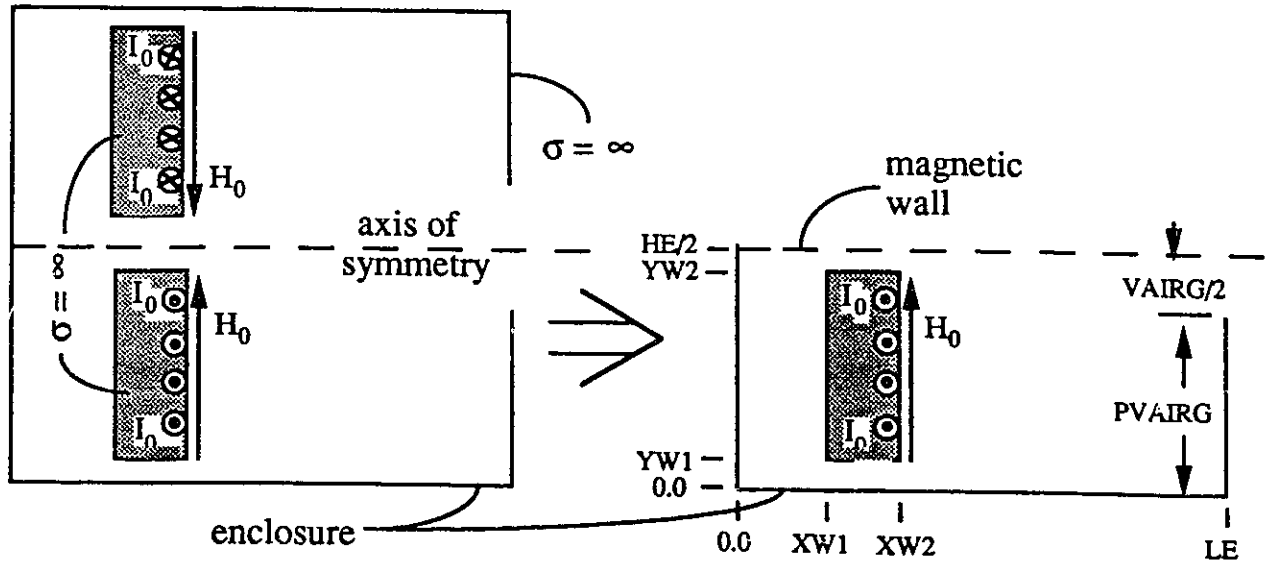


Figure 5.9: Emission problem under investigation.

and material of the enclosure's wall will be chosen in such a way that the diffusion process may be neglected, i.e. the skin depth is chosen to be much smaller than the wall thickness of the enclosure. The diffusion process is neglected in this section for two reasons:

- First to reduce the region to analyse for TLM
- Second, and more importantly, to demonstrate the versatility of both techniques in solving various situations.

5.3.1 Mathematical Formulation

TLM Formulation

The TLM formulation is the same as given in chapter 4. However, since we are interested in the magnetic fields rather than the electric fields, the boundary conditions associated with the source field will be imposed differently. For the shunt network

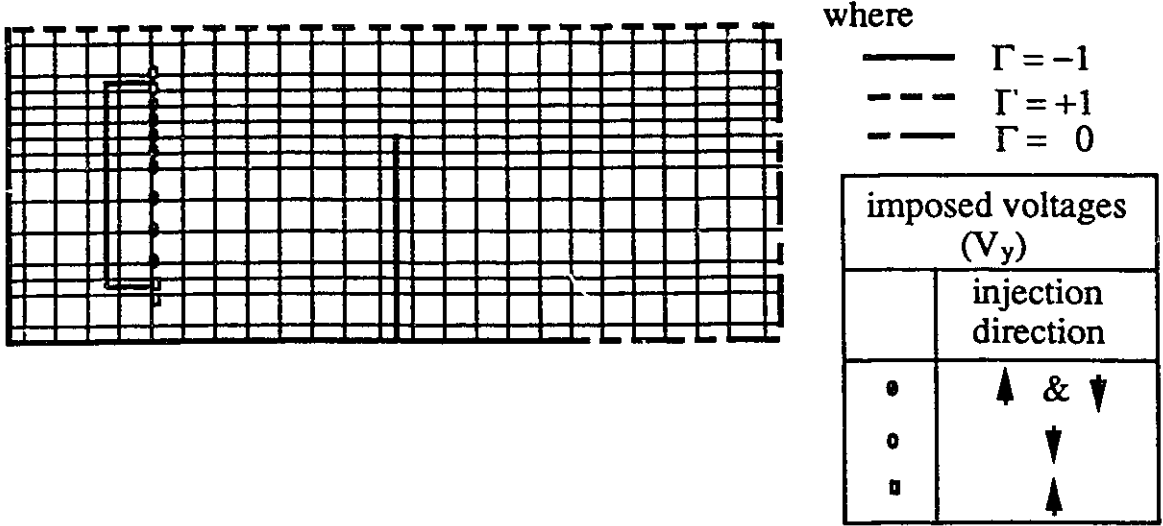


Figure 5.10: TLM mesh division for the emission study.

given in chapter 4, the fields are calculated as follows [42] (refer to figure 4.4):

$${}_k E_y \equiv {}_k V_y = \frac{2}{Y} \left(\sum_{m=1}^4 {}_k V_m^i + {}_k V_5^i Y_0 \right) \quad (5.11)$$

$$-{}_k H_x \equiv {}_k I_z = ({}_k V_2^i - {}_k V_4^i) / Z_0 \quad (5.12)$$

$${}_k H_z \equiv {}_k I_x = ({}_k V_1^i - {}_k V_3^i) / Z_0 \quad (5.13)$$

where $Y = 4 + Y_0$ and $Z_0 = \sqrt{L/C} = \sqrt{\mu_0/\epsilon_0}$ is the characteristic impedance of the lines. Therefore to create a constant magnetic field in the x -direction for example, one could set the incident voltages V_1 & V_3 at time $k * \Delta t$ to the same value, thus setting ${}_k H_z = 0$ and ${}_k H_x \neq 0$. This indirect approach is a very effective way of controlling the magnetic field in order to present a Dirichlet boundary condition in the TE formulation.

The magnetic walls are introduced to the incident voltage V_y by a reflection coefficient of $\Gamma = 1$ and the perfectly conducting walls by $\Gamma = -1$ [42]. As this is an unbounded problem, the transmission lines in the outside region may be terminated by loads matched to the characteristic impedance of air as seen by the lines, thus $\Gamma = 0$. The emission problem as given in figure 5.9 is represented in TLM, with the boundary conditions, as shown in figure 5.10.

FEM Formulation

This type of analysis will generate two magnetic field components, the horizontal and the vertical. Solving with FEM directly for the magnetic field, \vec{h} , would then require the solution of a system of equations that is proportional to twice the total number of nodes as there are two field components per node, i.e. two unknowns per node. This increases both the memory requirements and the CPU time. But solving for the magnetic vector potential, \vec{a} , one may reduce the number of unknowns by one half since there is only one component to solve for each node [43].

The magnetic vector potential, \vec{a} , is related to the magnetic flux density, \vec{b} , by

$$\vec{b}(t) = \nabla \times \vec{a}(t) \quad (5.14)$$

since the divergence of \vec{b} is always zero and the divergence of the curl of any vector is also zero. Substituting equation 5.14 into Faraday's law,

$$\nabla \times \vec{e}(t) = -\frac{\partial}{\partial t} \vec{b}(t) = -\nabla \times \left(\frac{\partial}{\partial t} \vec{a}(t) \right), \quad (5.15)$$

the following equivalence is obtained

$$\vec{e}(t) = -\frac{\partial}{\partial t} \vec{a}(t) - \nabla \phi \quad (5.16)$$

since the curl of the gradient of any scalar is always zero. Now to determine the characteristic equation associated with the vector and scalar potentials we replace the electric field and the flux density in the following equation

$$\nabla \times \vec{b}(t) = \mu\sigma \vec{e}(t) + \mu\epsilon \frac{\partial}{\partial t} \vec{e} \quad (5.17)$$

by equations (5.16) and (5.15) respectively, which gives

$$\nabla \times (\nabla \times \vec{a}(t)) = (\mu\sigma + \mu\epsilon \frac{\partial}{\partial t}) \left(-\frac{\partial}{\partial t} \vec{a}(t) - \nabla \phi \right) \quad (5.18)$$

$$\nabla^2 \vec{a}(t) - \mu\epsilon \frac{\partial^2}{\partial t^2} \vec{a}(t) - \mu\sigma \frac{\partial}{\partial t} \vec{a}(t) = \nabla \cdot (\nabla \vec{a}(t) + \mu\sigma \phi + \mu\epsilon \frac{\partial}{\partial t} \phi). \quad (5.19)$$

Equation (5.19) is very complicated as such, but by choosing the divergence of \vec{a} appropriately, it may be simplified considerably. A popular choice for the divergence of \vec{a} is the so-called Lorentz condition

$$\nabla \vec{a}(t) = -\mu\epsilon \frac{\partial}{\partial t} \phi. \quad (5.20)$$

But by choosing this, we are still left with a term on the right hand side of equation (5.19), which complicates the analysis. Thus an appropriate choice, in our case, would be the following [43],

$$\nabla \vec{a}(t) = -\mu\sigma\phi - \mu\epsilon \frac{\partial}{\partial t} \phi \quad (5.21)$$

which reduces equation (5.19) to the wave equation

$$\nabla^2 \vec{a}(t) - \mu\sigma \frac{\partial}{\partial t} \vec{a}(t) - \mu\epsilon \frac{\partial^2}{\partial t^2} \vec{a}(t) = 0. \quad (5.22)$$

By using this characteristic equation, only the boundary conditions need to be modified and not the core of the FEM formulation as presented in chapter 3.

The magnetic vector potentials, as defined in (5.14), is normal to the magnetic field, i.e. parallel to any flow of current. Since the current in the back plane is assumed to flow in the z -direction only, the magnetic vector potential will then have but one component directed in the z -axis. The relationship between these two magnetic “quantities” is as follows

$$\vec{h}(t) = \frac{1}{\mu} \nabla \times (a_z(t) \hat{z}) = \frac{1}{\mu} \left[\hat{x} \frac{\partial}{\partial y} a_z(t) - \hat{y} \frac{\partial}{\partial x} a_z(t) \right] \quad (5.23)$$

for a one-component formulation of \vec{a} .

The source field $h_0(t)$, a Dirichlet boundary, is then mapped to an inhomogeneous Neumann boundary in the magnetic vector formulation, given as

$$\frac{\partial \vec{a}(t)}{\partial \hat{n}} = -\mu_0 h_0(t) \hat{z} \quad (5.24)$$

where the normal \hat{n} is pointing outside of the region. This boundary condition is incorporated in the final system of equations through the surface integral matrix, U ,

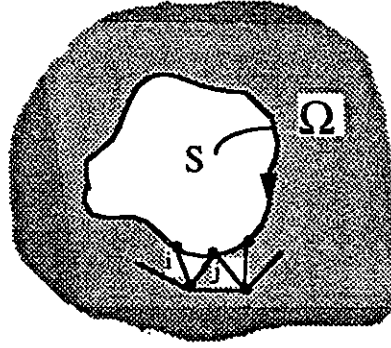


Figure 5.11: Inhomogeneous Neumann boundary.

given in equation (3.24). The shape function used to approximate the field on the surface is a contour type of function with the value a_i on node i and a_j on j [44]

$$\vec{a}(s, t) = \hat{z} \left(a_i(t) \frac{s_j - s}{s_j - s_i} + a_j(t) \frac{s_i - s}{s_i - s_j} \right) \quad (5.25)$$

in which s is a contour variable and s_i & s_j are the node positions of the segment l (see figure 5.11). The surface integral matrix, U , is then obtained as follows

$$\begin{aligned} U_{ij} &= \frac{\partial}{\partial a_i(t)} \int_{s_i}^{s_j} \left[2 \cdot \left(a_i(t) \frac{s_j - s}{s_j - s_i} + a_j(t) \frac{s_i - s}{s_i - s_j} \right) \hat{z} \cdot (-\mu_0 h_0(t) \hat{z}) \right] ds \\ &= -2\mu_0 h_0(t) \int_{s_i}^{s_j} \left(\frac{s_j - s}{s_j - s_i} \right) ds \\ &= -2\mu_0 h_0(t) \frac{(s_j - s_i)}{2} \end{aligned} \quad (5.26)$$

and similarly

$$U_{ji} = 2\mu_0 h_0(t) \frac{(s_i - s_j)}{2}. \quad (5.27)$$

Now since the region analysed is unbounded, a special type of element will be needed to somehow bound the region. One such type of elements are the infinite elements first introduced by Ungless [45] as reciprocal decay elements. But since Pissanetzky [46] has brought forward a simple and effective infinite element formulation, it will be chosen for this analysis.

The infinite elements, seen in figure 5.12, have two nodes on the boundary (i & j) and two nodes at infinity. To make the analysis more attractive and simpler, a new

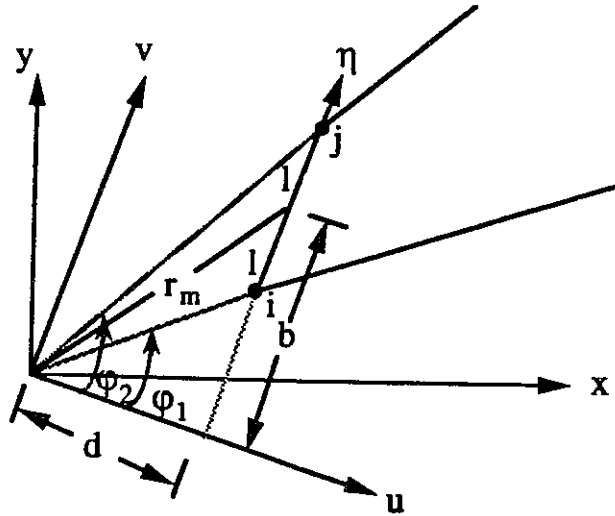


Figure 5.12: The infinite element.

coordinate system is chosen for each element. This rectangular coordinate system (u, v) has the v -axis parallel to the segment in question $(i - j)$. The angle ϕ is measured counter-clockwise from the u -axis and the length of the segment $i - j$ is $2l$.

The shape function in this case will vary linearly along the segment $i - j$ and will have the value of a_i and a_j on nodes i and j respectively

$$\vec{a}_{i-j}(t) = \hat{z} \frac{1}{2} [(1 - \eta)a_i(t) + (1 + \eta)a_j(t)] \quad (5.28)$$

where η is a coordinate that varies linearly along $i - j$ given as

$$\eta = \frac{d}{l} \tan \phi - \frac{b}{l}. \quad (5.29)$$

The coordinate η will then have the value of -1 when $a = a_i$, and of 1 when $a = a_j$.

The shape function should also decay as a function of r , the distance from the origin, towards infinity. Then, in terms of polar coordinates (r, ϕ) , the shape function is given as

$$\vec{a}(r, \phi, t) = \hat{z} \frac{f(r)}{2f(d/\cos\phi)} [(1 - \eta)a_i(t) + (1 + \eta)a_j(t)] \quad (5.30)$$

in which $d/\cos\phi$ is the distance from the origin to a particular point on the segment (when $r = d/\cos\phi$, equation (5.30) becomes equivalent to (5.28)).

When considering the case of reciprocal decay, $f(r) = 1/r^n$ with $n \geq 1$, the shape functions become

$$\vec{a}(r, \phi, t) = \hat{z} \frac{d^n}{2r^n \cos^n \phi} [(1 - \eta)a_i(t) + (1 + \eta)a_j(t)] \quad (5.31)$$

or in terms of the rectangular coordinate system u, v

$$\vec{a}(u, v, t) = \hat{z} \frac{d^n}{2u^n} \left[\left(1 + \frac{b}{l} - \frac{dv}{lu}\right) a_i(t) + \left(1 - \frac{b}{l} + \frac{dv}{lu}\right) a_j(t) \right]. \quad (5.32)$$

The contribution of the infinite elements to the final system of equations given in (3.24) is with respect to the matrices S and T . The contribution to the S matrix is [46]

$$\begin{aligned} S_{ii} &= \frac{1}{6nd} \left[(4n^2 + 2n + 1)l - 6nb + \frac{3r_m^2}{l} \right] \\ S_{ij} = S_{ji} &= \frac{1}{6nd} \left[(2n^2 - 2n - 1)l - \frac{3r_m^2}{l} \right] \\ S_{jj} &= \frac{1}{6nd} \left[(4n^2 + 2n + 1)l + 6nb + \frac{3r_m^2}{l} \right] \end{aligned} \quad (5.33)$$

and to the T matrix (see Appendix B),

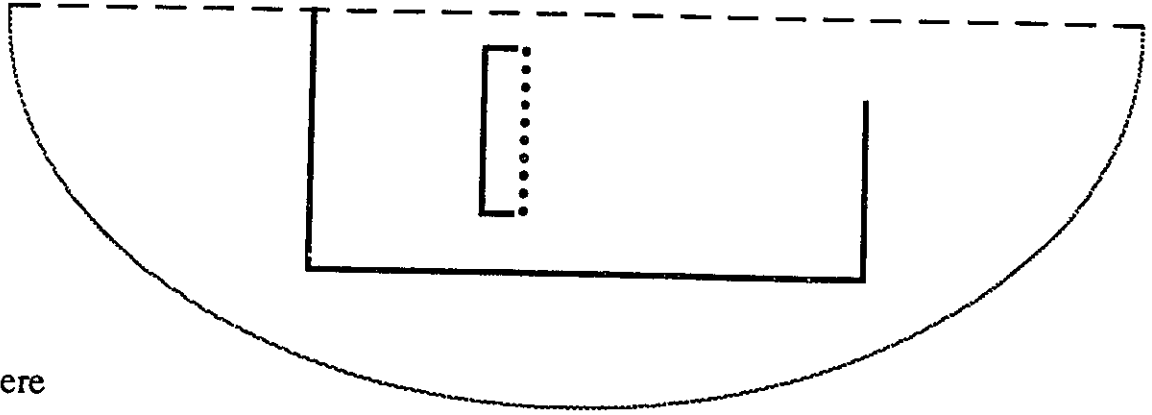
$$\begin{aligned} T_{ii} &= T_{jj} = \frac{2dl}{(3n - 3)} \\ T_{ij} &= T_{ji} = \frac{dl}{(3n - 3)} \end{aligned} \quad (5.34)$$

where $n \geq 2$.

The magnetic walls are introduced in the FEM by homogeneous Neumann boundary conditions ($\frac{\partial \vec{a}(t)}{\partial \vec{n}} = 0$) and the perfectly conducting walls by a Dirichlet boundary ($\vec{a}(t) = 0$). Therefore the emission problem as given in figure 5.9 is represented in FEM, with the boundary conditions, as shown in figure 5.13

5.3.2 Frequency Domain Comparison Between FEM and TLM

In the emission analysis, the walls of the enclosure are set to a high conductivity such that the skin depth is much lower than the wall thickness. This is readily obtained



where

- Dirichlet boundary $\{a(t) = 0\}$
- - Homogeneous Neumann boundary $\{\partial a(t)/\partial n = 0\}$
- ... Inhomogeneous Neumann boundary $\{\partial a(t)/\partial n = -\mu h_0(t)\}$
- Infinite elements

Figure 5.13: FEM boundary condition for the emission study.

by choosing an enclosure with a wall thickness of let's say 0.5mm and a conductivity of $0.6 \times 10^8 S/m$ (as for copper material) and with an operating frequency of 1GHz. With these choices, the skin depth is 243 times smaller than the wall thickness, thus a perfectly conducting wall may be assumed.

For such analysis, the limiting factors are again imposed by TLM but this time are determined by the cutoff frequency of the network and the number of iterations needed to reach steady-state. For a non-dielectric region, equation (4.37) determines the frequencies that are below the cutoff point. The precision of the TLM mesh size will be set to 1mm, for which the cutoff frequency is 21GHz. Therefore by choosing the frequency of analysis to be 1GHz we ensure a well posed TLM model.

Referring to figure 5.9, the parameters of the problems are listed below

$$\begin{aligned}
 LE &= 0.2m & ; & & HE/2 &= 0.1m \\
 XW1 &= 0.05m & ; & & XW2 &= 0.055m \\
 YW1 &= 0.05m & ; & & YW2 &= 0.087m \\
 PVAIRG &= 0.075m & ; & & VAIRG/2 &= 0.025m \\
 f &= 1.0GHz
 \end{aligned}$$

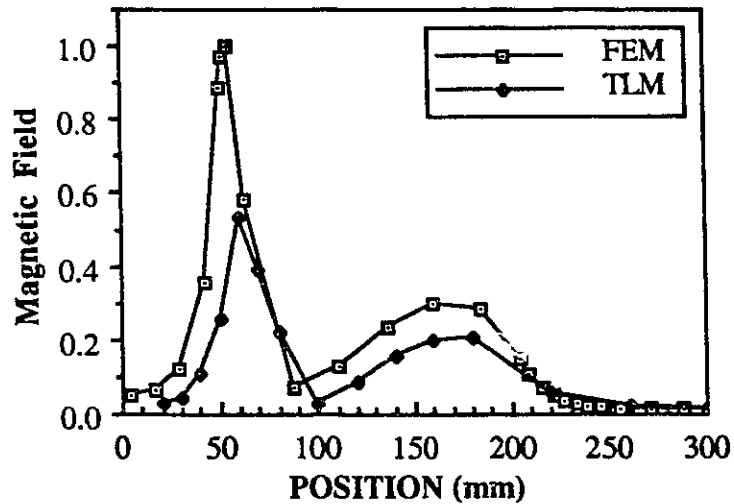


Figure 5.14: Frequency domain comparison between FEM and TLM, emission case.

$$TLM \left\{ \begin{array}{l} \#ofiterations = 15 \times [\#ofiter./cycle] \\ \Delta l = 1.0mm \end{array} \right\}.$$

In figure 5.14, the results of the analysis by both numerical techniques are presented for the magnitude of the magnetic fields as a function of the x -position at $y = 0.1m$ (in the middle of the aperture). Notice how close they compare. This comparison is extremely important as it shows very well the adaptability of both CAD tools in modeling complex boundary conditions such as a field created by a current source.

5.3.3 Time Domain Comparison Between FEM and TLM

The time domain analysis for the emission case is also conducted for an EMP type signal. The reason for choosing such a time signature is mainly for the simplicity of implementation in both tools. The analogy to a real situation could be as follows : an EMP field inducing a current, with a similar time signature, in a power line, finds its way into an improperly filtered enclosure on the back plane of a microstrip, thus radiating and affecting nearby equipment that were initially well filtered.

In this analysis, the current source will have the same time signature as the EMP

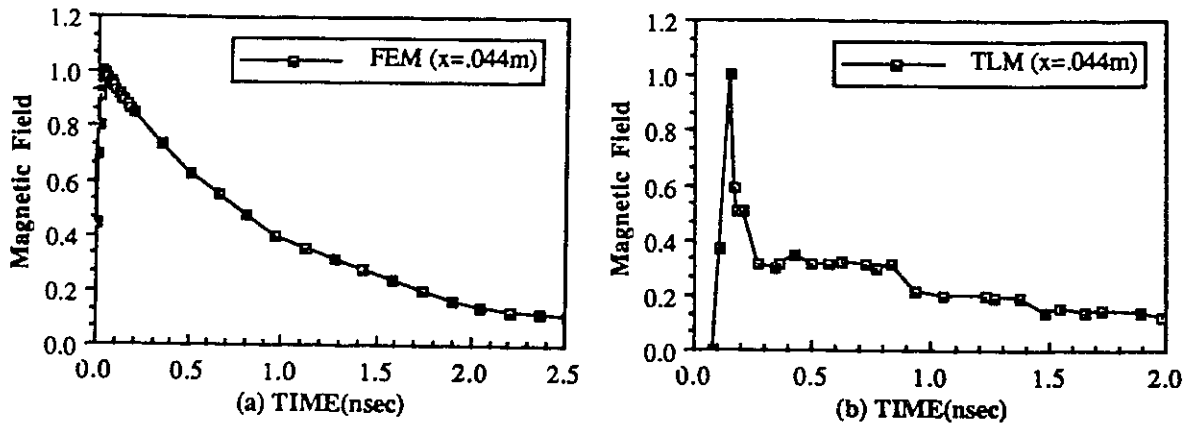


Figure 5.15: Time domain comparison between FEM and TLM, emission case.

type field from section 5.2.3. This current source will therefore generate a magnetic field of the same shape. The problem to investigate in the time domain emission analysis has the following parameters (see figure 5.9)

$$\begin{aligned}
 LE &= 0.04m & ; & & HE/2 &= 0.02m \\
 XW1 &= 0.01m & ; & & XW2 &= 0.011m \\
 YW1 &= 0.01m & ; & & YW2 &= 0.0174m \\
 PVAIRG &= 0.015m & ; & & VAIRG/2 &= 0.005m \\
 \alpha &= 10^9 & ; & & \beta &= 3 \times 10^{11}
 \end{aligned}$$

$$TLM\{\#ofiterations = 5000; \Delta l = 200\mu m\}.$$

The results of this analysis are presented in figure 5.15 in which the magnetic field's magnitude is plotted as a function of time at the position ($x = 0.044m$, $y = 0.019m$). In the TLM results the frequency components lower than 500 GHz do not figure in the results since, as explained in section 5.2.3, not enough iterations are considered for these frequencies which has the effect of reducing the overall field radiations.

5.4 Discussion

The comparison between these two completely different numerical techniques has greatly increased our confidence in the CAD tool for predicting the shielding effectiveness of enclosures.

The near perfect agreement in the frequency immunity analysis has shown us the ability of both techniques to predict the shielding effectiveness of enclosures with apertures. In the emission frequency analysis, the comparisons have demonstrated the adaptability of both methods to various situations.

In the time domain analysis some insights, into the TLM method, were brought forward. Mainly that the analysis of wide frequency band signals is not feasible because the effects of the lower frequencies are not included in this analysis initially. Nevertheless, in the initial and latter stage of the analysis, both techniques compare fairly well.

The analysis of the two types of situations, namely the immunity and the emission cases, has shown us the versatility of both methods.

Chapter 6

Time-Domain Analysis of Complex Shielding Situations with FEM

6.1 Introduction

In the previous chapter, both numerical techniques were proven to be very effective in predicting the shielding effectiveness of enclosures with apertures. Their comparison has greatly increased our confidence in solving such problems via CAD tools; even the emission analysis which has a much more complicated formulation yields a fairly good comparison between these two completely different numerical techniques. The tools at this point may be applied confidently to much more complex situations. Although TLM could also be used to analyse the problems presented in this section, only FEM will be used as it is more versatile for these types of analyses.

The analysis is conducted in the time domain since studies, in this domain, are rarely performed. The reason why this type of analysis is infrequent is the lack of measurement scheme to carry out such a complex investigation (especially for fast

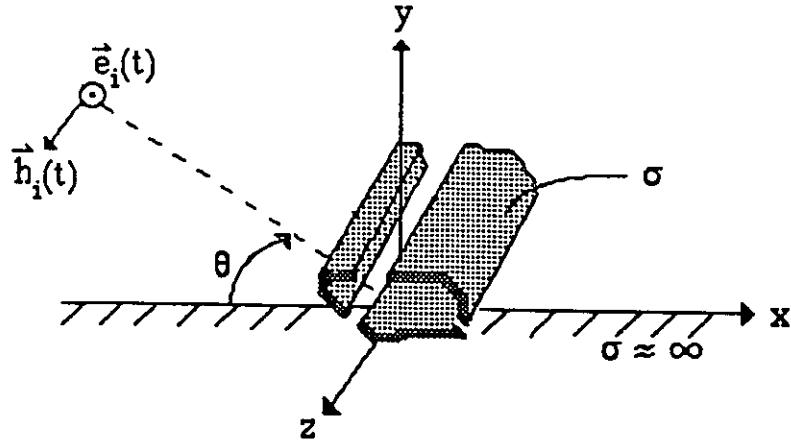


Figure 6.1: General immunity problem to investigate.

transients). The difficulty in measuring/predicting the field variations and penetrations in the time domain may be overcome by the introduction of CAD tools such as the ones presented here. With these tools, more possibilities exist now for the exploration of this new field.

As it was previously stated in chapter 5, “the length of the enclosure is assumed to be much longer than its width or height”, thus making it possible to reduce a three-dimensional problem into a two-dimensional one. The complexity of the problem is then diminished without sacrificing too much the generality of the analysis.

6.2 Immunity Analysis

The problem of interest consists of predicting the time-domain shielding performance of any arbitrarily shaped enclosure with apertures. The enclosure, lying above a ground plane of infinite conductivity, is subjected to a time varying plane wave impinging at a certain angle θ , as shown in figure 6.1.

The main interest of this analysis is to investigate the shielding performance of enclosures illuminated by a high-altitude nuclear electromagnetic pulse (HNEMP), therefore the study is conducted in the far field region for which the impinging fields are plane waves [20]. The fields can then be decomposed into TE and TM propagating

modes and analysed separately, thus reducing the number of field components from three to one, thereby reducing the system of equations to be solved by a factor of three. Both modes are treated in the FEM code presented here (see Appendix C).

6.2.1 Considerations

The fact that the enclosure is lying above a perfect ground plane ($\sigma = \infty$) may be taken into consideration by making use of the mirror image concept, as explained in section 5.2.

The use of a numerical technique such as the FEM requires that the problem be enclosed within a bounded region. In this analysis the field is known at a distance far from the enclosure therefore the region under investigation may then be enclosed by an imaginary Dirichlet boundary at a certain distance from the enclosure. The field values at this boundary are calculated by superimposing the impinging fields to the ground reflected fields. This imaginary boundary is chosen to be a half sphere of radius r equal to ten times the enclosure's longest dimension ¹. To obtain the value of the field on the half sphere as a function of the impinging field, location and time, one needs to first calculate the distance from the real and image sources to any point on the half sphere as shown in figure 6.2.

In figure 6.2, $d_i(\phi)$ and $d_{im}(\phi)$, are respectively the distance from the real and image sources to a certain position on the sphere of radius r and R_s is the distance of the source with respect to the enclosure. Since the impinging fields are plane waves, we may set R_s to any value, thus R_s is chosen to be equal to r . The distances are given in the following

$$d_i(\phi) = r(1 - \cos(\theta - \phi)) \quad (6.1)$$

$$d_{im}(\phi) = r(1 - \cos(\theta + \phi)). \quad (6.2)$$

Now from equations (6.1) and (6.2), the field value at any position on the half sphere,

¹The reason for specifying such a large radius is to allow the scattered fields on the enclosure to be negligible (although the option for including the scattered field is provided in the program)

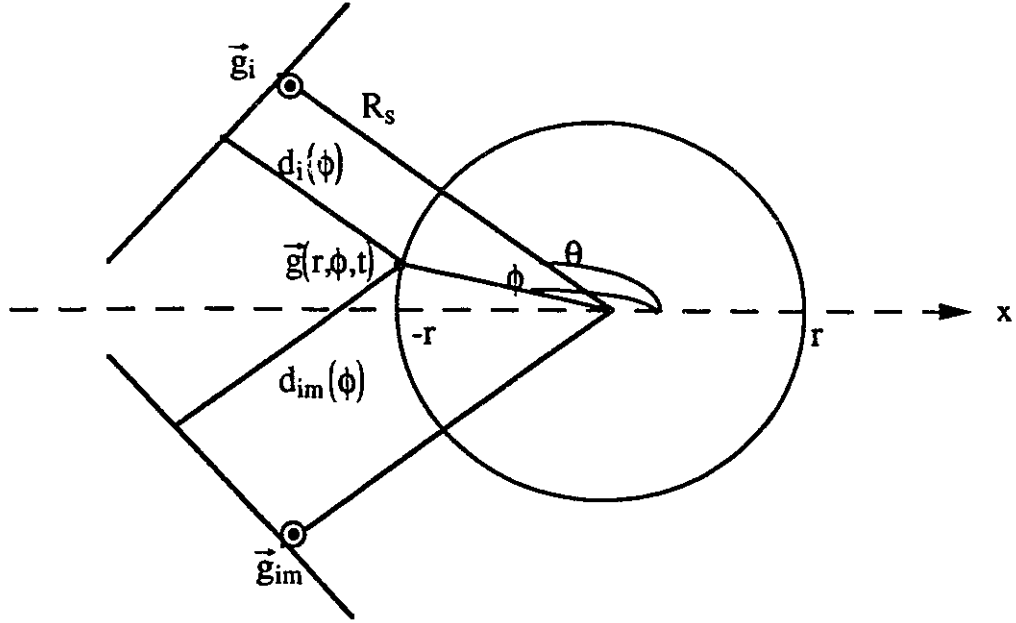


Figure 6.2: Distance from the real and image source to a boundary point.

when neglecting the scattered fields on the enclosure, is calculated as follows:

$$\begin{aligned}
 \vec{g}(r, \phi, t) &= \vec{g}_i \left(t - \frac{d_i(\phi)}{c_0} \right) + \vec{g}_{im} \left(t - \frac{d_{im}(\phi)}{c_0} \right) \\
 &= \vec{g}_i \left(t - \frac{d_i(\phi)}{c_0} \right) + \Gamma \vec{g}_i \left(t - \frac{d_{im}(\phi)}{c_0} \right)
 \end{aligned} \tag{6.3}$$

where $\Gamma = -1$ for the TE case and $\Gamma = +1$ for the TM case.

The enclosure analysed is presented in figure 6.3 where R_s is the distance to the source, θ , the angle of incidence, r , the radius of the half sphere boundary and $HE, LE, WE, PVAIRG, VAIRG$ correspond to the geometry of the enclosure. The division into triangular finite elements is similar to that of figure 6.4 only with a more refined mesh.

6.2.2 Results

The penetration of an NEMP incident field through an enclosure with apertures, similar to that shown in figure 6.3 is investigated. The geometry and field parameters

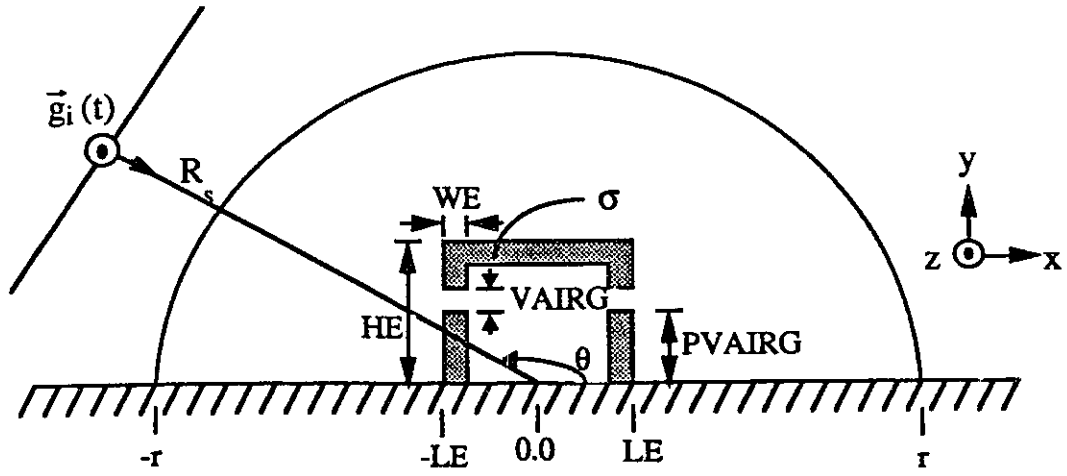


Figure 6.3: The analysed enclosure (immunity).

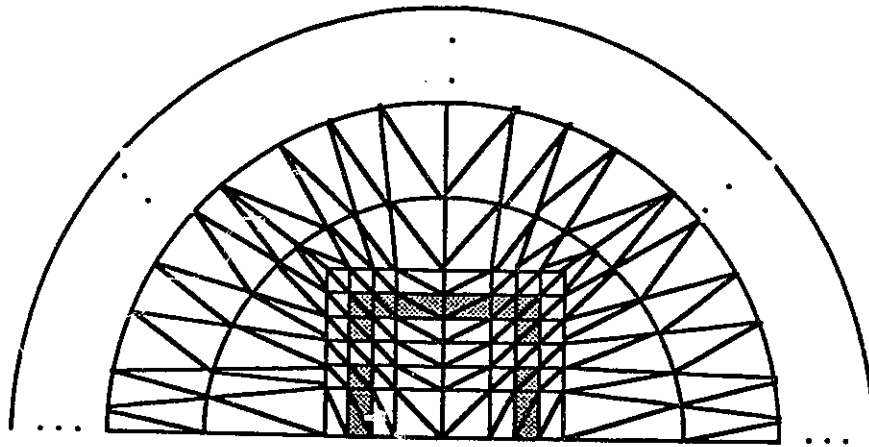


Figure 6.4: Division into FEs of region (immunity).

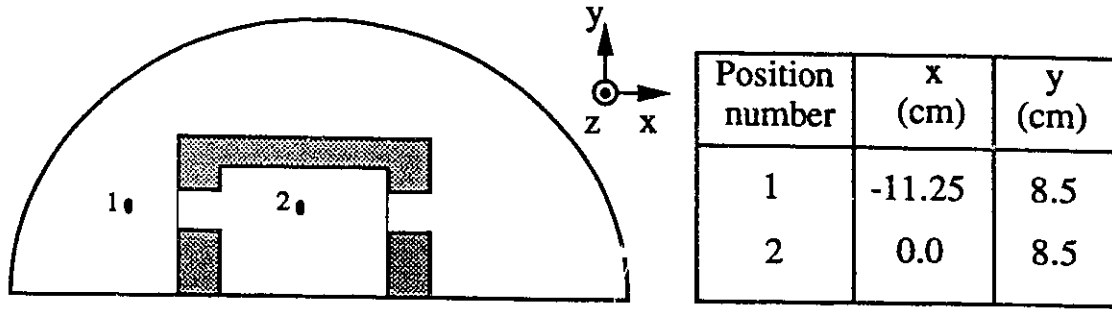


Figure 6.5: Position of the field calculation.

of the problem are given as :

$$LE = 0.1m \quad HE = 0.1m \quad WE = 0.1mm \quad PV AIRG = 0.08m$$

$$VAIRG = 0.01m \quad R_s = r = 1.0m \quad \theta = 160^\circ$$

$$E_0 = 5.25 \times 10^4 V/m \quad H_0 = E_0/\eta_0 = 1.39 \times 10^2 A/m$$

$$\alpha = 4.0 \times 10^6 \quad \beta = 4.76 \times 10^8$$

where E_0 and H_0 correspond respectively to the electric and magnetic field constants as in equation (2.11) and η_0 is the free space characteristic impedance ($\eta_0 = \sqrt{\frac{\mu_0}{\epsilon_0}} \approx 377\Omega$).

The results of this analysis are plotted in figures 6.6 to 6.9 for which the numbers 1 & 2 determine the position of the field calculation points (see figure 6.5).

In figures 6.6 and 6.8 the electric and magnetic field penetration are plotted as a function of time. Notice here the time delay and the flatter response of the predicted magnetic field in the middle of the enclosure. The effect of the ground plane on the electric field signature is shown in figure 6.6, the waveform reveals to be rather complex due to the ground plane reflections.

The shielding effectiveness (SE) of enclosures is generally defined in the frequency domain as the ratio of the measured or calculated field without the enclosure to the field with the enclosure [47].

$$SE(\omega) = 20 \log_{10} \left\{ \frac{|\vec{G}_{no\ enclosure}(\omega)|}{|\vec{G}_{with\ enclosure}(\omega)|} \right\} \quad (6.4)$$

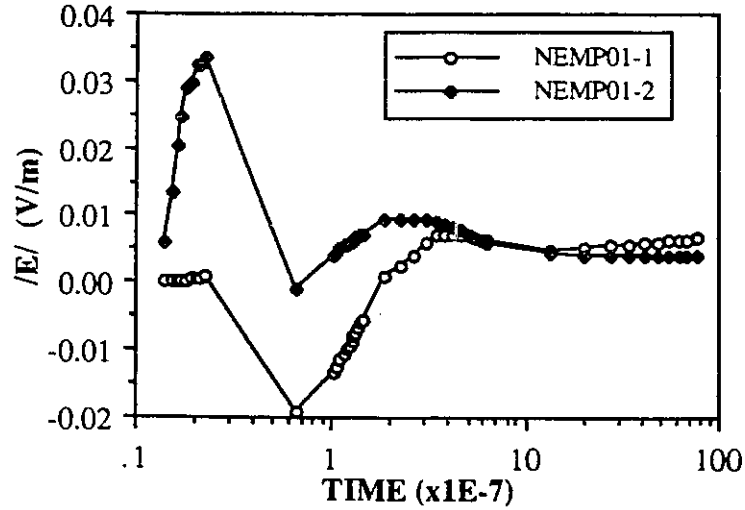


Figure 6.6: Electric field penetration at positions 1 & 2.

where \vec{G} is the field in question. In this analysis we define the time domain shielding effectiveness as

$$SE(t) = 20 \log_{10} \left\{ \frac{|\vec{g}_{no\ enclosure}(t)|}{|\vec{g}_{with\ enclosure}(t)|} \right\} \quad (6.5)$$

which is also given in decibels, dBs. Thus the time domain shielding effectiveness of the enclosure presented here, is plotted in figures 6.7 and 6.9 for the position #2 inside the enclosure for both TE and TM cases, respectively. It is seen that initially the SE of the enclosure is very high since the higher frequency components of the impinging field are greatly attenuated by the enclosure, but as time progress, the lower frequency components predominate thus reducing the overall shielding effectiveness.

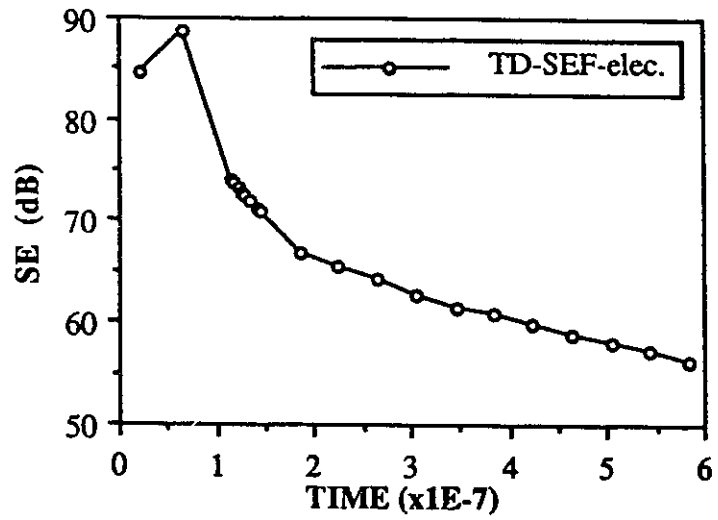


Figure 6.7: Time domain electric SE at position 2.

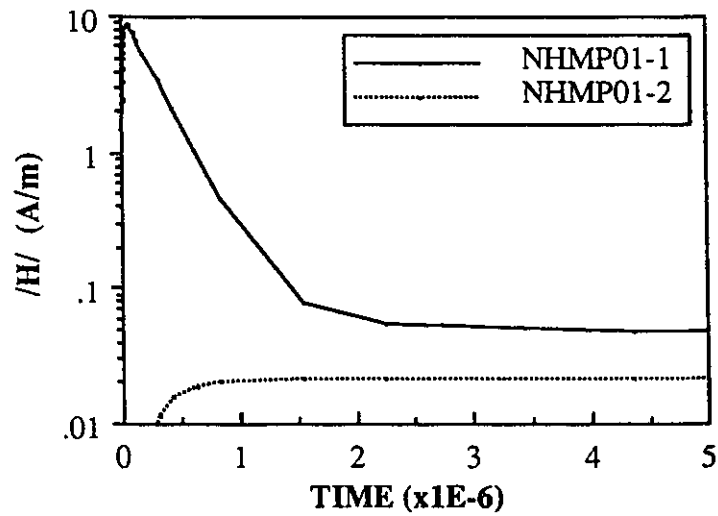


Figure 6.8: Magnetic field penetration at positions 1 & 2.

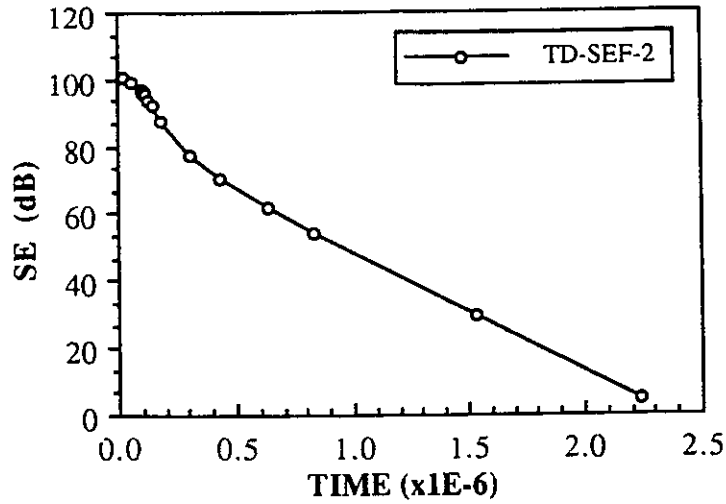


Figure 6.9: Time domain magnetic SE at position 2.

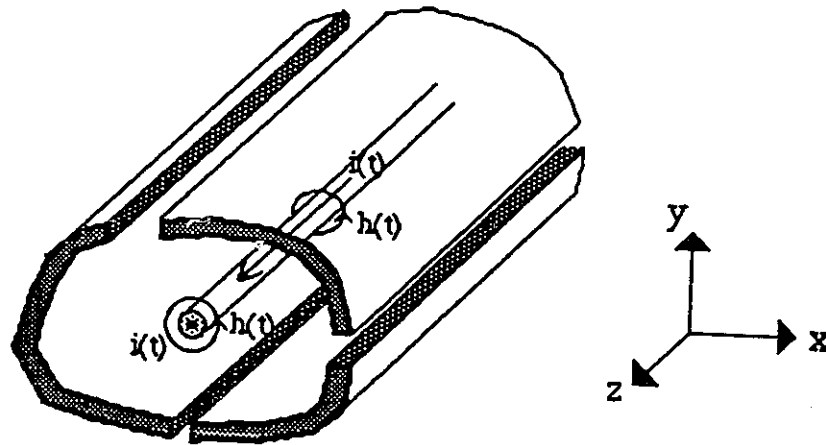


Figure 6.10: General emission problem under investigation.

6.3 Emission Analysis

This section treats the time-domain shielding effectiveness of an enclosure in which a radiating conductor is located. Contrary to the immunity case, we are interested in keeping as much energy as possible confined within the enclosure and its walls. The conductor, situated inside an arbitrarily shaped enclosure, is carrying a time varying current from which an associated magnetic field is generated (see figure 6.10).

The interest here lies in the analysis of the shielding performance of an enclosure in which a current flowing in a conductor, has a time signature similar to a digital pulse

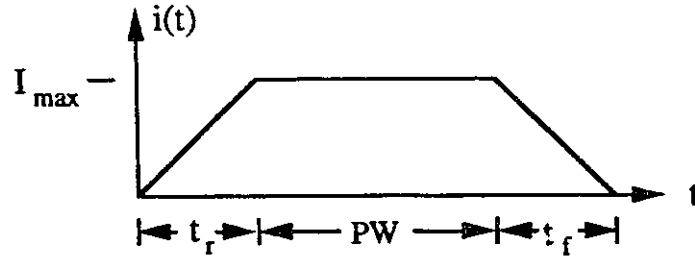


Figure 6.11: Current time signature.

signal. This signal will be assumed to have a rise and fall time varying linearly and a constant magnitude throughout the pulse width (see figure 6.11). The associated magnetic field will have the same shape as the current and a magnitude that is governed by the following equation [41]

$$h(t) = \frac{i(t)}{2\pi a} \quad (6.6)$$

where a is the radius of the conductor. Equation 6.6 is valid at a close proximity of the conductor. Again, to reduce the size of the final system of equations to be solved, the analysis is conducted using the magnetic vector potential, $\vec{a}(t)$, see section 5.3.1 for more details.

6.3.1 Considerations

The comparison, in section 5.3, between FEM and TLM for the emission case was carried out by neglecting the diffusion process and also by imposing symmetry to the problem. This was done to limit the processing time required by the TLM method, especially in the time domain analysis. Here neither a low skin depth nor a symmetry shall be imposed. We will then be at liberty to place the conductor anywhere within the enclosure since the finite element division code (see Appendix D) is written for general problems.

The region of analysis is unbounded, thus there is a need for infinite elements to bound such a region. The derivation of these infinite elements is found in section 5.3.1 as well as in Appendix B.

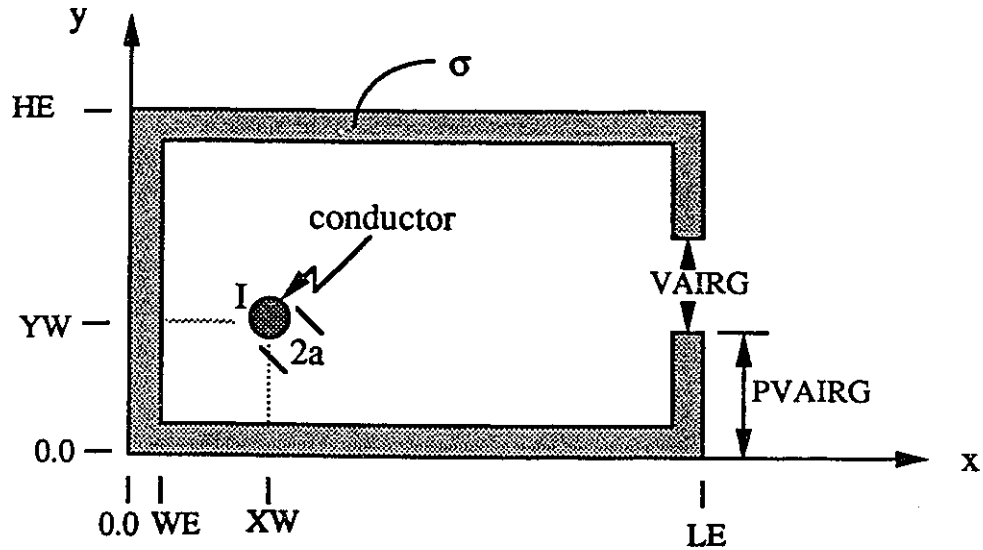


Figure 6.12: The analysed enclosure (emission).

The emission problem analysed is shown in figure 6.12 where LE , HE , WE , $PVAIRG$, $VAIRG$ correspond to the geometry of the enclosure, XW and YW are the position of the conducting wire and σ is the conductivity of the walls.

6.3.2 Results

The emission problem under investigation has a wire conducting a current from a digital circuit that is inside an enclosure with an aperture, see figure 6.12. Two analysis were conducted in which the conductor was positioned differently. In one analysis the conductor is far from the aperture ($XW = 0.03m$, $YW = 0.03m$) and in the other it is set closer ($XW = 0.07m$, $YW = 0.07m$). The geometry and current parameters are given as follows

$$\begin{aligned}
 LE &= 0.1m & HE &= 0.1m & WE &= 0.1mm & 2a &= 1.0mm \\
 PVAIRG &= 0.045m & VAIRG &= 0.01m & \sigma &= 0.6 \times 10^8 S/m \\
 I_{max} &= 1.0mA & t_r &= 1.0ns & PW &= 10.0ns & t_f &= 1.0ns
 \end{aligned}$$

The effect of the current source position on the radiated energy is well observed in figure 6.14 where the time domain magnetic field is presented, in both cases, at

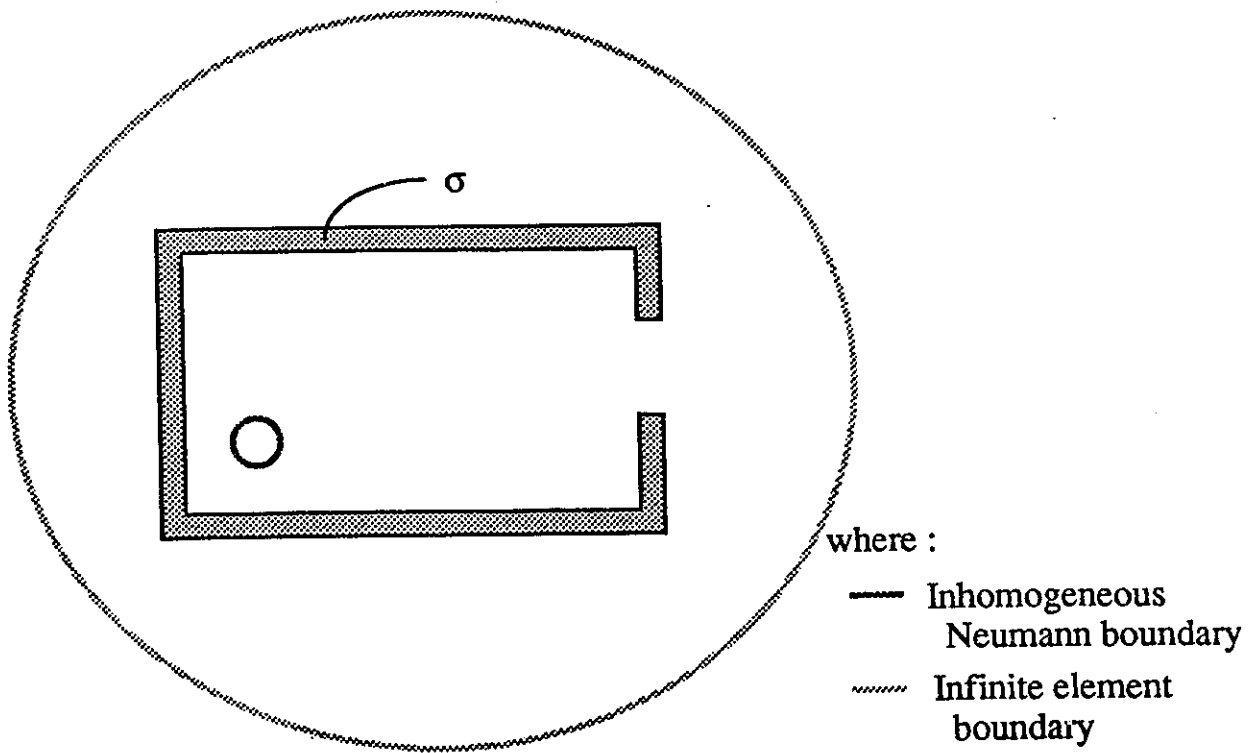


Figure 6.13: FEM boundary conditions (emission).

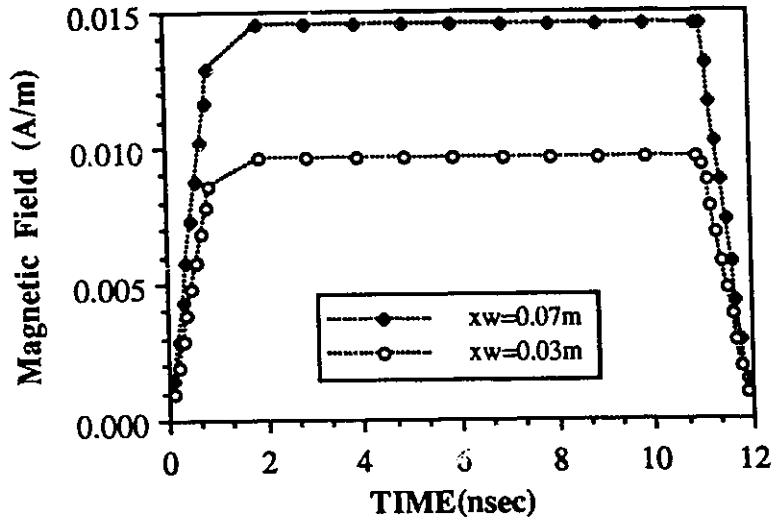


Figure 6.14: Magnetic field radiation for different positions of source.

a position just outside the enclosure's aperture ($x = 0.139m, y = 0.055m$). Notice that the radiated field almost doubles when the current source is near the aperture as compared to the furthest one.

Chapter 7

Conclusion

The object of this whole analysis was to develop a CAD tool capable of solving shielding effectiveness problems both in time and frequency domains. To achieve this task we have chosen the finite element method as the foundation for the tool. This numerical technique was proven over the years to be a very efficient and versatile method.

The CAD tool's performance was analysed in a methodic manner, starting from very simple problems and working our way up to complex situations. The derivation of an analytical solution as a means of validation, in the initial phase, proved to be an excellent choice as it provided a solid means by which the operating range of the numerical techniques may be determined. With the availability of this analytical formulation, rules of thumb regarding the diffusion process could be easily verified thus increasing our confidence in the numerical methods.

The introduction of a second tool gave us the opportunity to validate the finite element code for slightly more involved analysis which included apertures (needed to communicate with the outside world and to allow the dissipation of the heat generated by the electronic device) in the shield.

This comparison was very instructive for both techniques as it provided further information on their operating range. Moreover, it was seen that the time-domain

analysis through TLM is not feasible for wide frequency band signals because this analysis does not take into consideration the effect of the lower frequencies.

With full confidence in the CAD tool for predicting shielding effectiveness of enclosures within known limits, the tool was then applied to more realistic situations.

The main contributions of this thesis are summarized below:

- development of a CAD tool to predict shielding effectiveness of enclosures
- analytical formulation of both frequency and time diffusion problems
- devising new applications of the FEM
- devising new applications of the TLM method
- deriving rules of thumb for both FEM and TLM regarding diffusion problems
- time-domain analysis of the diffusion problem with FEM (to the authors' knowledge, no other analysis of such problems has been reported)
- better understanding of diffusion processes

Appendix A

Time Domain Analytical Formulation

The general solution for the time domain analysis is given in equations (2.14) and (2.15) and repeated here for convenience

$$\vec{E}_2(x, s) = \hat{z}[A \cos(\sqrt{-s\mu\sigma} x) + B \sin(\sqrt{-s\mu\sigma} x)] \quad (\text{A.1})$$

$$\vec{E}_3(x, s) = \hat{z}C \cosh(\sqrt{s^2\mu_0\epsilon_0} x) \quad (\text{A.2})$$

where A , B , and C are determined by the boundary conditions. The derivation leads to the following

$$A = L(s)(\cosh \phi \cos \gamma - \delta \sinh \phi \sin \gamma)/R(s) \quad (\text{A.3})$$

$$B = L(s)(\cosh \phi \sin \gamma + \delta \sinh \phi \cos \gamma)/R(s) \quad (\text{A.4})$$

$$C = L(s)/R(s) \quad (\text{A.5})$$

where

$$R(s) = [\cosh \phi \cos(\gamma - \theta) - \delta \sinh \phi \sin(\gamma - \theta)]$$

$$L(s) = \mathcal{L}\{E_0(e^{-\alpha t} - e^{-\beta t})\} = \frac{E_0(\beta - \alpha)}{(s + \alpha)(s + \beta)}.$$

Then (A.1) and (A.2) may be rewritten as:

$$\vec{E}_2(x, s) = \hat{z}P_2(s)/Q(s) \quad (\text{A.6})$$

$$\vec{E}_3(x, s) = \hat{z}P_3(s)/Q(s) \quad (\text{A.7})$$

in which

$$P_2(s) = E_0(\beta - \alpha) \{ (\cosh \phi \cos \gamma - \delta \sinh \phi \sin \gamma) \cos(\sqrt{-s\mu\sigma} x) + (\cosh \phi \sin \gamma + \delta \sinh \phi \cos \gamma) \sin(\sqrt{-s\mu\sigma} x) \}$$

$$P_3(s) = E_0(\beta - \alpha) \cosh(\sqrt{s^2\mu_0\epsilon_0} x)$$

$$Q(s) = (s + \alpha)(s + \beta)R(s)$$

The time domain response can be obtained by transforming (A.6) and (A.7) with Heaviside's formula

$$e(t) = \sum_{k=1}^{\infty} \frac{P(s_k)}{Q'(s_k)} e^{s_k t} \quad (\text{A.8})$$

with s_k being the poles of $Q(s)$ are given as:

- $s_1 = -\alpha$
- $s_2 = -\beta$
- s_n , the roots of the following equation

$$\tanh(\sqrt{s_n^2\mu_0\epsilon_0} D_1) = \eta_0 \sqrt{\frac{\sigma}{-s_n\mu}} \cot(\sqrt{-s_n\mu\sigma} (D_1 - D_2))$$

and $\dot{Q}(s)$ the derivative of $Q(s)$ with respect to s . The derivative of $Q(s)$ is given as

$$\dot{Q}(s) = \{(2s + \alpha + \beta)R(s) + (s + \alpha)(s + \beta)\dot{R}(s)\} \quad (\text{A.9})$$

where

$$\begin{aligned} \dot{R}(s) = & \left[\sinh \phi \frac{\partial \phi}{\partial s} \cos(\gamma - \theta) - \cosh \phi \sin(\gamma - \theta) \frac{\partial(\gamma - \theta)}{\partial s} - \right. \\ & \frac{\partial \delta}{\partial s} \sinh \phi \sin(\gamma - \theta) - \delta \cosh \phi \frac{\partial \phi}{\partial s} \sin(\gamma - \theta) - \\ & \left. \delta \sinh \phi \cos(\gamma - \theta) \frac{\partial(\gamma - \theta)}{\partial s} \right] \end{aligned}$$

$$\begin{aligned}\frac{\partial\phi}{\partial s} &= \sqrt{\mu_0\epsilon_0} D_1 \\ \frac{\partial\delta}{\partial s} &= \frac{-1}{2\eta_0} \sqrt{\frac{\mu}{-s\sigma}} \\ \frac{\partial(\gamma - \theta)}{\partial s} &= -\sqrt{\frac{\mu\sigma}{-s}} \frac{(D_1 - D_2)}{2}\end{aligned}$$

Now by introducing the poles of $Q(s)$ in equation (A.8), the time domain counterpart of (A.6) and (A.7) are obtained

$$\vec{e}_{2/3}(x, t) = \hat{z} \left[\frac{P_{2/3}(s_1)}{Q(s_1)} e^{s_1 t} + \frac{P_{2/3}(s_2)}{Q(s_2)} e^{s_2 t} + \sum_{n=1}^{\infty} \frac{P_{2/3}(s_n)}{Q(s_n)} e^{s_n t} \right] \quad (\text{A.10})$$

Appendix B

Infinite Element Contribution to the System of Equations

The contribution to the T matrix given in the general equation of (3.24) is calculated as follows. For the finite elements located on the open boundary (infinite boundary), an additional contribution must be included in the final system of equations. On this boundary, the field may be approximated by the following linear shape function, as described in section 5.3.1,

$$\begin{aligned}\vec{a}(u, v, t) &= \hat{z} \frac{d^n}{2u^n} \left[\left(1 + \frac{b}{l} - \frac{dv}{lu} \right) a_i(t) + \left(1 - \frac{b}{l} + \frac{dv}{lu} \right) a_j(t) \right] \\ &= \hat{z} [N_i a_i(t) + N_j a_j(t)]\end{aligned}\quad (\text{B.1})$$

Now replacing equation (B.1) into the integral related to the T matrix we get the following

$$T_l = \int_{\Omega_l} \left[N_i^2 a_i^2(t) + N_j^2 a_j^2(t) + 2N_i N_j a_i(t) a_j(t) \right] d\Omega_l \quad (\text{B.2})$$

where

$$\begin{aligned}N_i^2 &= \frac{d^{2n}}{4n^{2n}} \left(1 + \frac{b^2}{l^2} + \frac{d^2 v^2}{l^2 u^2} + \frac{2b}{l} - \frac{2dv}{lu} - \frac{2bdv}{l^2 u} \right) \\ N_j^2 &= \frac{d^{2n}}{4n^{2n}} \left(1 + \frac{b^2}{l^2} + \frac{d^2 v^2}{l^2 u^2} - \frac{2b}{l} + \frac{2dv}{lu} - \frac{2bdv}{l^2 u} \right)\end{aligned}$$

$$2N_i N_j = \frac{d^{2n}}{2n^{2n}} \left(1 - \frac{b^2}{l^2} - \frac{d^2 v^2}{l^2 u^2} + \frac{2bdv}{l^2 u} \right)$$

Taking the first variation of (B.2) with respect to the unknown and setting it equal to zero

$$T_{ii} = \frac{\partial}{\partial a_i(t)} T_l = 2 \int_d^\infty \int_{u(\frac{b-l}{d})}^{u(\frac{b+l}{d})} N_i^2 dv du \quad (\text{B.3})$$

$$T_{jj} = \frac{\partial}{\partial a_j(t)} T_l = 2 \int_d^\infty \int_{u(\frac{b-l}{d})}^{u(\frac{b+l}{d})} N_j^2 dv du \quad (\text{B.4})$$

$$T_{ij} = T_{ji} = \frac{\partial}{\partial a_{i-j}(t)} T_l = 2 \int_d^\infty \int_{u(\frac{b-l}{d})}^{u(\frac{b+l}{d})} N_i N_j dv du \quad (\text{B.5})$$

Solving the integrals of (B.3) to (B.5) gives

$$T_{ii} = T_{jj} = \frac{2dl}{(3n-3)} \quad (\text{B.6})$$

$$T_{ij} = T_{ji} = \frac{dl}{(3n-3)} \quad (\text{B.7})$$

Appendix C

FEM Computer Program for Immunity Problems in Time Domain


```

C >
C >> X,Y : COORDINATES OF THE TRIANGLE VERTICES < SEM00560
C >> SIGMA,MIUR : CONDUCTIVITY & RELATIVE PERMEABILITY OF TRIANGLE< SEM00570
C >> NV,DIRP : # ASSOCIATED TO EACH NODES & BOUNDARY CONDITION < SEM00580
C >> : SEM00590
C >> A,AP : THE VALUE & DERIVATIVE OF THE FIELD AT EACH NODE< SEM00600
C >> W,RWORK,IWORK : WORKING SPACE REQUIRED BY "DDASSL" < SEM00610
C >> R,S,SE : MATRICES RELATED TO THE SYSTEM OF EQUATIONS < SEM00620
C >> Q,TQ : REALTED TO P. SILVESTER'S SHAPE FUNCTIONS < SEM00630
C >> INFO : INFORMATIONS REQUIRED BY "DDASSL" < SEM00640
C >> PIMN1 - PIMX3 : CRITICAL ANGLES WHEN CONSIDERING SCATTERED FIELD< SEM00650
C >> VMIUO,CO : PERMEABILITY & SPEED OF LIGHT IN AIR < SEM00660
C >> : SEM00670
C >> : SEM00680
C >> : SEM00690
C >> : SEM00700
C >> : SEM00710
C >> : SEM00720
C >> : SEM00730
C >> : SEM00740
C >> : SEM00750
C >> : SEM00760
C >> : SEM00770
C >> : SEM00780
C >> : SEM00790
C >> : SEM00800
C >> : SEM00810
C >> : SEM00820
C >> : SEM00830
C >> : SEM00840
C >> : SEM00850
C >> : SEM00860
C >> : SEM00870
C >> : SEM00880
C >> : SEM00890
C >> : SEM00900
C >> : SEM00910
C >> : SEM00920
C >> : SEM00930
C >> : SEM00940
C >> : SEM00950
C >> : SEM00960
C >> : SEM00970
C >> : SEM00980
C >> : SEM00990
C >> : SEM01000
C >> : SEM01010
C >> : SEM01020
C >> : SEM01030
C >> : SEM01040
C >> : SEM01050
C >> : SEM01060
C >> : SEM01070
C >> : SEM01080
C >> : SEM01090
C >> : SEM01100

```

PARAMETER (NUNK=680,NTRI=1280,MLMX=90,MUMX=90)
IMPLICIT REAL*8(A-H,O-Z)

C >> VALUES FROM SUBROUTINE GETINF < SEM00750
REAL*8 PVAIRG(5),VAIRG(5),HE,LE,WE < SEM00760
REAL*8 SIG,MIURW,EO,ALPHA,BETA,TETAS < SEM00770
REAL*8 X1(10),Y1(10),X2(10),Y2(10),TINT(50) < SEM00780
INTEGER NVAIRG, TM, SCAT, NREG, IOUT, NINT < SEM00790

C >> VALUES FROM TRIANG SUBROUTINE < SEM00800
REAL*8 X(NUNK),Y(NUNK),SIGMA(NTRI),MIUR(NTRI),RB,RS < SEM00810
INTEGER NV(NTRI,3) < SEM00820
LOGICAL*4 DIRP(NUNK) < SEM00830

C >> VALUES FOR PROGRAM SEMPTDDA < SEM00840
REAL*8 A(NUNK),AP(NUNK) < SEM00850
REAL*8 RWORK(40+9*NUNK+(2*MLMX+MUMX+1)*NUNK) < SEM00860
REAL*8 RWORK(40+9*NUNK+NUNK*NUNK) < SEM00870
REAL*8 R(NUNK,MLMX+MUMX+1),S(NUNK,MLMX+MUMX+1),SE(3,3),T(200) < SEM00880
INTEGER Q(4,15,15,3),TQ(4,15,15),INFO(15),IWORK(20+NUNK) < SEM00890

C >> : SEM00900
C >> : SEM00910
C >> : SEM00920
C >> : SEM00930
C >> : SEM00940
C >> : SEM00950
C >> : SEM00960
C >> : SEM00970
C >> : SEM00980
C >> : SEM00990
C >> : SEM01000
C >> : SEM01010
C >> : SEM01020
C >> : SEM01030
C >> : SEM01040
C >> : SEM01050
C >> : SEM01060
C >> : SEM01070
C >> : SEM01080
C >> : SEM01090
C >> : SEM01100

THE FOLLOWING IS THE COMMON BLOCK LINK TO THE
SUBROUTINES AND FUNCTIONS

COMMON /GETIN/PVAIRG,VAIRG,HE,LE,WE,SIG,MIURW,EO,TINT,ALPHA,
& BETA,TETAS,X1,Y1,X2,Y2,NVAIRG, TM, SCAT, NREG, IOUT, NINT SEM00970
COMMON /TRIAN/X,Y,SIGMA,MIUR,RB,RS,NOPTL,NDIR,NV,ML,MU DIRP SEM00980
COMMON /PHI/PIMN1,PIMN2,PIMX1,PIMX2,PIMN3,PIMX3 SEM00990
& PIMN1,PIMN2,PIMN3,PIMX1,PIMX2,PIMX3 SEM01000
COMMON /OUT/A SEM01010
COMMON /RAS/R,S,NEQ/SIMPL/Q,TQ SEM01020

C >> : SEM01030
C >> : SEM01040
C >> : SEM01050
C >> : SEM01060
C >> : SEM01070
C >> : SEM01080
C >> : SEM01090
C >> : SEM01100

EXTERNAL RES,JAC

$P(A1,B1,A2,B2,A3,B3) = A1*B2 - A2*B1 + A2*B3 - A3*B2 + A3*B1 - A1*B3$

```

C > HERE ARE THE OPENING STATEMENTS < SEM01110
C > _____ < SEM01120
C OPEN(UNIT=7,FILE='NEMP01.INPUT',STATUS='OLD') SEM01130
C OPEN(UNIT=9,FILE='NEMP01.SEMPTDDA',STATUS='NEW') SEM01140
C PI = DACOS(-1.0D0) SEM01150
C VMIUO = 4.0D-07*PI SEM01160
C CO = 3.0D08 SEM01170
C SEM01180
C SEM01190
C SEM01200
C > THE FOLLOWING CALL GETS THE NECESSARY INFORMATION < SEM01210
C > CONCERNING THE GEOMETRY & THE FIELD < SEM01220
C > _____ < SEM01230
C CALL GETINF SEM01240
C SEM01250
C SEM01260
C > THE FOLLOWING CALL PRINTS THE INFORMATION ON THE OUTPUT FILE < SEM01270
C > _____ < SEM01280
C CALL PRNINF SEM01290
C SEM01300
C SEM01310
C SEM01320
C > THIS CALL TO "TRIANG" WILL TRIANGULARIZE THE REGION OF < SEM01330
C > INTEREST AND DETERMINE THE DIRICHLET BOUNDARIES < SEM01340
C > _____ < SEM01350
C CALL TRIANG SEM01360
C NN = NOPTL - NDIR SEM01370
C SEM01380
C SEM01390
C SEM01400
C > THIS CALL TO "PHICAL" WILL CALCULATE THE CRITICAL < SEM01410
C > ANGLES OF SCATTERING ON THE ENCLOSURE (IF REQUIRED) < SEM01420
C > _____ < SEM01430
C IF (SCAT .EQ. 1) CALL PHICAL SEM01440
C SEM01450
C SEM01460
C SEM01470
C SEM01480
C > NEXT WE DETERMINE THE TIME STEPS AND THE FINAL TIME < SEM01490
C > FOR THE ANALYSIS OF THIS PARTICULAR PROBLEM < SEM01500
C > _____ < SEM01510
C SEM01520
C SMIU = SIG*VMIUO*MIURW SEM01530
C TSTA = (RS - 0.990D0*RB)/CO SEM01540
C TPEAK = DLOG(BETA/ALPHA)/(BETA - ALPHA) SEM01550
C TDIF = SMIU*WE**2 SEM01560
C TPIN = TSTA + TPEAK + TDIF/(2.0D0**((DLOG10(ALPHA) - 4)) SEM01570
C EPEAK = DEXP(-ALPHA*TPEAK) - DEXP(-BETA*TPEAK) SEM01580
C DO 100 I = 2, 10000 SEM01590
C IF (-BETA*TPEAK*REAL(I) .LE. -120.D0) THEN SEM01600
C IF (DEXP(-ALPHA*TPEAK*REAL(I)) .LT. 0.10D0*EPEAK) GO TO 200 SEM01610
C ELSE SEM01620
C IF ((DEXP(-ALPHA*TPEAK*REAL(I)) - DEXP(-BETA*TPEAK*REAL(I))) SEM01630
C & .LT. 0.10D0*EPEAK) GO TO 200 SEM01640
C SEM01650

```

100	CONTINUE	SEMO1660
200	CONTINUE	SEMO1670
	TFIN = REAL(1)*TPEAK	SEMO1680
	N1 = I	SEMO1690
	TSTEP = TPEAK/10.000	SEMO1700
	IF (N1 .GT. 15) THEN	SEMO1710
	N1 = 15	SEMO1720
	TSTEP2 = TFIN/15.000	SEMO1730
	ELSE	SEMO1740
	TSTEP2 = TPEAK	SEMO1750
	ENDIF	SEMO1760
	TSTEP3 = TDIF	SEMO1770
	T(1) = TSTA	SEMO1780
C		SEMO1790
C		SEMO1800
C		SEMO1810
C		SEMO1820
C	> THEN THE DISCRETE TIMES ARE CALCULATED	SEMO1830
C		SEMO1840
C		SEMO1850
	K = 0	SEMO1860
	DO 300 I = 2 , 20 + N1	SEMO1870
	IF (I .LE. 10) THEN	SEMO1880
	T(I+K) = T(I+K-1) + TSTEP	SEMO1890
	ELSE IF (I .LE. 10 + N1) THEN	SEMO1900
	T(I+K) = T(I+K-1) + TSTEP2	SEMO1910
	ELSE	SEMO1920
	T(I+K) = T(I+K-1) + TSTEP3	SEMO1930
	ENDIF	SEMO1940
	IF (T(I+K-1) .LT. TPIN .AND. T(I+K) .GE. TPIN) THEN	SEMO1950
	STEPX = (T(I+K) - T(I+K-1))/10.000	SEMO1960
	T(I+K) = T(I+K-1) + STEPX	SEMO1970
	DO 400 K = 1 , 10	SEMO1980
	T(I+K) = T(I+K-1) + STEPX	SEMO1990
400	CONTINUE	SEMO2000
	K = K - 1	SEMO2010
	ENDIF	SEMO2020
300	CONTINUE	SEMO2030
C		SEMO2040
C		SEMO2050
C	> NEXT THE TIME REQUIRED BY THE USER ARE MERGED	SEMO2060
C	> WITH THE CALCULATED TIMES (IF THERE ARE ANY!!!)	SEMO2070
C		SEMO2080
C		SEMO2090
	IF (NINT .NE. 0) THEN	SEMO2100
	DO 500 I = 1 , NINT	SEMO2110
	TINT(I) = TINT(I) + TSTA	SEMO2120
500	CONTINUE	SEMO2130
	K = 1	SEMO2140
	DO 600 I = 2 , 30 + N1 + NINT	SEMO2150
	IF (T(I) .GT. TINT(K) .AND. T(I-1) .LT. TINT(K)) THEN	SEMO2160
	DO 700 J = 30 + N1 + K , I , -1	SEMO2170
	T(J) = T(J-1)	SEMO2180
700	CONTINUE	SEMO2190
		SEMO2200

```

        T(I) = TINT(K)
        K   = K + 1
        ENDIF
600     CONTINUE
        DO 800 I = 30 + N1 + K , 30 + N1 + NINT
            T(I) = TINT(K)
            K   = K + 1
800     CONTINUE
        ENDIF
C
C > THIS CALL TO "SIMPLX" DEFINES THE SHAPE FUNCTIONS AS
C > GIVEN IN P. SILVESTER'S BOOK ON THE FEM
C < SEMO2310
C < SEMO2320
C < SEMO2330
C < SEMO2340
        CALL SIMPLX(1)
C
C > WE CAN NOW SET-UP THE "S" AND "R" MATRICES AT THE
C > INITIAL TIME "T(1)"
C < SEMO2380
C < SEMO2390
C < SEMO2400
C < SEMO2410
        DO 900 I = 1 , NUNK
            DO 900 J = 1 , MLMX+MUMX+1
                R(I,J) = 0.000
                S(I,J) = 0.000
900     CONTINUE
        DO 1000 ITR = 1 , NOTR
            VM = VMIUO*MIUR(ITR)
            I1 = NV(ITR,1)
            I2 = NV(ITR,2)
            I3 = NV(ITR,3)
C        WRITE(9,111) ITR,I1,I2,I3,SIGMA(ITR),MIUR(ITR)
            DET = P(X(I1),Y(I1),X(I2),Y(I2),X(I3),Y(I3))
            IF (DET .EQ. 0.000) GO TO 8888
            AR = ABS(DET)/2.000
            R12 = (X(I1) - X(I2))*(X(I1) - X(I2))
            &      + (Y(I1) - Y(I2))*(Y(I1) - Y(I2))
            R13 = (X(I1) - X(I3))*(X(I1) - X(I3))
            &      + (Y(I1) - Y(I3))*(Y(I1) - Y(I3))
            R23 = (X(I2) - X(I3))*(X(I2) - X(I3))
            &      + (Y(I2) - Y(I3))*(Y(I2) - Y(I3))
            COSA1 = (R12 + R13 - R23)/(2.00*DSQRT(R12*R13))
            IF (COSA1 .GE. 1.000) WRITE(9,'(5HCOSA1,2X,F5.3)') COSA1
            COSA2 = (R12 + R23 - R13)/(2.00*DSQRT(R12*R23))
            IF (COSA2 .GE. 1.000) WRITE(9,'(5HCOSA2,2X,F5.3)') COSA2
            COSA3 = (R13 + R23 - R12)/(2.00*DSQRT(R13*R23))
            IF (COSA3 .GE. 1.000) WRITE(9,'(5HCOSA3,2X,F5.3)') COSA3
            COTA1 = COSA1/DSQRT(1.000 - COSA1*COSA1)
            COTA2 = COSA2/DSQRT(1.000 - COSA2*COSA2)
            COTA3 = COSA3/DSQRT(1.000 - COSA3*COSA3)
            DO 1100 I = 1 , 3
                DO 1100 J = 1 , 3
                    SE(I,J) = (COTA1*REAL(Q(1,I,J,1)) + COTA2*
& REAL(Q(1,I,J,2)) + COTA3*REAL(Q(1,I,J,3)))/2.000
                    SEMO2210
                    SEMO2220
                    SEMO2230
                    SEMO2240
                    SEMO2250
                    SEMO2260
                    SEMO2270
                    SEMO2280
                    SEMO2290
                    SEMO2300
                    SEMO2310
                    SEMO2320
                    SEMO2330
                    SEMO2340
                    SEMO2350
                    SEMO2360
                    SEMO2370
                    SEMO2380
                    SEMO2390
                    SEMO2400
                    SEMO2410
                    SEMO2420
                    SEMO2430
                    SEMO2440
                    SEMO2450
                    SEMO2460
                    SEMO2470
                    SEMO2480
                    SEMO2490
                    SEMO2500
                    SEMO2510
                    SEMO2520
                    SEMO2530
                    SEMO2540
                    SEMO2550
                    SEMO2560
                    SEMO2570
                    SEMO2580
                    SEMO2590
                    SEMO2600
                    SEMO2610
                    SEMO2620
                    SEMO2630
                    SEMO2640
                    SEMO2650
                    SEMO2660
                    SEMO2670
                    SEMO2680
                    SEMO2690
                    SEMO2700
                    SEMO2710
                    SEMO2720
                    SEMO2730
                    SEMO2740
                    SEMO2750
                
```

```

1100 CONTINUE
      DO 1200 I = 1 , 3
      L = NV(ITR,I)
      IF(DIRP(L)) GO TO 1200
      DO 1300 K = 1 , 3
      LC = NV(ITR,K)
      IF (.NOT.DIRP(LC)) THEN
      LC = LC - L + ML + 1
      S(L,LC) = S(L,LC) + SE(I,K)
      R(L,LC) = R(L,LC) + VM*SIGMA(ITR)*TQ(1,I,K)*AR/12.0DO
      ENDIF
1300 CONTINUE
1200 CONTINUE
1000 CONTINUE
C
C >-----<
C > THE "S" & "R" MATRICES NEED TO BE SHIFTED UP BY NDIR <
C > AND ALSO SIDEWAYS <
C >-----<
C
      DO 1400 I = 1 , NOPTL
      IF (DIRP(I)) GO TO 1400
      DO 1500 K = 1 , ML + MU + 1
      IF (K .EQ. 1) K1 = 0
1800 CONTINUE
      L = K + I - ML - 1 + K1
      IF (L .LT. 1 .OR. K .EQ. ML+1) GO TO 1500
      IF (L .GT. NOPTL) GO TO 1400
      IF (DIRP(L)) THEN
      IF (K .EQ. 1) THEN
      R(I,K) = 0.0DO
      S(I,K) = 0.0DO
      ELSE IF (K .EQ. ML+MU+1) THEN
      R(I,K) = 0.0DO
      S(I,K) = 0.0DO
      ELSE IF (K .LT. ML+1) THEN
      DO 1600 J = K , 2 , -1
      R(I,J) = R(I,J-1)
      S(I,J) = S(I,J-1)
1600 CONTINUE
      R(I,1) = 0.0DO
      S(I,1) = 0.0DO
      ELSE IF (K .GT. ML+1) THEN
      DO 1700 J = K , ML+MU
      R(I,J) = R(I,J+1)
      S(I,J) = S(I,J+1)
1700 CONTINUE
      R(I,ML+MU+1) = 0.0DO
      S(I,ML+MU+1) = 0.0DO
      K1 = K1 + 1
      GO TO 1800
      ENDIF
1500 CONTINUE
1400 CONTINUE

```

SEM02760
SEM02770
SEM02780
SEM02790
SEM02800
SEM02810
SEM02820
SEM02830
SEM02840
SEM02850
SEM02860
SEM02870
SEM02880
SEM02890
SEM02900
SEM02910
SEM02920
SEM02930
SEM02940
SEM02950
SEM02960
SEM02970
SEM02980
SEM02990
SEM03000
SEM03010
SEM03020
SEM03030
SEM03040
SEM03050
SEM03060
SEM03070
SEM03080
SEM03090
SEM03100
SEM03110
SEM03120
SEM03130
SEM03140
SEM03150
SEM03160
SEM03170
SEM03180
SEM03190
SEM03200
SEM03210
SEM03220
SEM03230
SEM03240
SEM03250
SEM03260
SEM03270
SEM03280
SEM03290
SEM03300

```

M1 = 0
DO 1900 I = 1 , NOPTL
  IF (.NOT. DIRP(I)) THEN
    DO 2000 K = 1 , ML + MU + 1
      R(I-M1,K) = R(I,K)
      S(I-M1,K) = S(I,K)
2000  CONTINUE
    ELSE
      M1 = M1 + 1
    ENDIF
1900 CONTINUE
C
C >-----<
C > SET-UP THE INITIAL VALUES FOR THE CALL TO "DDASSL" <
C >-----<
C
DO 2100 I = 1 , NN
  A(I) = 0.0D+00
  AP(I) = 0.0D+00
2100 CONTINUE
DO 2200 I = 1 , 15
  INFO(I) = 0
2200 CONTINUE
  INFO(5) = 1
  INFO(6) = 1
  IWORK(1) = ML
  IWORK(2) = MU
  NEQ = NN
  RTOL = 0.001D0
  ATOL = 0.001D0*EO
  LRW = 40 + 9*NUNK + (2*MLMX+MUMX+1)*NUNK
  C LRW = 40 + 9*NUNK + NUNK*NUNK
  LIW = 20 + NUNK
  IPAR = NEQ
C
C >-----<
C > SOLVE WITH "DDASSL", THE SUBROUTINE WRITTEN BY <
C > LINDA R. PETZOLD <
C >-----<
C
DO 2300 I = 2 , 30 + N1 + NINT
  CALL DDASSL(RES,NEQ,T(I-1),A,AP,T(I),INFO,RTOL,ATOL, IDID,RWORK,
  & LRW,IWORK,LIW,RPAR,IPAR,JAC)
  IF (IDID .LT. 0) THEN
    GO TO 2500
  ELSE
    IF (IOUT .EQ. 0) THEN
      CALL OUTP(T(I))
    ELSE
      DO 2400 J = 1 , NINT
        IF (T(I) .GE. 0.999D0*TINT(J) .AND. T(I) .LE. 1.001D0*
        & TINT(J)) CALL OUTP(T(I))
2400 CONTINUE
      ENDIF
    ENDIF
  ENDIF

```

SEM03310
SEM03320
SEM03330
SEM03340
SEM03350
SEM03360
SEM03370
SEM03380
SEM03390
SEM03400
SEM03410
SEM03420
SEM03430
SEM03440
SEM03450
SEM03460
SEM03470
SEM03480
SEM03490
SEM03500
SEM03510
SEM03520
SEM03530
SEM03540
SEM03550
SEM03560
SEM03570
SEM03580
SEM03590
SEM03600
SEM03610
SEM03620
SEM03630
SEM03640
SEM03650
SEM03660
SEM03670
SEM03680
SEM03690
SEM03700
SEM03710
SEM03720
SEM03730
SEM03740
SEM03750
SEM03760
SEM03770
SEM03780
SEM03790
SEM03800
SEM03810
SEM03820
SEM03830
SEM03840
SEM03850


```

ELSE
  WRITE(9,333) TIME
  WRITE(9,444)
ENDIF
N1 = 1
DO 100 I = 1 , NOPTL
  IF (NREG .EQ. 0) THEN
C
C >-----<
C > THE USER WANTS TO PRINT OUT THE WHOLE REGION <
C >-----<
    IF (DIRP(I)) THEN
      IF (Y(I) .EQ. 0.000 .AND. TM .EQ. 0) THEN
        WRITE(9,555) X(I),Y(I),0.000
      ELSE
        WRITE(9,555) X(I),Y(I),EFLD(TIME,X(I),Y(I),0)
      ENDIF
    ELSE
      WRITE(9,555) X(I),Y(I),A(N1)
      N1 = N1 + 1
    ENDIF
  ELSE
C
C >-----<
C > THE USER WANTS TO PRINT OUT ONLY PARTS OF THE REGION <
C >-----<
    DO 200 J = 1 , NREG
      IF ((X(I) .GE. X1(J) .AND. X(I) .LE. X2(J)) .AND.
        & (Y(I) .GE. Y1(J) .AND. Y(I) .LE. Y2(J))) THEN
        IF (DIRP(I)) THEN
          IF (Y(I) .EQ. 0.000 .AND. TM .EQ. 0) THEN
            WRITE(9,555) X(I),Y(I),0.000
          ELSE
            WRITE(9,555) X(I),Y(I),EFLD(TIME,X(I),Y(I),0)
          ENDIF
        ELSE
          WRITE(9,555) X(I),Y(I),A(N1)
          N1 = N1 + 1
        ENDIF
      ENDIF
    CONTINUE
  ENDIF
100 CONTINUE
111 FORMAT(////,10X,'/',30('-'),',',10X,'/',30X,'/',10X,
& '/ POSITION AND ASSOCIATED
&/,10X,'/',5X,'ELECTRIC FIELD (V/m)',
& ,5X,'/',10X,'/',6X,'AT T = ',E10.4,7X,'/',10X,'/',30X,'/',
& 10X,'/',30('-'),',',10X,'/',
222 FORMAT(6X,'X',11X,'Y',15X,'|E|',/)
333 FORMAT(////,10X,'/',30('-'),',',10X,'/',30X,'/',10X,
& '/ POSITION AND ASSOCIATED
&/,10X,'/',5X,'MAGNETIC FIELD (A/m)',
& ,5X,'/',10X,'/',6X,'AT T = ',E10.4,7X,'/',10X,'/',30X,'/',

```

SEM04410
SEM04420
SEM04430
SEM04440
SEM04450
SEM04460
SEM04470
SEM04480
SEM04490
SEM04500
SEM04510
SEM04520
SEM04530
SEM04540
SEM04550
SEM04560
SEM04570
SEM04580
SEM04590
SEM04600
SEM04610
SEM04620
SEM04630
SEM04640
SEM04650
SEM04660
SEM04670
SEM04680
SEM04690
SEM04700
SEM04710
SEM04720
SEM04730
SEM04740
SEM04750
SEM04760
SEM04770
SEM04780
SEM04790
SEM04800
SEM04810
SEM04820
SEM04830
SEM04840
SEM04850
SEM04860
SEM04870
SEM04880
SEM04890
SEM04900
SEM04910
SEM04920
SEM04930
SEM04940
SEM04950


```

C > SEM05510
C > THE "B" VECTOR (THE SOURCE VECTOR) NEED TO BE SET-UP < SEM05520
C > AT "TIME" < SEM05530
C > SEM05540
C > SEM05550
DO 200 ITR = 1 , NOTR SEM05560
  VM = VMIUO*MIUR(ITR) SEM05570
  I1 = NV(ITR,1) SEM05580
  I2 = NV(ITR,2) SEM05590
  I3 = NV(ITR,3) SEM05600
  DET = P(X(I1),Y(I1),X(I2),Y(I2),X(I3),Y(I3)) SEM05610
  IF (DET .EQ. 0.000) GO TO 9999 SEM05620
  AR = ABS(DET)/2.000 SEM05630
  R12 = (X(I1) - X(I2))*(X(I1) - X(I2)) SEM05640
  & + (Y(I1) - Y(I2))*(Y(I1) - Y(I2)) SEM05650
  R13 = (X(I1) - X(I3))*(X(I1) - X(I3)) SEM05660
  & + (Y(I1) - Y(I3))*(Y(I1) - Y(I3)) SEM05670
  R23 = (X(I2) - X(I3))*(X(I2) - X(I3)) SEM05680
  & + (Y(I2) - Y(I3))*(Y(I2) - Y(I3)) SEM05690
  COSA1 = (R12 + R13 - R23)/(2.DO*DSQRT(R12*R13)) SEM05700
  IF (COSA1 .GE. 1.000) WRITE(9, '(5HCOSA1,2X,F5.3)') COSA1 SEM05710
  COSA2 = (R12 + R23 - R13)/(2.DO*DSQRT(R12*R23)) SEM05720
  IF (COSA2 .GE. 1.000) WRITE(9, '(5HCOSA2,2X,F5.3)') COSA2 SEM05730
  COSA3 = (R13 + R23 - R12)/(2.DO*DSQRT(R13*R23)) SEM05740
  IF (COSA3 .GE. 1.000) WRITE(9, '(5HCOSA3,2X,F5.3)') COSA3 SEM05750
  COTA1 = COSA1/DSQRT(1.000 - COSA1*COSA1) SEM05760
  COTA2 = COSA2/DSQRT(1.000 - COSA2*COSA2) SEM05770
  COTA3 = COSA3/DSQRT(1.000 - COSA3*COSA3) SEM05780
  DO 300 I = 1 , 3 SEM05790
    DO 300 J = 1 , 3 SEM05800
      SE(I,J) = (COTA1*REAL(Q(1,I,J,1)) + REAL(COTA2*Q(1,I,J,2)) + SEM05820
        COTA3*REAL(Q(1,I,J,3)))/2.000 SEM05830
    CONTINUE SEM05840
  DO 400 I = 1 , 3 SEM05850
    L = NV(ITR,I) SEM05860
    IF(DIRP(L)) GO TO 400 SEM05870
    DO 500 K = 1 , 3 SEM05880
      LC = NV(ITR,K) SEM05890
      IF (DIRP(LC)) THEN SEM05900
        IF ((Y(LC) .NE. 0.000 .AND. TM .EQ. 0) .OR. SEM05910
          TM .EQ. 1) THEN SEM05920
          & B(L) = B(L) - EFLD(TIME,X(LC),Y(LC),0)*SE(I,K) - SEM05930
          & EFLD(TIME,X(LC),Y(LC),1)* SEM05940
          & VM*SIGMA(ITR)*TQ(1,I,K)*AR/12.000 SEM05950
        ENDIF SEM05960
      ENDIF SEM05970
    CONTINUE SEM05980
  DO 200 CONTINUE SEM05990
  CONTINUE SEM06000
C > SEM06010
C > THE "B" VECTOR NEED TO BE SHIFTED UP BY NDIR < SEM06020
C > SEM06030
C > SEM06040
C > SEM06050

```

N1 = 0	SEM06060
DO 600 I = 1 , NOPTL	SEM06070
IF (.NOT. DIRP(I)) THEN	SEM06080
B(I-N1) = B(I)	SEM06090
ELSE	SEM06100
N1 = N1 + 1	SEM06110
ENDIF	SEM06120
600 CONTINUE	SEM06130
C	SEM06140
C	SEM06150
C > WE THEN CALCULATE DELTA = G(TIME,A,AP)	SEM06160
C >	SEM06170
C	SEM06180
DO 800 I = 1 , NEQ	SEM06190
SUM = 0.000	SEM06200
DO 900 J = 1 , NEQ	SEM06210
K = J - I + ML + 1	SEM06220
IF (K .GT. 0 .AND. K .LE. ML+MU+1) THEN	SEM06230
SUM = SUM + R(I,K)*AP(J) + S(I,K)*A(J)	SEM06240
ENDIF	SEM06250
900 CONTINUE	SEM06260
DELTA(I) = SUM - B(I)	SEM06270
800 CONTINUE	SEM06280
RETURN	SEM06290
9999 CONTINUE	SEM06300
WRITE(9,*) ' ITR = ', ITR	SEM06310
WRITE(9,*) ' ITR = ', ITR	SEM06320
STOP	SEM06330
END	SEM06340
C	SEM06350
C	SEM06360
C >	SEM06370
C >	SEM06380
C >	SEM06390
C >	SEM06400
C >	SEM06410
C >	SEM06420
C >	SEM06430
C >	SEM06440
C >	SEM06450
C >	SEM06460
C	SEM06470
SUBROUTINE JAC (T,A,AP,PD,CJ,RPAR,IPAR)	SEM06480
PARAMETER (NUNK=680,NTRI=1280,MLMX=90,MUMX=90)	SEM06490
IMPLICIT REAL*8(A-H,O-Z)	SEM06500
C > VALUES FROM TRIANG SUBROUTINE	SEM06510
REAL*8 X(NUNK),Y(NUNK),SIGMA(NTRI),MIUR(NTRI),RB,RS	SEM06520
INTEGER NV(NTRI,3)	SEM06530
LOGICAL*4 DIRP(NUNK)	SEM06540
C > VALUES FOR SUBROUTINE JAC	SEM06550
REAL*8 A(NUNK),AP(NUNK),PD(2*ML+MU+1,IPAR)	SEM06560
REAL*8 R(NUNK,MLMX+MUMX+1),S(NUNK,MLMX+MUMX+1),T,CJ	SEM06570
C	SEM06580
C >	SEM06590
C >	SEM06600

```

C > THE FOLLOWING IS THE COMMON BLOCK LINK TO THE          < SEM06610
C > SUBROUTINES AND FUNCTIONS                               < SEM06620
C >-----< SEM06630
C COMMON /TRIAN/X,Y,SIGMA,MIUR,RB,RS,NOTR,NOPTL,NDIR,NV,ML,MU,DIRPSEM06640
COMMON /RAS/R,S,NEQ SEM06650
C SEM06660
C SEM06670
C SEM06680
C >-----< SEM06690
C > AS THE "S" AND "R" MATRICES ARE INDEPENDENT OF TIME, < SEM06700
C > THE JACOBIAN IS ALSO TIME INDEPENDENT                 < SEM06710
C >-----< SEM06720
C DO 100 I = 1 , NEQ SEM06730
  DO 100 J = 1 , NEQ SEM06740
    K = J - I + ML + 1 SEM06750
    IF (K .GT. 0 .AND. K .LE. ML+MU+1) THEN SEM06760
      IROW = I - J + ML + MU + 1 SEM06770
      PD(IROW,J) = S(I,K) + CJ*R(I,K) SEM06780
    ENDIF SEM06790
100 CONTINUE SEM06800
RETURN SEM06810
END SEM06820
C SEM06830
C SEM06840
C >-----< SEM06850
C > FUNCTION EFLD                                          < SEM06860
C >-----< SEM06870
C > THIS FUNCTION CALCULATES THE FIELD, AS A FUNCTION    < SEM06880
C > TIME, ON THE SPHERICAL BOUNDARY                     < SEM06890
C >-----< SEM06900
C >-----< SEM06910
C >-----< SEM06920
C >-----< SEM06930
C >-----< SEM06940
C >-----< SEM06950
C FUNCTION EFLD(TIME,XA,YA,IDER) SEM06960
C SEM06970
C SEM06980
C IMPLICIT REAL*8(A-H,O-Z) SEM06990
C PARAMETER (NUNK=680,NTRI=1280,MLMX=90,MUMX=90) SEM07000
C >-----< SEM07010
C > VALUES FROM SUBROUTINE GETINF SEM07020
C REAL*8 PVAIRG(5),VAIRG(5),HE,LE,WE SEM07030
C REAL*8 SIG,MIURW,EO,ALPHA,BETA,TETAS SEM07040
C REAL*8 X1(10),Y1(10),X2(10),Y2(10),TINT(50) SEM07050
C >-----< SEM07060
C > VALUES FROM TRIANG SUBROUTINE SEM07070
C REAL*8 X(NUNK),Y(NUNK),SIGMA(NTRI),MIUR(NTRI),RB,RS SEM07080
C INTEGER NV(NTRI,3) SEM07090
C >-----< SEM07100
C > VALUES FOR EFLD FUNCTION SEM07110
C REAL*8 TIME,XA,YA,PHI,HP,FACT(5),RF(5),TD(5),EFLD SEM07120
C >-----< SEM07130
C > THE FOLLOWING IS THE COMMON BLOCK LINK TO THE          < SEM07140
C > SUBROUTINES AND FUNCTIONS                               < SEM07150

```

```

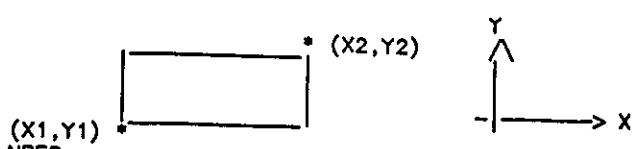
C >-----< SEM07160
C COMMON /GETIN/PVAIRG,VAIRG,HE,LE,WE,SIG,MIURW,EO,TINT,ALPHA, SEM07170
& BETA,TETAS,X1,Y1,X2,Y2,NVAIRG,TM,SCAT,NREG,IOUT,NINT, SEM07180
COMMON /TRIAN/X,Y,SIGMA,MIUR,RB,RS,NOTR,NOPTL,NDIR,NV,ML,MU,DIRP SEM07190
COMMON /PHI/PIMN1,PIMN1,PIMMX1,PIMN2,PIMN2,PIMMX2, SEM07200
& PIMN3,PIMX3 SEM07210
C CO = 3.0008 SEM07220
PHI = DATAN2(YA,XA) SEM07230
DO 100 I = 1, 5 SEM07240
  FACT(I) = 0.000 SEM07250
CONTINUE SEM07260
100 IF (TM .EQ. 0) THEN SEM07270
  IF (TM .EQ. 0) THEN SEM07280
    RF(1) = 1.000 SEM07290
    RF(2) = 0.000 SEM07300
    RF(3) = -1.000 SEM07310
    RF(4) = 0.000 SEM07320
    RF(5) = -1.000 SEM07330
  ELSE SEM07340
    RF(1) = 1.000 SEM07350
    RF(2) = 1.000 SEM07360
    RF(3) = 1.000 SEM07370
    RF(4) = 1.000 SEM07380
    RF(5) = 1.000 SEM07390
  ENDIF SEM07400
  IF (SCAT .EQ. 0) THEN SEM07410
    I1 = 2 SEM07420
    TD(1) = (RS-RB*DCOS(TETAS - PHI))/CO SEM07430
    FACT(1) = 1.000 SEM07440
    TD(2) = (RS-RB*DCOS(TETAS + PHI))/CO SEM07450
    FACT(2) = 1.000 SEM07460
  ELSE SEM07470
    I1 = 5 SEM07480
    IF (PHI .GE. PIMN1) THEN SEM07490
      TD(1) = (RS-RB*DCOS(TETAS - PHI))/CO SEM07500
      FACT(1) = 1.000 SEM07510
    ENDIF SEM07520
    IF (PHI .GE. PIMN1 .OR. PHI .LE. PIMMX1) THEN SEM07530
      TD(2) = (RS-RB*DCOS(TETAS + PHI))/CO SEM07540
      FACT(2) = 1.000 SEM07550
    ENDIF SEM07560
    IF (PHI .GE. PIMN2) THEN SEM07570
      HI = DSQRT(LE**2 + (-(LE + RB*DCOS(PHI))*DTAN(TETAS) + SEM07580
& RB*DSIN(PHI))**2) SEM07590
& TD(3) = ((LE + RB*DCOS(PHI))/DCOS(TETAS) + RS - SEM07600
& HI*DCOS(TETAS - PI/2.000 - DASIN(LE/HI)))/CO SEM07610
      FACT(3) = 1.000 SEM07620
    ENDIF SEM07630
    IF (PHI .GE. PIMN2 .AND. PHI .LE. PIMMX2) THEN SEM07640
      HIM = DSQRT(LE**2 + ((LE + RB*DCOS(PHI))*DTAN(TETAS) + SEM07650
& RB*DSIN(PHI))**2) SEM07660
& TD(4) = ((LE + RB*DCOS(PHI))/DCOS(TETAS) + RS - SEM07670
& HIM*DCOS(PI - TETAS - DACOS(LE/HIM)))/CO SEM07680
      FACT(4) = 1.000 SEM07690
    ENDIF SEM07700
  
```


	REAL*8	X(NUNK),Y(NUNK),SIGMA(NTRI),MIUR(NTRI),RB,RS	SEM08260
	INTEGER	NV(NTRI,3)	SEM08270
	LOGICAL*4	DIRP(NUNK)	SEM08280
C			SEM08290
C	>	----->	SEM08300
C	>	THE FOLLOWING IS THE COMMON BLOCK LINK TO THE	< SEM08310
C	>	SUBROUTINES AND FUNCTIONS	< SEM08320
C	>	----->	SEM08330
	COMMON	/GETIN/PVAIRG,VAIRG,HE,LE,WE,SIG,MIURW,EO,TINT,ALPHA,	SEM08340
&		BETA,TETAS,X1,Y1,X2,Y2,NVAIRG,TM,SCAT,NREG,IOUT,NINT	SEM08350
COMMON		/TRIAN/X,Y,SIGMA,MIUR,RB,RS,NOTR,NOPTL,NDIR,NV,ML,MU,DIRP	SEM08360
COMMON		/PHI/PIMN1,PIMN1,PIMX1,PIMN2,PIMM2,PIMX2,	SEM08370
&		PIMN3,PIMX3	SEM08380
C			SEM08390
	PI	= DACOS(-1.000)	SEM08400
C	LH2	= DSQRT(LE**2 + HE**2)	SEM08410
			SEM08420
	PIMN1	= TETAS - PI + DASIN((LH2*DSIN(DATAN(LE/HE) + TETAS -	SEM08430
&		PI/2.000))/RB)	SEM08440
PIMN1	=	PI - TETAS - DASIN(((LE - HE*DCOTAN(TETAS))*DSIN(TETAS))/	SEM08450
&		RB)	SEM08460
PIMX1	=	PI - TETAS + DASIN(((LE - HE*DCOTAN(TETAS))*DSIN(TETAS))/	SEM08470
&		RB)	SEM08480
PIMN2	=	-TETAS - DASIN((LH2*DSIN(DATAN(LE/HE) + TETAS -	SEM08490
&		PI/2.000))/RB)	SEM08500
PIMN2	=	TETAS - DASIN((LH2*DSIN(DATAN(LE/HE) - TETAS +	SEM08510
&		1.5000*PI))/RB)	SEM08520
PIMX2	=	TETAS + DASIN((LH2*DSIN(DATAN(LE/HE) + TETAS -	SEM08530
&		PI/2.000))/RB)	SEM08540
PIMN3	=	PI - TETAS + DASIN((LH2*DSIN(DATAN(LE/HE) - TETAS +	SEM08550
&		1.5000*PI))/RB)	SEM08560
PIMX3	=	PI - TETAS + DASIN((LH2*DSIN(DATAN(HE/LE) - TETAS +	SEM08570
&		PI))/RB)	SEM08580
C			SEM08590
	RETURN		SEM08600
	END		SEM08610
			SEM08620


```

WRITE(6,*) :
WRITE(6,*) :
WRITE(6,*) : FIRST WOULD YOU LIKE TO ANALYZE THE WHOLE
WRITE(6,*) : REGION (Y/N)?
READ(IUNIT, '(A1)') CHAR
IF (CHAR .EQ. 'Y' .OR. CHAR .EQ. 'y') GO TO 400
WRITE(6,10) :
WRITE(6,*) :
WRITE(6,*) :
WRITE(6,*) : HOW MANY REGIONS THEN WOULD YOU LIKE TO
WRITE(6,*) : ANALYZE (PLEASE DO ENTER LARGE ENOUGH
WRITE(6,*) : RECTANGULAR REGIONS AS THE
WRITE(6,*) : TRIANGULARIZATION IS AUTOMATED)
I1 = 0
500 WRITE(6,*) :
WRITE(6,*) : # OF REGIONS ?
READ(IUNIT,*) NREG
IF (NREG .GT. 10) THEN
WRITE(6,*) :
WRITE(6,*) : THE NUMBER OF MAXIMUM REGIONS IS TEN (10)
WRITE(6,*) : PLEASE ENTER OVER THE NUMBER OF REGIONS
IF (I1 .GT. 3) STOP
I1 = I1 + 1
GO TO 500
ENDIF
C
WRITE(6,*) :
WRITE(6,*) :
WRITE(6,*) :
WRITE(6,*) :
WRITE(6,*) :
WRITE(6,*) :
WRITE(6,*) :
DO 600 I = 1, NREG
WRITE(6,*) :
WRITE(6,*) : (20H FOR REGION #, I2, 15H PLEASE ENTER :) I
WRITE(6,*) : X1, Y1 ? (in meters)
READ(IUNIT,*) X1(I), Y1(I)
WRITE(6,*) : X2, Y2 ? (in meters)
READ(IUNIT,*) X2(I), Y2(I)
600 CONTINUE
400 CONTINUE
WRITE(6,10) :
WRITE(6,*) :
WRITE(6,*) :
WRITE(6,*) : AS A FINAL QUESTION, DO YOU PREFER TO SET
WRITE(6,*) : THE TIMES FOR AT WHICH THE FIELDS ARE TO
WRITE(6,*) : BE DETERMINED (OUT = 1), OR USE THE DEFAULT
WRITE(6,*) : VALUES CALCULATED INTERNALLY (OUT = 0)?
WRITE(6,*) : (IF YOU CHOOSE OUT = 1 SOME CRITICAL
WRITE(6,*) : TIME VALUES SHALL BE GIVEN TO YOU)
WRITE(6,*) :
WRITE(6,*) : OUT ?
READ(IUNIT,*) IOUT
IF (IOUT .EQ. 1) THEN

```



- * GET02760
- * GET02770
- * GET02780
- * GET02790
- * GET02800
- * GET02810
- * GET02820
- * GET02830
- * GET02840
- * GET02850
- * GET02860
- * GET02870
- * GET02880
- * GET02890
- * GET02900
- * GET02910
- * GET02920
- * GET02930
- * GET02940
- * GET02950
- * GET02960
- * GET02970
- * GET02980
- * GET02990
- * GET03000
- * GET03010
- * GET03020
- * GET03030
- * GET03040
- * GET03050
- * GET03060
- * GET03070
- * GET03080
- * GET03090
- * GET03100
- * GET03110
- * GET03120
- * GET03130
- * GET03140
- * GET03150
- * GET03160
- * GET03170
- * GET03180
- * GET03190
- * GET03200
- * GET03210
- * GET03220
- * GET03230
- * GET03240
- * GET03250
- * GET03260
- * GET03270
- * GET03280
- * GET03290
- * GET03300


```

C
WRITE(6,*) : GET03860
WRITE(6,*) : IF THE INVESTIGATION IS CARRIED OUT THROUGH 'GET03870
WRITE(6,*) : CONSTANT TIME STEPS ENTER 1, 0 OTHERWISE 'GET03880
WRITE(6,*) : 'GET03890
WRITE(6,*) : 1 or 0 ? 'GET03900
READ(IUNIT,*) NSTE 'GET03910
IF (NSTE .EQ. 0) THEN GET03920
DO 1000 I = 1 , NINT GET03930
WRITE(6,*) : GET03940
WRITE(6,*(40H PLEASE ENTER INTEGRATION TIME # ,I2)') I 'GET03950
WRITE(6,*) : (in seconds) 'GET03960
WRITE(6,*) : 'GET03970
READ(IUNIT,*) TINT(I) 'GET03980
WRITE(6,*) : 'GET03990
1000 CONTINUE 'GET04000
ELSE 'GET04010
WRITE(6,*) : 'GET04020
WRITE(6,*) : PLEASE ENTER THE INTEGRATION TIME STEP 'GET04030
WRITE(6,*) : (in seconds) 'GET04040
WRITE(6,*) : 'GET04050
READ(IUNIT,*) TINTS 'GET04060
WRITE(6,*) : 'GET04070
TINT(1) = TINTS 'GET04080
DO 1100 I = 2 , NINT 'GET04090
TINT(I) = TINT(I-1) + TINTS 'GET04100
1100 CONTINUE 'GET04110
ENDIF 'GET04120
ENDIF 'GET04130
C 'GET04140
C 'GET04150
C >-----> 'GET04160
C > RETURN TO THE MAIN PROGRAM < 'GET04170
C >-----> 'GET04180
C 'GET04190
10 FORMAT('1') 'GET04200
RETURN 'GET04210
END 'GET04220
'GET04230

```

Appendix D

FEM Computer Program for Emission Problems in Time Domain


```

C > IOUT          : TIME PARAMETER (PARAM.)          < SMT00560
C >              < SMT00570
C > X,Y          : COORDINATES OF THE TRIANGLE VERTICES < SMT00580
C > SIGMA,MIUR   : CONDUCTIVITY & RELATIVE PERMEABILITY OF TRIANGLE< SMT00590
C > NV,DIRP      : # ASSOCIATED TO EACH NODES & BOUNDARY CONDITION < SMT00600
C >              < SMT00610
C > A,AP         : THE VALUE & DERIVATIVE OF THE FIELD AT EACH NODE< SMT00620
C > W,RWORK,IWORK : WORKING SPACE REQUIRED BY "DDASSL"      < SMT00630
C > R,S,SE       : MATRICES RELATED TO THE SYSTEM OF EQUATIONS < SMT00640
C > Q,TQ        : REALTED TO P. SILVESTER'S SHAPE FUNCTIONS < SMT00650
C > INFO        : INFORMATIONS REQUIRED BY "DDASSL"        < SMT00660
C > VMIUO,CO     : PERMEABILITY & SPEED OF LIGHT IN AIR   < SMT00670
C >              < SMT00680
C >              < SMT00690
C >              < SMT00700
C >              < SMT00710
C >              < SMT00720
C >              < SMT00730
C >              < SMT00740
C >              < SMT00750
C > PARAMETER (NUNK=780,NTRI=1500,MLMX=300,MUMX=300)
C > IMPLICIT REAL*8(A-H,O-Z)
C > ----- VALUES FROM SUBROUTINE GETINF ----- < SMT00760
C > REAL*8 PVAIRG,VAIRG,HE,LE,WE,XW,YW SMT00770
C > REAL*8 SIG,MIURW,HO,ALPHA,BETA SMT00780
C > REAL*8 XR1(10),YR1(10),XR2(10),YR2(10),TINT(50) SMT00790
C > INTEGER IBND,TM,NREG,IOUT,NINT SMT00800
C > ----- VALUES FROM TRIANG SUBROUTINE ----- < SMT00810
C > REAL*8 X(NUNK),Y(NUNK),POT(NUNK),SIGMA(NTRI),MIUR(NTRI) SMT00820
C > INTEGER NV(NTRI,3),NC(100,2),NI(100,2) SMT00830
C > LOGICAL*4 DIRP(NUNK) SMT00840
C > ----- VALUES FOR PROGRAM SEMPTDDA ----- < SMT00850
C > REAL*8 A(NUNK),AP(NUNK) SMT00860
C > REAL*8 RWORK(40+9*NUNK+(2*MLMX+MUMX+1)*NUNK) SMT00870
C > REAL*8 R(NUNK,MLMX+MUMX+1),S(NUNK,MLMX+MUMX+1),SE(3,3),T(200) SMT00880
C > INTEGER Q(4,15,15,3),TQ(4,15,15),INFO(15),IWORK(20+NUNK) SMT00890
C >              < SMT00900
C >              < SMT00910
C > THE FOLLOWING IS THE COMMON BLOCK LINK TO THE < SMT00920
C > SUBROUTINES AND FUNCTIONS < SMT00930
C > ----- < SMT00940
C > COMMON /GETIN/PVAIRG,VAIRG,HE,LE,WE,SIG,MIURW,HO,TINT,ALPHA, SMT00950
C > &BETA,XR1,YR1,XR2,YR2,XW,YW,AW,TR,PW,TF, SMT00960
C > &IBND,TM,NREG,IOUT,NINT,IFIELD,ITIME SMT00970
C > COMMON /TRIWR/SIGMA,MIUR, SMT00980
C > &X,Y,POT,NOTR,NOPTL,NDIR,NV,NS,NC,NIE,NI,ML,MU,DIRP SMT00990
C > COMMON /OUT/A SMT01000
C > COMMON /RAS/R,S,NEQ/SIMPL/Q,TQ SMT01010
C > SMT01020
C > SMT01030
C > SMT01040
C > SMT01050
C > SMT01060
C > SMT01070
C > SMT01080
C > SMT01090
C > SMT01100

```

```

EXTERNAL RES,JAC

```

```

P(A1,B1,A2,B2,A3,B3) = A1*B2-A2*B1+A2*B3-A3*B2+A3*B1-A1*B3

```

```

PI = DACOS(-1.000)

```

```

VMIUO = 4.0D-07*PI

```

```

CO = 3.0D08

```

```

C
C
C >-----< SMT01110
C > THE FOLLOWING CALL GETS THE NECESSARY INFORMATION < SMT01120
C > CONCERNING THE GEOMETRY & THE FIELD < SMT01130
C >-----< SMT01140
C CALL GETWTD SMT01150
C SMT01160
C SMT01170
C SMT01180
C >-----< SMT01190
C > THE FOLLOWING CALL PRINTS THE INFORMATION ON THE OUTPUT FILE < SMT01200
C >-----< SMT01210
C CALL PRNINF SMT01220
C SMT01230
C SMT01240
C >-----< SMT01250
C > THIS CALL TO "TRIANG" WILL TRIANGULARIZE THE REGION OF < SMT01260
C > INTEREST AND DETERMINE THE DIRICHLET BOUNDARIES < SMT01270
C >-----< SMT01280
C IF (IFIELD .EQ. 0) THEN SMT01290
C   CALL TRWRD SMT01300
C ELSE SMT01310
C   CALL TRIBPT SMT01320
C ENDIF SMT01330
C NN = NOPTL - NDIR SMT01340
C SMT01350
C SMT01360
C >-----< SMT01370
C > NEXT WE DETERMINE THE TIME STEPS AND THE FINAL TIME < SMT01380
C > FOR THE ANALYSIS OF THIS PARTICULAR PROBLEM < SMT01390
C >-----< SMT01400
C IF (IFIELD .EQ. 1) THEN SMT01410
C   SMIU = SIG*VMIUO*MIURW SMT01420
C   TSTA = 0.000 SMT01430
C   TPEAK = DLOG(BETA/ALPHA)/(BETA - ALPHA) SMT01440
C   TDIF = SMIU*WE**2 SMT01450
C   TPIN = TSTA + TPEAK + TDIF/(2.000**((DLOG10(ALPHA) - 4))) SMT01460
C   EPEAK = DEXP(-ALPHA*TPEAK) - DEXP(-BETA*TPEAK) SMT01470
C   DO 100 I = 2 , 10000 SMT01480
C     IF (-BETA*TPEAK*REAL(I) .LE. -120.00) THEN SMT01490
C       IF (DEXP(-ALPHA*TPEAK*REAL(I)) .LT. 0.1000*EPEAK) SMT01500
C         GO TO 200 SMT01510
C     ELSE SMT01520
C       IF ((DEXP(-ALPHA*TPEAK*REAL(I)) - SMT01530
C         DEXP(-BETA*TPEAK*REAL(I))) .LT. 0.1000*EPEAK) GO TO 200 SMT01540
C     ENDIF SMT01550
C   CONTINUE SMT01560
C CONTINUE SMT01570
C   TFIN = REAL(I)*TPEAK SMT01580
C   N1 = I SMT01590
C   TSTEP = TPEAK/10.000 SMT01600
C   IF (N1 .GT. 15) THEN SMT01610
C     N1 = 15 SMT01620
C     TSTEP2 = TFIN/15.000 SMT01630
C   ELSE SMT01640
C     SMT01650

```

```

        TSTEP2 = TPEAK
    ENDIF
    TSTEP3 = TDIF
    IF (TDIF .EQ. 0.000) TSTEP3 = TSTEP2
    T(1) = TSTA
ELSE
    TSTEP = TR/10.000
    TSTEP2 = PW/10.000
    TSTEP3 = TF/10.000
    TSTEP4 = (TR + PW + TF)/2.000
ENDIF
C
C
C
C >-----<
C > THEN THE DISCRETE TIMES ARE CALCULATED <
C >-----<
C
    IF (IFIELD .EQ. 1) THEN
        K = 0
        DO 300 I = 2 , 20 + N1
            IF (I .LE. 10) THEN
                T(I+K) = T(I+K-1) + TSTEP
            ELSE IF (I .LE. 10 + N1) THEN
                T(I+K) = T(I+K-1) + TSTEP2
            ELSE
                T(I+K) = T(I+K-1) + TSTEP3
            ENDIF
            IF (T(I+K-1) .LT. TPIN .AND. T(I+K) .GE. TPIN) THEN
                STEPX = (T(I+K) - T(I+K-1))/10.000
                T(I+K) = T(I+K-1) + STEPX
                DO 400 K = 1 , 10
                    T(I+K) = T(I+K-1) + STEPX
                CONTINUE
            K = K - 1
        ENDIF
    CONTINUE
300 CONTINUE
ELSE
    T(1) = 0.000
    DO 350 I = 2 , 50
        IF (I .LE. 10) THEN
            T(I+K) = T(I+K-1) + TSTEP
        ELSE IF (I .LE. 20) THEN
            T(I+K) = T(I+K-1) + TSTEP2
        ELSE IF (I .LE. 40) THEN
            T(I+K) = T(I+K-1) + TSTEP3
        ELSE
            T(I+K) = T(I+K-1) + TSTEP4
        ENDIF
    CONTINUE
350 CONTINUE
ENDIF
C
C >-----<
C > NEXT THE TIME REQUIRED BY THE USER ARE MERGED <
C > WITH THE CALCULATED TIMES (IF THERE ARE ANY!!!) <
C >-----<

```

SMT01660
 SMT01670
 SMT01680
 SMT01690
 SMT01700
 SMT01710
 SMT01720
 SMT01730
 SMT01740
 SMT01750
 SMT01760
 SMT01770
 SMT01780
 SMT01790
 SMT01800
 SMT01810
 SMT01820
 SMT01830
 SMT01840
 SMT01850
 SMT01860
 SMT01870
 SMT01880
 SMT01890
 SMT01900
 SMT01910
 SMT01920
 SMT01930
 SMT01940
 SMT01950
 SMT01960
 SMT01970
 SMT01980
 SMT01990
 SMT02000
 SMT02010
 SMT02020
 SMT02030
 SMT02040
 SMT02050
 SMT02060
 SMT02070
 SMT02080
 SMT02090
 SMT02100
 SMT02110
 SMT02120
 SMT02130
 SMT02140
 SMT02150
 SMT02160
 SMT02170
 SMT02180
 SMT02190
 SMT02200

```

C >-----< SMT02210
C < SMT02220
  IF (NINT .NE. 0) THEN SMT02230
  DO 500 I = 1 , NINT SMT02240
    TINT(I) = TINT(I) + TSTA SMT02250
500 CONTINUE SMT02260
    K = 1 SMT02270
    DO 600 I = 2 , 30 + N1 + NINT SMT02280
      IF (T(I) .GT. TINT(K) .AND. T(I-1) .LT. TINT(K)) THEN SMT02290
        DO 700 J = 30 + N1 + K , I , -1 SMT02300
          T(J) = T(J-1) SMT02310
700 CONTINUE SMT02320
          T(I) = TINT(K) SMT02330
          K = K + 1 SMT02340
        ENDIF SMT02350
800 CONTINUE SMT02360
        DO 800 I = 30 + N1 + K , 30 + N1 + NINT SMT02370
          T(I) = TINT(K) SMT02380
          K = K + 1 SMT02390
        CONTINUE SMT02400
      ENDIF SMT02410
C < SMT02420
C >-----< SMT02430
C > THIS CALL TO "SIMPLX" DEFINES THE SHAPE FUNCTIONS AS < SMT02440
C > GIVEN IN P. SILVESTER'S BOOK ON THE FEM < SMT02450
C >-----< SMT02460
C < SMT02470
  CALL SIMPLX(1) SMT02480
C < SMT02490
C >-----< SMT02500
C > WE CAN NOW SET-UP THE "S" AND "R" MATRICES AT THE < SMT02510
C > INITIAL TIME "T(1)" < SMT02520
C >-----< SMT02530
C < SMT02540
  DO 900 I = 1 , NUNK SMT02550
  DO 900 J = 1 , MLMX+MUMX+1 SMT02560
    R(I,J) = 0.000 SMT02570
    S(I,J) = 0.000 SMT02580
900 CONTINUE SMT02590
  DO 1000 ITR = 1 , NOTR SMT02600
    VM = MIUR(ITR)*VMIUO SMT02610
    I1 = NV(ITR,1) SMT02620
    I2 = NV(ITR,2) SMT02630
    I3 = NV(ITR,3) SMT02640
C WRITE(9,111) ITR,I1,I2,I3,SIGMA(ITR),MIUR(ITR) SMT02650
  DET = P(X(I1),Y(I1),X(I2),Y(I2),X(I3),Y(I3)) SMT02660
  IF (DET .EQ. 0.000) GO TO 8888 SMT02670
  AR = ABS(DET)/2.000 SMT02680
  R12 = (X(I1) - X(I2))*(X(I1) - X(I2)) SMT02690
  & + (Y(I1) - Y(I2))*(Y(I1) - Y(I2)) SMT02700
  & R13 = (X(I1) - X(I3))*(X(I1) - X(I3)) SMT02710
  & + (Y(I1) - Y(I3))*(Y(I1) - Y(I3)) SMT02720
  & R23 = (X(I2) - X(I3))*(X(I2) - X(I3)) SMT02730
  & + (Y(I2) - Y(I3))*(Y(I2) - Y(I3)) SMT02740
  COSA1 = (R12 + R13 - R23)/(2.DO*DSQRT(R12*R13)) SMT02750

```

```

IF (COSA1 .GE. 1.0D0) WRITE(9, '(5HCOSA1,2X,F5.3)') COSA1
COSA2 = (R12 + R23 - R13)/(2.D0*DSQRT(R12*R23))
IF (COSA2 .GE. 1.0D0) WRITE(9, '(5HCOSA2,2X,F5.3)') COSA2
COSA3 = (R13 + R23 - R12)/(2.D0*DSQRT(R13*R23))
IF (COSA3 .GE. 1.0D0) WRITE(9, '(5HCOSA3,2X,F5.3)') COSA3
COTA1 = COSA1/DSQRT(1.0D0 - COSA1*COSA1)
COTA2 = COSA2/DSQRT(1.0D0 - COSA2*COSA2)
COTA3 = COSA3/DSQRT(1.0D0 - COSA3*COSA3)
DO 1100 I = 1, 3
  DO 1100 J = 1, 3
    SE(I,J) = (COTA1*REAL(Q(1,I,J,1)) + COTA2*
& REAL(Q(1,I,J,2)) + COTA3*REAL(Q(1,I,J,3)))/2.0D0
1100 CONTINUE
DO 1200 I = 1, 3
  L = NV(ITR,I)
  IF(DIRP(L)) GO TO 1200
  DO 1300 K = 1, 3
    LC = NV(ITR,K)
    IF (.NOT.DIRP(LC)) THEN
      LC = LC - L + ML + 1
      S(L,LC) = S(L,LC) + SE(I,K)
      IF (SIG .NE. 0.0D0) THEN
        R(L,LC) = R(L,LC) + VM*SIGMA(ITR)*TQ(1,I,K)*AR/12.0D0
      ENDIF
    ENDIF
1300 CONTINUE
1200 CONTINUE
1000 CONTINUE
C
C >-----<
C > THE CONTRIBUTION OF THE INFINITE ELEMENT BOUNDARY <
C > IS ADDED TO THE "R" AND "S" MATRICES <
C >-----<
C
N = 1
DO 1350 I = 1, NIE
  L1 = NI(I,1)
  L2 = NI(I,2)
  LI = DSQRT((X(L2) - X(L1))**2 + (Y(L2) - Y(L1))**2)/2.0D0
  XMI = (X(L1) + X(L2))/2.0D0
  YMI = (Y(L1) + Y(L2))/2.0D0
  RMI = DSQRT(XMI**2 + YMI**2)
  TETA = DATAN2(YMI,XMI)
  PHIE = DATAN2(Y(L2) - Y(L1), X(L2) - X(L1)) - PI/2.0D0
  D = RMI*DCOS(TETA - PHIE)
  B = RMI*DSIN(TETA - PHIE)
  LC = ML + 1
  LC21 = L1 - L2 + ML + 1
  LC12 = L2 - L1 + ML + 1
  S(L1,LC) = S(L1,LC) + 1.0D0/(6.0D0*N*D)*((4.0D0*N**2 + 2.0D0*N
& + 1)*LI - 6.0D0*N*B + 3.0D0*RMI**2/LI)
  S(L2,LC) = S(L2,LC) + 1.0D0/(6.0D0*N*D)*((4.0D0*N**2 + 2.0D0*N
& + 1)*LI + 6.0D0*N*B + 3.0D0*RMI**2/LI)
  S(L1,LC12) = S(L1,LC12) + 1.0D0/(6.0D0*N*D)*((2.0D0*N**2
& - 2.0D0*N - 1)*LI - 3.0D0*RMI**2/LI)

```

SMT02760
SMT02770
SMT02780
SMT02790
SMT02800
SMT02810
SMT02820
SMT02830
SMT02840
SMT02850
SMT02860
SMT02870
SMT02880
SMT02890
SMT02900
SMT02910
SMT02920
SMT02930
SMT02940
SMT02950
SMT02960
SMT02970
SMT02980
SMT02990
SMT03000
SMT03010
SMT03020
SMT03030
SMT03040
SMT03050
SMT03060
SMT03070
SMT03080
SMT03090
SMT03100
SMT03110
SMT03120
SMT03130
SMT03140
SMT03150
SMT03160
SMT03170
SMT03180
SMT03190
SMT03200
SMT03210
SMT03220
SMT03230
SMT03240
SMT03250
SMT03260
SMT03270
SMT03280
SMT03290
SMT03300

```

      S(L2,LC21) = S(L2,LC21) + 1.000/(6.000*N*D)*((2.000*N**2
&      -2.000*N - 1)*LI - 3.000*RMI**2/LI)
1350 CONTINUE
C
C >-----<
C > THE "S" & "R" MATRICES NEED TO BE SHIFTED UP BY NDIR <
C > AND ALSO SIDWAYS <
C >-----<
C
DO 1400 I = 1 , NOPTL
  IF (DIRP(I)) GO TO 1400
  DO 1500 K = 1 , ML + MU + 1
    IF (K .EQ. 1) K1 = 0
1800 CONTINUE
    L = K + I - ML - 1 + K1
    IF (L .LT. 1 .OR. K .EQ. ML+1) GO TO 1500
    IF (L .GT. NOPTL) GO TO 1400
    IF (DIRP(L)) THEN
      IF (K .EQ. 1) THEN
        R(I,K) = 0.000
        S(I,K) = 0.000
      ELSE IF (K .EQ. ML+MU+1) THEN
        R(I,K) = 0.000
        S(I,K) = 0.000
      ELSE IF (K .LT. ML+1) THEN
        DO 1600 J = K , 2 , -1
          R(I,J) = R(I,J-1)
          S(I,J) = S(I,J-1)
1600 CONTINUE
          R(I,1) = 0.000
          S(I,1) = 0.000
        ELSE IF (K .GT. ML+1) THEN
          DO 1700 J = K , ML+MU
            R(I,J) = R(I,J+1)
            S(I,J) = S(I,J+1)
1700 CONTINUE
            R(I,ML+MU+1) = 0.000
            S(I,ML+MU+1) = 0.000
            K1 = K1 + 1
            GO TO 1800
          ENDIF
        ENDIF
1500 CONTINUE
1400 CONTINUE
    M1 = 0
    DO 1900 I = 1 , NOPTL
      IF (.NOT. DIRP(I)) THEN
        DO 2000 K = 1 , ML + MU + 1
          R(I-M1,K) = R(I,K)
          S(I-M1,K) = S(I,K)
2000 CONTINUE
        ELSE
          M1 = M1 + 1
        ENDIF
1900 CONTINUE

```

```

SMT03310
SMT03320
SMT03330
SMT03340
SMT03350
SMT03360
SMT03370
SMT03380
SMT03390
SMT03400
SMT03410
SMT03420
SMT03430
SMT03440
SMT03450
SMT03460
SMT03470
SMT03480
SMT03490
SMT03500
SMT03510
SMT03520
SMT03530
SMT03540
SMT03550
SMT03560
SMT03570
SMT03580
SMT03590
SMT03600
SMT03610
SMT03620
SMT03630
SMT03640
SMT03650
SMT03660
SMT03670
SMT03680
SMT03690
SMT03700
SMT03710
SMT03720
SMT03730
SMT03740
SMT03750
SMT03760
SMT03770
SMT03780
SMT03790
SMT03800
SMT03810
SMT03820
SMT03830
SMT03840
SMT03850

```

```

C
C >-----<
C > SET-UP THE INITIAL VALUES FOR THE CALL TO "DDASSL" <
C >-----<
C
DO 2100 I = 1 , NN
  A(I) = 0.0D+00
  AP(I) = 0.0D+00
2100 CONTINUE
DO 2200 I = 1 , 15
  INFO(I) = 0
2200 CONTINUE
  INFO(5) = 1
  INFO(6) = 1
  IWORK(1) = ML
  IWORK(2) = MU
  NEQ = NN
  RTOL = 0.001D0
  ATOL = 0.001D0*HO
  LRW = 40 + 9*NUNK + (2*MLMX+MUMX+1)*NUNK
  LIW = 20 + NUNK
  IPAR = NEQ
  WRITE(9,*) NEQ
C
C >-----<
C > SOLVE WITH "DDASSL", THE SUBROUTINE WRITTEN BY <
C > LINDA R. PETZOLD <
C >-----<
C
I2 = 50 + NINT
IF (IFIELD .EQ. 1) I2 = 30 + N1 + NINT
DO 2300 I = 2 , 30 + N1 + NINT
  CALL DDASSL(RES,NEQ,T(I-1),A,AP,T(I),INFO,RTOL,ATOL, IDID,RWORK,
& LRW,IWORK,LIW,RPAR,IPAR,JAC)
  IF (IDID .LT. 0) THEN
    GO TO 2500
  ELSE
    IF (ITIME .EQ. 0) THEN
      CALL OUTP(T(I))
    ELSE
      DO 2400 J = 1 , NINT
        IF (T(I) .GE. 0.999D0*TINT(J) .AND. T(I) .LE. 1.001D0*
& TINT(J)) CALL OUTP(T(I))
2400 CONTINUE
      ENDIF
    ENDIF
2300 CONTINUE
  STOP
2500 CONTINUE
  WRITE(6,333) IDID
  WRITE(9,333) IDID
  STOP
8888 CONTINUE
  WRITE(9,'(5X,23HDETERMINANT OF TRIANGLE,14,10H = 0.01111)' ) ITR
  WRITE(6,'(5X,23HDETERMINANT OF TRIANGLE,14,10H = 0.01111)' ) ITR

```

SMT03860
 SMT03870
 SMT03880
 SMT03890
 SMT03900
 SMT03910
 SMT03920
 SMT03930
 SMT03940
 SMT03950
 SMT03960
 SMT03970
 SMT03980
 SMT03990
 SMT04000
 SMT04010
 SMT04020
 SMT04030
 SMT04040
 SMT04050
 SMT04060
 SMT04070
 SMT04080
 SMT04090
 SMT04100
 SMT04110
 SMT04120
 SMT04130
 SMT04140
 SMT04150
 SMT04160
 SMT04170
 SMT04180
 SMT04190
 SMT04200
 SMT04210
 SMT04220
 SMT04230
 SMT04240
 SMT04250
 SMT04260
 SMT04270
 SMT04280
 SMT04290
 SMT04300
 SMT04310
 SMT04320
 SMT04330
 SMT04340
 SMT04350
 SMT04360
 SMT04370
 SMT04380
 SMT04390
 SMT04400


```

C > THE USER WANTS TO PRINT OUT THE WHOLE REGION < SMT04960
C >-----< SMT04970
C > SMT04980
C > IF (DIRP(I)) THEN SMT04990
C > WRITE(9,333) X(I),Y(I),POT(I) SMT05000
C > ELSE SMT05010
C > WRITE(9,333) X(I),Y(I),A(N1) SMT05020
C > N1 = N1 + 1 SMT05030
C > ENDIF SMT05040
C > ELSE SMT05050
C > SMT05060
C >-----< SMT05070
C > THE USER WANTS TO PRINT OUT ONLY PARTS OF THE REGION < SMT05080
C >-----< SMT05090
C > SMT05100
C > DO 200 J = 1 , NREG SMT05110
C > IF ((X(I) .GE. XR1(J) .AND. X(I) .LE. XR2(J)) .AND. SMT05120
C > (Y(I) .GE. YR1(J) .AND. Y(I) .LE. YR2(J))) THEN SMT05130
C > & IF (DIRP(I)) THEN SMT05140
C > WRITE(9,333) X(I),Y(I),POT(I) SMT05150
C > ELSE SMT05160
C > WRITE(9,333) X(I),Y(I),A(N1) SMT05170
C > N1 = N1 + 1 SMT05180
C > ENDIF SMT05190
C > ENDIF SMT05200
200 CONTINUE SMT05210
C > ENDIF SMT05220
100 CONTINUE SMT05230
C > SMT05240
C >-----< SMT05250
C > SMT05260
C > NEXT WE'LL CALCULATE THE MAGNETIC FIELD < SMT05270
C > WITHIN EACH TRIANGLES < SMT05280
C >-----< SMT05290
C > SMT05300
C > N1 = NOPTL - NDIR SMT05310
C > DO 300 I = NOPTL , 1 , -1 SMT05320
C > IF (DIRP(I)) THEN SMT05330
C > B(I) = POT(I) SMT05340
C > ELSE SMT05350
C > B(I) = A(N1) SMT05360
C > N1 = N1 - 1 SMT05370
C > ENDIF SMT05380
300 CONTINUE SMT05390
C > DO 400 ITR = 1 , NOTR SMT05400
C > I1 = NV(ITR,1) SMT05410
C > I2 = NV(ITR,2) SMT05420
C > I3 = NV(ITR,3) SMT05430
C > DET = P(X(I1),Y(I1),X(I2),Y(I2),X(I3),Y(I3)) SMT05440
C > DADX = ((Y(I2) - Y(I3))*B(I1) + (Y(I3) - Y(I1))*B(I2) + SMT05450
C > (Y(I1) - Y(I2))*B(I3))/DET SMT05460
C > & DADY = ((X(I3) - X(I2))*B(I1) + (X(I1) - X(I3))*B(I2) + SMT05470
C > (X(I2) - X(I1))*B(I3))/DET SMT05480
C > HX(ITR) = DADY SMT05490
C > HY(ITR) = -DADX SMT05500

```



```

C >----- VALUES FROM SUBROUTINE GETINF -----> SMT06060
REAL*8   PVAIRG,VAIRG,HE,LE,WE,XW,YW          SMT06070
REAL*8   SIG,MIURW,HO,ALPHA,BETA             SMT06080
REAL*8   XR1(10),YR1(10),XR2(10),YR2(10),TINT(50) SMT06090
INTEGER  IBND,TM,NREG,IOUT,NINT              SMT06100
C >----- VALUES FROM TRIANG SUBROUTINE -----> SMT06110
REAL*8   X(NUNK),Y(NUNK),POT(NUNK),SIGMA(NTRI),MIUR(NTRI) SMT06120
INTEGER  NV(NTRI,3),NC(100,2),NI(100,2)      SMT06130
LOGICAL*4 DIRP(NUNK)                         SMT06140
C >----- VALUES FROM PROGRAM SEMPTDDA -----> SMT06150
REAL*8   R(NUNK,MLMX+MUMX+1),S(NUNK,MLMX+MUMX+1) SMT06160
INTEGER  Q(4,15,15,3),TQ(4,15,15)           SMT06170
C >----- VALUES FOR SUBROUTINE RES -----> SMT06180
REAL*8   TIME,A(NUNK),AP(NUNK),B(NUNK),DELTA(IPAR),SE(3,3),EFLD SMT06190
C >-----> SMT06200
C >-----> SMT06210
C > THE FOLLOWING IS THE COMMON BLOCK LINK TO THE < SMT06220
C > SUBROUTINES AND FUNCTIONS < SMT06230
C >-----> SMT06240
C >-----> SMT06250
COMMON  /GETIN/PVAIRG,VAIRG,HE,LE,WE,SIG,MIURW,HO,TINT,ALPHA, SMT06260
&BETA,XR1,YR1,XR2,YR2,XW,YW,AW,TR,PW,TF, SMT06270
&IBND,TM,NREG,IOUT,NINT,IFIELD,ITIME SMT06280
COMMON  /TRIWR/SIGMA,MIUR, SMT06290
&X,Y,POT,NOTR,NOPTL,NDIR,NV,NS,NC,NIE,NI,ML,MU,DIRP SMT06300
COMMON  /RAS/R,S,NEQ/SIMPL/Q,TQ SMT06310
C >-----> SMT06320
C P(A1,B1,A2,B2,A3,B3) = A1*B2-A2*B1+A2*B3-A3*B2+A3*B1-A1*B3 SMT06330
C >-----> SMT06340
C PI = DACOS(-1.0D0) SMT06350
C VMIUD = 4.0D-07*PI SMT06360
C CO = 3.0D08 SMT06370
C DO 100 I = 1, NUNK SMT06380
C   B(I) = 0.0D0 SMT06390
100 CONTINUE SMT06400
C >-----> SMT06410
C >-----> SMT06420
C > THE "B" VECTOR (THE SOURCE VECTOR) NEED TO BE SET-UP < SMT06430
C > AT "TIME" < SMT06440
C >-----> SMT06450
C > THE CONTRIBUTION OF THE INEOMOGENEOUS NEUMANN BOUNDARY < SMT06460
C > IS ADDED TO THE "B" VECTOR < SMT06470
C >-----> SMT06480
C >-----> SMT06490
IF (IFIELD .EQ. 1) THEN SMT06500
  VALUE = HO*(DEXP(-ALPHA*TIME) - DEXP(-BETA*TIME)) SMT06510
ELSE SMT06520
  IF (TIME .LE. TR) THEN SMT06530
    VALUE = HO*TIME/TR SMT06540
  ELSE IF (TIME .LE. TR+PW) THEN SMT06550
    VALUE = HO SMT06560
  ELSE IF (TIME .LE. TR+PW+TF) THEN SMT06570
    VALUE = -HO/TF*(TIME - TR - PW) + HO SMT06580
  ELSE SMT06590
    VALUE = 0.0D0 SMT06600
  END IF
END IF

```



```

C > THIS SUBROUTINE DEFINES THE JACOBIAN, THE MATRIX OF < SMT07160
C > PARTIAL DERIVATIVES : < SMT07170
C > PD = DG/DA + CJ*DG/DAP < SMT07180
C > < SMT07190
C >-----< SMT07200
C < SMT07210
C < SMT07220
C SUBROUTINE JAC (T,A,AP,PD,CJ,RPAR,IPAR) < SMT07230
C PARAMETER (NUNK=780,NTRI=1500,MLMX=300,MUMX=300) < SMT07240
C IMPLICIT REAL*8(A-H,O-Z) < SMT07250
C >-----VALUES FROM TRIANG SUBROUTINE-----< SMT07260
C REAL*8 X(NUNK),Y(NUNK),POT(NUNK),SIGMA(NTRI),MIUR(NTRI) < SMT07270
C INTEGER NV(NTRI,3),NC(100,2),NI(100,2) < SMT07280
C LOGICAL*4 DIRP(NUNK) < SMT07290
C >-----VALUES FOR SUBROUTINE JAC-----< SMT07300
C REAL*8 A(NUNK),AP(NUNK),PD(2*ML+MU+1,IPAR) < SMT07310
C REAL*8 R(NUNK,MLMX+MUMX+1),S(NUNK,MLMX+MUMX+1),T,CJ < SMT07320
C < SMT07330
C >-----< SMT07340
C > THE FOLLOWING IS THE COMMON BLOCK LINK TO THE < SMT07350
C > SUBROUTINES AND FUNCTIONS < SMT07360
C >-----< SMT07370
C < SMT07380
C COMMON /TRIWR/SIGMA,MIUR, < SMT07390
C &X,Y,POT,NOTR,NOPTL,NDIR,NV,NS,NC,NIE,NI,ML,MU,DIRP < SMT07400
C COMMON /RAS/R,S,NEQ < SMT07410
C < SMT07420
C < SMT07430
C >-----< SMT07440
C > AS THE "S" AND "R" MATRICES ARE INDEPENDENT OF TIME, < SMT07450
C > THE JACOBIAN IS ALSO TIME INDEPENDENT < SMT07460
C >-----< SMT07470
C < SMT07480
C DO 100 I = 1 , NEQ < SMT07490
C DO 100 J = 1 , NEQ < SMT07500
C K = J - I + ML + 1 < SMT07510
C IF (K .GT. 0 .AND. K .LE. ML+MU+1) THEN < SMT07520
C IROW = I - J + ML + MU + 1 < SMT07530
C IF (SIG .EQ. 0.0D0) THEN < SMT07540
C PD(IROW,J) = S(I,K) < SMT07550
C ELSE < SMT07560
C PD(IROW,J) = S(I,K) + CJ*R(I,K) < SMT07570
C ENDIF < SMT07580
C ENDIF < SMT07590
100 CONTINUE < SMT07600
C RETURN < SMT07610
C END < SMT07620

```



```

WRITE(6,*) '
WRITE(6,*) '          tpeak          tfin          'GET02760
WRITE(6,*) '          WHERE f(tfin) = 0.1 * f(tpeak) 'GET02770
WRITE(6,*) ' 'GET02780
WRITE(6,*) ' 'GET02790
WRITE(6,*) ' 'GET02800
C          GET02810
TPEAK = DLOG(BETA/ALPHA)/(BETA-ALPHA) GET02820
EPEAK = DEXP(-ALPHA*TPEAK) - DEXP(-BETA*TPEAK) GET02830
DO 700 I = 2, 10000 GET02840
  IF (-BETA*TPEAK*REAL(I) .LE. -120.00) THEN GET02850
  IF (DEXP(-ALPHA*TPEAK*REAL(I)) .LT. 0.1000*EPEAK) GO TO 800 GET02860
  ELSE GET02870
  IF ((DEXP(-ALPHA*TPEAK*REAL(I)) - DEXP(-BETA*TPEAK*REAL(I))) GET02880
& .LT. 0.1000*EPEAK) GO TO 800 GET02890
  ENDIF GET02900
700 CONTINUE GET02910
800 CONTINUE GET02920
  TFIN = REAL(I)*TPEAK GET02930
  TDIFF = 4.00-07*PI*MIURW*SIG*WE**2 GET02940
  TFINA = TFIN + TDIFF GET02950
  WRITE(6,*) ' 'GET02960
  WRITE(6,*) '          HERE ARE THE CRITICAL TIME VALUES : 'GET02970
  WRITE(6,*) ' 'GET02980
  WRITE(6,*) ' 'GET02990
  WRITE(6,*) '(7X,8Htpeak = ,E10.4,5X,7Htfin = ,E10.4)' TPEAK,TFIN GET03000
  WRITE(6,*) '(7X,8Htdiff = ,E10.4,5X,9Htfinal = ,E10.4)' TDIFF,TFIN GET03010
  WRITE(6,*) ' 'GET03020
  WRITE(6,*) '          tdiff IS THE REQUIRED TIME FOR DIFFUSION 'GET03030
  WRITE(6,*) '          AND tfinal IS THE OVERALL FINAL INTEGRATION 'GET03040
  WRITE(6,*) '          TIME CALCULATED AS tfinal = tfin + tdiff 'GET03050
  WRITE(6,*) ' 'GET03060
  WRITE(6,*) '          PLEASE ENTER THE NUMBER OF SPECIFIC TIMES 'GET03070
  WRITE(6,*) '          FOR WHICH YOU ARE INTERESTED FOR THE 'GET03080
  WRITE(6,*) '          INVESTIGATION 'GET03090
900 WRITE(6,*) ' 'GET03100
  WRITE(6,*) '          # OF INTEGRATION TIME ? 'GET03110
  READ(IUNIT,*) NINT GET03120
  IF (NINT .GT. 50) THEN GET03130
  WRITE(6,*) ' 'GET03140
  WRITE(6,*) '          THE MAXIMUM # OF INT. TIMES IS FIFTY (50) 'GET03150
  WRITE(6,*) '          PLEASE ENTER OVER THE NUMBER OF INT. TIME 'GET03160
  IF (I1 .GT. 3) STOP GET03170
  I1 = I1 + 1 GET03180
  GO TO 900 GET03190
  ENDIF GET03200
C          GET03210
  WRITE(6,*) ' 'GET03220
  WRITE(6,*) '          IF THE INVESTIGATION IS CARRIED OUT THROUGH 'GET03230
  WRITE(6,*) '          CONSTANT TIME STEPS ENTER 1, 0 OTHERWISE 'GET03240
  WRITE(6,*) ' 'GET03250
  WRITE(6,*) '          1 or 0 ? 'GET03260
  READ(IUNIT,*) NSTE GET03270
  IF (NSTE .EQ. 0) THEN GET03280
  DO 1000 I = 1, NINT GET03290
  WRITE(6,*) ' 'GET03300

```

```

WRITE(6, '(40H          PLEASE ENTER INTEGRATION TIME # ,12)') I GET03310
WRITE(6,*) : (in seconds) 'GET03320
WRITE(6,*) : 'GET03330
READ(IUNIT,*) TINT(I) GET03340
WRITE(6,*) : 'GET03350
1000 CONTINUE GET03360
ELSE GET03370
WRITE(6,*) : 'GET03380
WRITE(6,*) : PLEASE ENTER THE INTEGRATION TIME STEP 'GET03390
WRITE(6,*) : (in seconds) 'GET03400
WRITE(6,*) : 'GET03410
READ(IUNIT,*) TINTS GET03420
WRITE(6,*) : 'GET03430
TINT(I) = TINTS GET03440
DO 1100 I = 2 , NINT GET03450
TINT(I) = TINT(I-1) + TINTS GET03460
1100 CONTINUE GET03470
ENDIF GET03480
ENDIF GET03490
C GET03500
C GET03510
C >-----< GET03520
C > RETURN TO THE MAIN PROGRAM < GET03530
C >-----< GET03540
C GET03550
10 FORMAT('1') GET03560
RETURN GET03570
END GET03580

```

Bibliography

- [1] Clough, R.W., "The finite element method in plane stress analysis," Proc. 2nd Conf. Electronic Comput., ASCE, Pittsburg, Pa., 1960.
- [2] Winslow, A.M., "Magnetic field calculation in an irregular triangular mesh," Lawrence Radiation Laboratory, Livermore, California, UCRL-7784-T, Rev. 1, 1965.
- [3] Costache, G.H., "Calculation of eddy currents and skin effect in nonmagnetic conductors by the finite element method," Rev. Roum. Sci. Techn.-Electrotechn. et Energ., Bucarest, vol. 21, no. 3, pp. 357-363, 1976.
- [4] Silvester, P. and C.R.S. Haslam, "Magnetotelluric modelling by the finite element method," Geophysical Prospecting, vol.20, pp. 872-891, 1972.
- [5] Brauer, J.R. "Finite elements calculation of eddy currents and skin effects," IEEE Trans. Magn., vol. MAG-18, NO. 2, PP.504- 509, March 1982.
- [6] Silvester, P. and M.V.K. Chari, "Finite element solution of saturable magnetic field problems," IEEE Trans. PAS, vol. PAS- 89, 1642-1651, 1970.
- [7] Anderson, O.W., "Laplacian electrostatic field calculations by finite elements with automatic grid generation," IEEE Trans. PAS, vol. PAS-92, 1973.
- [8] Chari, M.V.K. and P. Silvester, "Analysis of turbo-alternator magnetic fields by finite elements," IEEE Trans PAS, vol. PAS- 90, PP. 454-464, 1971.

- [9] Wexler, A., "Finite-element analysis of inhomogeneous anisotropic reluctance machine rotor," IEEE Trans. PAS, vol. PAS-92, no.1, pp. 145-149, 1973.
- [10] Akhtarzad S. and P.B. Johns, "Numerical solution of lossy waveguides: T.L.M. computer program," Electron. Lett., vol. 10, no. 15, pp. 309-311, July 25, 1974.
- [11] Akhtarzad S. and P.B. Johns, "Three dimensional transmission-line matrix computer analysis of microstrip resonators," IEEE Trans. Microwave Theory Tech., vol. MTT-23, pp. 990-997, Dec. 1975.
- [12] Akhtarzad S. and P.S. Johns, "Solution of Maxwell's equations in three space dimensions and time by the T.L.M. method of analysis," Proc. Inst. Elec. Eng., vol. 122, no.12, pp. 1344- 1348, Dec. 1975.
- [13] Al. Mukhtar D. A. and J.E. Sitch, "Transmission-line matrix method with irregularly graded space," Proc. Inst. Elec. Eng., vol. 128, no. 6, pp. 299-305, Dec. 1981.
- [14] Shih, Y.-C. and W.J.R. Hoefer, "Dominant and second-order mode cutoff frequencies in fin lines calculated with a two-dimensional TLM program," IEEE Trans. Microwave Theory Tech., vol. MTT-28, pp. 1443-1448, Dec. 1980.
- [15] Shih, Y.-C., " The analysis of fin lines using transmission line matrix and transverse resonance methods," M.A.Sc. thesis, Univ. of Ottawa, Canada, 1980
- [16] Yoshida, N. I. Fukai and J.Fukuoka, "Transient analysis of two-dimensional Maxwell's equations by Bergeron's method," Trans. IECE Japan, vol. J62B, pp. 511-518, June 1979.
- [17] Yoshida, N., I. Fukai and J. Fukuoka, "Application of Bergeron's method to anisotropic medias," Trans. IECE Japan, vol. J64B, pp. 1242-1249, Nov. 1981.

- [18] Hoefel, W.J.R., "The transmission-line matrix method — Theory and applications," *IEEE Trans. Microwave Theory Tech.*, vol. MTT-33, no.10, pp. 882-893, Oct. 1985.
- [19] Spiegel, M.R., *Theory and Problems of Laplace Transforms*, Schaum's Outline Series, McGraw-Hill, 1965.
- [20] Shermann, R., R.A. DeMoss, W.C. Freeman, G.J. Greco, D.G. Larson, L. Levey, and D. S. Wilson, *EMP Engineering and Design Principles*, Bell Laboratories, Whippany, New Jersey, 1975.
- [21] Rektorys, K., *Variational Methods in Mathematics, Science and Engineering*, Reidel Publication Co, 1980.
- [22] Foggia, A., J.C. Sabonnadiere and P. Silvester, "Finite element solution of saturated travelling magnetic field problems," *IEEE Trans. Power Ap. Sys.*, vol. PAS-94, no. 3, pp.866-871, May/June 1975.
- [23] Kreyszig, E., *Advanced Engineering Mathematics*, John Wiley & Sons, New York, 1983.
- [24] Silvester, P.P., *Finite Elements for Electrical Engineers*, Cambridge University Press, Cambridge, 1983.
- [25] Silvester, P.P., "Higher-order polynomial triangle finite elements for potential problems," *Int. J. Eng. Science*, vol. 7, no.8-F, pp. 849-860, 1969.
- [26] Cheng, D.K., *Field and Wave Electromagnetics*, Addison-Wesley, Massachusetts, 1983.
- [27] Anton, H., *Elementary Linear Algebra*, John Wiley & Sons, New York, 1981.
- [28] Ney, M. and G. Costache, "Penetration des impulsions electromagnetiques dans les blindages cylindriques de section arbitraire," *Colloque international en compatibilite electromagnetique*, Limoges, juin 1987.

- [29] International Mathematical and Statistical Libraries, inc., "IMSL library reference manual," Texas, Houston, 1982.
- [30] Petzold, L., "Differential/algebraic equations are not ODE's," SIAM J. Sci. Stat. Comput., vol. 3, no. 3, Sept. 1982.
- [31] Petzold, L.R., "A description of DDASSL: a differential/algebraic system solver," Sandia National Laboratories, Livermore, SAND82-8637, Sept. 1982.
- [32] Huygens, C., *Traite de la lumiere*, Leiden, 1690.
- [33] Johns, P.B. and R.L. Beurle, "Numerical solution of 2-dimensional scattering problems using a transmission-line matrix," Proc. Inst. Elec. Eng., vol. 118, no. 9, pp. 1203-1208, Sept. 1971.
- [34] Johns, P.B., "The solution of inhomogeneous waveguide problems using transmission-line matrix," IEEE Trans. Microwave Theory Tech., vol. MTT-22, no. 3, pp. 209-215, March 1974.
- [35] Akhtarzad, S. and P.B. Johns, "Generalized elements for t.l.m. of numerical analysis," Proc. Inst. Elec. Eng., vol. 122, no. 12, pp. 1349-1352, Dec. 1975
- [36] Saguet, P., E. Pic, "Le maillage rectangulaire et le changement de maille dans la methode TLM en deux dimensions," Electron. Lett., vol. 17, no. 7, pp. 277-279, April 2, 1981.
- [37] Saguet, P., "Analyse des milieux guides, la methode MTLM," Ph.D. thesis, Universite Scientifique et Medicale - Institut National Polytechnique de Grenoble, Dec. 1985.
- [38] Konrad, A., "A direct three-dimensional finite element method for the solution of electromagnetic fields in cavities", IEEE Trans. Magn., vol. MAG-21, no. 6, pp. 2276-2279, November 1985.

- [39] Akhtarzad, S. and P.B. Johns, "Solution of G-component electromagnetic fields in three sapce dimensions and time by the T.L.M. method, " *Electron. Lett.*, vol. 10, no. 25/26, pp. 535-537, Dec. 12, 1974.
- [40] *FCC Part 15J Rules and Regulations*, 1980.
- [41] Shen, L.C. and J.A. Kong, *Applied Electromagnetism*, PWS, Massachusetts, Boston, 1983.
- [42] Hoefler, W.J.R., The Transmission Line Matrix (TLM) Method, in T. Itoh: *Numerical Techniques for Microwave and Millimeter Wave Passive Structures*, John Wiley & Sons, New York, 1989.
- [43] Chari, M.V.K. and P.P. Silvester, *Finite Elements in Electrical and Magnetic Field Problems*, John Wiley & Sons, New York, 1980.
- [44] Costache, G.I., "Finite element method applied to skin-effect problems in strip transmission lines", *IEEE Trans. Microwave Theory Tech.*, vol. MTT-35, no. 11, pp. 1009-1013, Nov. 1987.
- [45] Ungless, R.F., "An infinite element", M.A. Sc. Thesis, University of British Columbia, 1973.
- [46] Pissanetzky, S., "A simple infinite element", *Int. J. Comput. Math. Elec. Eng.*, vol. 3, no. 2, pp. 107-114, 1984.
- [47] Wilson, P.F. and M.T.Ma, "A study of techniques for measuring the electromagnetic shielding effectiveness of materials", National Bureau of Standards, Colorado, NBS Technical Note 1095, 1986.